Firing Properties of Spiral Ganglion Neurons: Functional Contribution of Hyperpolarization-Activated, Cyclic Nucleotide-Gated Channels in Primary Auditory Neurons of the Mouse Inner Ear

Ye-Hyun Kim
Kassel, Germany; Ansan, Korea

B.A., The College of Wooster, 2007

A Dissertation presented to the Graduate Faculty
of the University of Virginia in Candidacy for the Degree of
Doctor of Philosophy

Department of Neuroscience

University of Virginia
May, 2014

Abstract

The hyperpolarization-activated current, I_h, is carried by members of the *Hcn* channel family and contributes to resting potential and firing properties in excitable cells of various systems, including the auditory system. I_h has been identified in spiral ganglion neurons (SGNs), however, its molecular correlates and their functional relevance have not been established. To examine the molecular composition of the channels that carry I_h in SGNs, we examined *Hcn* mRNA harvested from spiral ganglia of wild-type (WT) neonatal and adult mice using quantitative RT-PCR. We show expression of *Hcn1*, *2*, and *4* subunits in SGNs, with *Hcn1* being the most highly expressed at both stages. To determine the physiological expression of HCN subunits in SGN cell bodies, we used the whole-cell, tight-seal technique in voltage-clamp mode to record I_h from WT SGNs and those deficient in *Hcn1*, *Hcn2* or both. We found that HCN1 is a major functional subunit contributing to I_h in SGNs. Deletion of *Hcn1* resulted in significantly reduced conductance, slower activation kinetics, and hyperpolarized half-activation potentials. To investigate the contribution of I_h to SGN function, we recorded membrane responses in current-clamp mode. We demonstrate that I_h contributes to depolarized resting potentials, sag and rebound potentials, accelerates rebound spikes following hyperpolarization, and minimizes spike jitter for small depolarizing stimuli. Auditory brainstem responses of *Hcn1*-deficient mice showed longer latencies, suggesting that HCN1-mediated I_h is critical for synchronized action potential firing in SGNs. Together, our data indicate I_h contributes to SGN membrane properties and plays a role in temporal aspects of signal transmission between the cochlea and the brain, which are critical for normal auditory function.

To further investigate how temporal auditory signal processing is achieved between SGNs and Inner hair cells (IHCs), we have developed a new intact preparation and recording paradigm, where mechanotransduction of the IHCs and recording of SGN responses are possible in simultaneous fashion. We demonstrate, for the first time, that SGNs are capable of transmitting signals in response to mechanical stimulation of IHC hair bundles as early as postnatal day one, at the base of the cochlea. In addition to processing mechanically driven IHC stimuli, we show that early postnatal SGNs fire spontaneous action potential in a position-dependent manner, similar to spontaneous Ca^{2+} spike patterns seen in immature IHCs before the onset of hearing.

Table of Contents

Table of Figures

List of Common Abbreviations

AP	Action Potential
ABR	Auditory Brainstem Response
AVCN	Anteroventral Cochlear Nucleus
CV	Coefficient of Variation
DV	Driving Voltage
E	Embryonic day
EPSP	Excitatory Post Synaptic Potential
IHC	Inner Hair Cell
I_h	Hyperpolarization-activated current
ISI	Inter-Spike Interval
MSO	Medial Superior Olive
MNTB	Medial Nucleus of Trapezoid Body
OHC	Outer Hair Cell
P	Postnatal day
SGN	Spiral Ganglion Neuron
SD	Standard Deviation
SEM	Standard Error of Means

Dedication

First and foremost, I am thankful for my graduate advisor Dr. Jeffrey Holt for giving me the opportunity to learn and grow under his watchful eyes. The past years in the lab has been one of the most invaluable experience in my life, and it has been a wonderful journey and I am forever grateful for everything you have done for me. Thank you very much for showing me how to do good science, but also teaching me how to be a confident scientist with a great heart. Thank you for giving me the freedom to explore the unknown world of spiral ganglion neurons, and supporting me in every possible way.

I would also like to thank my committee members: Dr. David Hill, Dr. Xiaowei Lu, Dr, Manoj Patel, and Dr. Jung-Bum Shin for all their help and guidance they provided me throughout my graduate years. Thank you very much for your constructive advice and encouragement throughout all these years.

My thanks to the UVa Neuroscience Graduate Program, especially Tracy Mourton and graduate program directors Dr. Sue Moentor, Dr. Bettina Winckler, and Dr. Manoj Patel for all their support.

I am especially grateful for the current and past Holt/Géléloc lab members, Dr. Gwen Géléloc, Yukako, Michaela, Geoff, Charlie, BiFeng, Ping, Erin, and Emily who have become my friends and home away from home. Thank you very much for all the laughters and memories you shared with me. Thank you for your kindness and trust and always lending me your ears and shoulders when I needed the most. Thank you very much.

I would also like to send my warmest gratitude to all my colleagues and friends I have made in Charlottesville and in Boston. My deepest thanks to my dear friends and family who are thousands of miles away, and to my dear uncle's family who took me under their wings for the past years. Thank you, aunt and uncle, John, Peter, and Liz, for all your love and your prayers. This would have not been possible without you.

And lastly, I am grateful for my parents for everything they have given me, and for teaching me the joy of learning and the beauty that comes within, and believing in me. Words cannot express how grateful I am for you. This I dedicate to you.

Chapter I: Background and Introduction

Hearing, or *audition*, by definition, refers to the process or ability to perceive sound. As one of the five traditional senses, hearing enables humans to detect, locate, and perceive sound stimuli, and make sense of the auditory scene (Bregman, 1990). The sense of hearing not only allows us to quickly recognize and respond to salient sound cues from the environment thereby alerting us to nearby activities, but also enables efficient everyday communication, such as speech and language, much of which is carried by acoustic sound. In parallel, hearing serves similar functions in animals, where it has evolved as essential means for many species' survival and communication (Fay and Popper, 2000; Gans, 1992; Hauser, 1997).

In order to perform these important tasks of hearing, the mammalian auditory end organ is equipped with a remarkable system, which rapidly captures the sound waves and precisely transforms and transmits into neural representations that preserve the spatio-temporal structure of sound information along the auditory pathway in the brain. In the heart of this dynamic process lies the cochlea – small, yet the most complex mechanical apparatus in the mammalian inner ear responsible for auditory signal processing.

The Mammalian Inner Ear: The Cochlea

The coiled-shaped mammalian cochlea is composed of array of cell types, all of which help the organ to accurately transmit sound signals from the external world. Among those, two major players are the mechano-sensitive hair cells and spiral ganglion neurons.

Auditory Signal Processing in the Cochlea: A synopsis

Auditory hair cells are the sensory receptors in the mammalian inner ear, which are situated within the cochlear sensory epithelium, called the organ of Corti (**Fig. 1-1**). There are two types of hair cells: A single row of inner hair cells (IHCs) and three rows of outer hair cells (OHCs). IHCs are primary sensory receptors that are responsible for transducing sound vibration into electrical signals that the brain can understand. OHCs, on the other hand, function as active amplifiers that aid IHC function by enhancing sound-driven mechanical input through electromotile amplification, contributing to cochlear nonlinearity (Brownell et al, 1985; Hudspeth, 1985; Lieberman et al. 2002).

In mature system, auditory processing commences when sound pressure waves deflects the mechanically-sensitive, stereocilliary hair bundles of IHCs - actin-rich microvilli that protrudes from the apical surface and pivot at their bases -, toward the tallest stereocillium. This positive deflection leads to opening of the cation-selective mechanotransduction channels (Kawashima et al., 2011; Pan et al., 2013) at the tip of the stereocilia (Beurg et al., 2009; Denk et al., 1995), allowing Ca^{2+} ions to flow into the cell. Depolarization of IHCs leads to graded receptor potential changes that result in activation of the voltage gated L-type calcium channels (Ca_v 1.3) near the basolateral membrane (Brandt et al., 2003; Platzer et al., 2000). Ca^{2+} influx triggers the release of neurotransmitter, glutamate, via exocytosis (Glowatzki and Fuchs, 2002; Khimich et al., 2005) from the ribbon synapse (Sobkowicz et al., 1982). Glutamate binds to the α-amino-3-hydroxy-5-methyl-4-isoxazolepropionic acid (AMPA) receptors (GluR 2/3 and 4) (Matsubara et al., 1996; Niedzielski and Wenthold, 1995; Ruel et al., 1999) in the afferent boutons of spiral ganglion neurons (SGNs) (Glowatzki and Fuchs, 2002). The

resulting neural impulse in the periphery is relayed to the cochlear nucleus, via the auditory nerve (8^{th} nerve) formed by the central axons of SGNs. Upon entering the brainstem, central axons of SGNs bifurcates into projections to dorsal cochlear nucleus (DCN) to form the efferent system, and ascending projections to anteroventral cochlear nucleus (AVCN) (Fekete et al., 1984). The bilateral projections from AVCN ascend to various locations of auditory brainstems that are important in sound localization, including the lateral superior olive (LSO), medial superior olive (MSO), and the medial nucleus of trapezoid body (MNTB). The information from the auditory brainstem nuclei is then relayed to the inferior colliculus and the medial geniculate nucleus in the thalamus, and finally to the primary auditory cortex in the brain (Sanes and Walsh, 1998).

Spiral Ganglion Neurons (SGNs)

Spiral ganglion neurons (SGNs) are the primary afferent neurons in the auditory system. SGNs are bipolar cells whose peripheral fibers contact the hair cells in the organ of Corti, while their central axons form the auditory nerve and innervate the cochlear nucleus in the brainstem (**Fig 1-1**). The cell bodies of the SGNs are encapsulated within the Rosenthal's canal (**Fig 1-1*A*)**, which is a bony channel found near the modiolus and it is thought to provide additional layer of protection for these neurons.

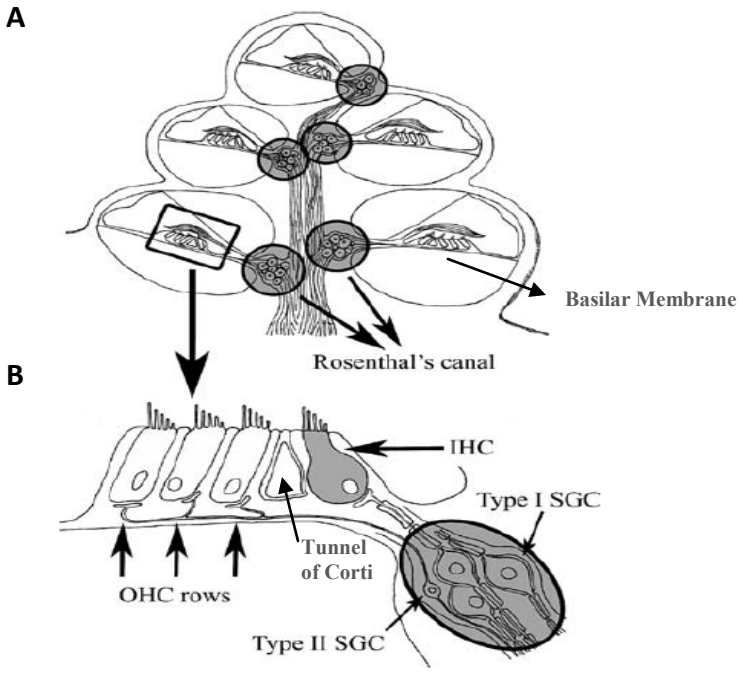

Figure 1-1. **Schematic view of the cochlea and spiral ganglion neurons (SGNs).** ***A,*** Sagital view of the cochlea. The rectangular box indicates the organ of Corti. The soma of SGNs resides within the Rosenthal's canal, close to the cochlea modiolus (axis). ***B,*** Overview of innervation pattern and morphology of Type I and Type II SGNs. Adapted from Rusznák & Szűcs (2009), with permission from Springer.

SGNs can be categorized into type I and type II neurons based on their somatic morphology, abundance, and peripheral innervation pattern (Kiang et al., 1984; Spoendlin, 1973) (**Fig. 1-1*A, B***). Type I neurons, which constitute 90-95 % of the entire SGN population, innervate the IHCs and are responsible for precise sound information transfer between the IHCs and the central auditory neurons (Kiang 1982; Liberman, 1980; 1982; Spoendlin, 1969). Type I neurons are highly myelinated (Romand and Romand, 1987). The myelin sheath tightly covers the fibers and loosely wraps around the soma, ensuring high velocity signal conduction from IHCs to the central pathway. In general,

type I neurons have larger soma size compared to type II neurons, although some variability exists (Rusznák and Szűcs, 2009).

Type II neurons, which comprise the remaining ~5 % of SGNs, on the other hand, innervate the OHCs (Kiang et al., 1982; Perkins and Morest, 1975; Spoendlin, 1969). Unlike type I neuron peripheral fibers that extend in radial direction, the outer spiral fibers of type II neurons pass the tunnel of Corti (**Fig. 1-1*B***) and turn towards the base of the cochlea, spanning hundreds of microns and forming multiple contacts with OHCs (Liberman and Simmons, 1985). Type II neurons are unmyelinated and have relatively smaller soma size than type I neurons (Berglund and Ryugo, 1987; Perkins and Morest, 1975; Romand and Romand, 1987), however, their functions have not been well understood.

In contrast to type I SGNs, whose function as cochlear primary afferent is well established, the functional studies of type II SGNs have been hampered by its scarcity in the number and its thin peripheral fibers (0.5 μm, Liberman, 1980), which make physiological recordings of these cells virtually difficult. As a result, their specific function and physiology have remained largely elusive, despite the efforts (Robertson et al, 1999). The few existing single unit recordings data suggested a role in loud sound processing (Brown, 1984; Robertson, 1984), but it was not until very recently, a more definitive function of type II SGNs started to unveil (Reid et al., 2004; Weisz et al., 2009; 2012). With the use of *in-vitro* whole-cell tight-seal technique, recent findings from rat type II SGN afferent fibers revealed that these cells have high threshold (–25mV) for action potential firing and require summation of EPSPs from multiple OHCs to fire one single action potential (Weisz et al., 2014), indicating that type II SGNs are very difficult

to excite by acoustic sound. These findings conform to the previously held view in the field, that type II SGNs may not be involved directly in afferent signaling as type I SGNs. Rather, considering their unmyelinated peripheral processes and multiple OHCs innervation pattern, it is plausible that these cells have a modulatory function, either through the efferent system (Ginzberg and Morest, 1984; Liberman and Brown, 1986) or local OHC circuitry, regulating auditory signal output, especially those for extremely loud sound. While the aforementioned statement is purely speculative, the functional significance of type II cells in auditory processing still awaits for a conclusive answer. In the context of this thesis, thus, SGNs will only refer to the type I neurons, unless specified otherwise.

Function of SGNs in Auditory Signal Processing

As the primary auditory afferent in the cochlea, SGNs transmit signals from hair cells to the brain in a manner that preserves the frequency, intensity, and temporal aspects of sound information. This faithful signal transmission between the hair cells and the SGNs is critical for normal auditory function and sound localization.

One of the most important and fundamental tasks in auditory signal processing is decomposing complex sound signals into its constituent frequencies as evidenced by tonotopic specialization of the IHCs. This arise in part due to basilar membrane (**Fig. 1-1A**) structural mechanics (von Békésy, 1970), in which the systematic variation of membrane stiffness and width along the cochlear length provides the membrane to act as a *spectral decomposer* (Hudspeth, 1985), such that the traveling wave will vibrate with

greatest amplitude only the parts of the membrane that correspond to its frequency. As a result, IHCs located in the basal part of the cochlea encode high frequency sound, and those located in the apical region encode low frequency sound. This tonotopic specialization is retained throughout the auditory pathway at each level as frequency maps (**Fig. 1-2**), including the SGNs, where the auditory neurons are topographically organized to reflect the tonotopic arrangement of IHCs at the surface of the cochlear sensory epithelium (Rubel and Fritzsch, 2002), reinforcing the importance of frequency specific coding in auditory processing.

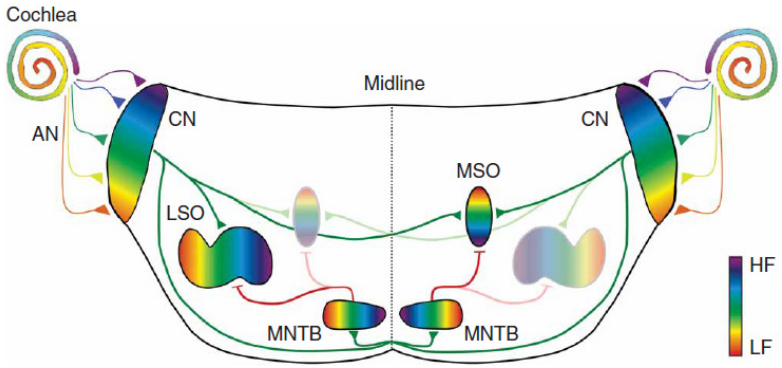

Figure 1-2. **Tonotopic arrangement of mammalian auditory system.** Note that the topographic arrangement of auditory brainstem neurons reflects the tonotopic specialization in the cochlea. AN: Auditory Nerve; CN: Cochlear Nucleus; LSO: Lateral Superior Olive; MSO: Medial Superior Olive; MNTB: Medial Nucleus of Trapezoid Body; HF: High Frequency; LF: Low Frequency. Reproduced from Kandler et al. (2009), with permission from Nature Publishing Group.

SGNs incorporate distinct morphological and signature electrophysiological features to resolve precision in the aforementioned frequency specific signal processing between the IHCs and the central auditory pathway. In mature auditory system, SGNs innervate IHCs in a one to one ratio, while each individual IHC is innervated by groups

of 20 to 40 SGNs (Lieberman, 1980; Spoendlin, 1969). This unique IHC-SGN innervation pattern ensures that the activity of SGNs is strictly dependent on the activity of presynaptic counterpart. Furthermore, the contact between SGN and IHC is made via ribbon synapse (Sobkowicz et al. 1982), an unusual synaptic specialization that is morphologically and physiologically distinct from conventional synapse, enabling fast and reliable signal transmission in SGNs in response to graded changes in IHCs receptor potentials (Buran et al., 2010; Khimich et al., 2005).

Not only in the periphery, but also the central projections of SGNs show morphological features that reflects the cochlear tonotopic specialization, in which SGN soma size and central fiber length are graded along the cochlear axis. That is, SGNs with larger soma size and shorter central fibers are found in the base, and those with smaller soma size and longer central axons are clustered in the apex of the cochlea (Echteler and Nofsinger, 2000; Liberman and Oliver, 1984). Considering the cable theory for action potential (AP) conduction, where conduction velocity is inversely proportional to length, this systematic variation of SGN central axon length makes sense, as SGNs innervating high frequency region (cochlear base) will conduct their impulses faster to their central target, while those innervating low frequency region (cochlear apex) will conduct their impulses slower, thus arriving with a delay. In the context of cable theory, however; the fact that cells with larger soma are found in the base is quite contradicting, as the increased membrane surface will decrease the membrane capacitance - the cells ability to charge the membrane-, thus slowing signal conduction velocity. While this issue has been examined elsewhere (Hossain et al., 2005; Robertson, 1976), from energy expenditure stand point, the large soma in the base is quite intuitive. That is, to sustain

the demand of high frequency firing in the base, more organelles that generate energy are needed, therefore larger soma size.

Complementing the morphological specializations, SGNs have intrinsic firing properties that mirror cochlear frequency tuning by graded expression of voltage-gated ion channels along the cochlear partition (Adamson et al., 2002; Mo and Davis, 1997; Mo et al., 2002). Electrophysiological recordings from *in-vitro* postnatal mouse SGN culture have shown that apical SGNs fire slowly accommodating action potentials with delay in AP latency, slow onset kinetics, longer AP duration, whereas those from the base fire sharp, phasic action potentials with shortened AP latency, fast onset kinetics, and shorter AP durations in response to membrane depolarization (Adamson et al., 2002). These differences in firing properties based on cochlear location are, in part, attributed to the graded expression of voltage-gated K^+ and Ca^{2+}channels in SGN cell bodies. Immunolocalization and pharmacological studies indicate K_v 1.1, K_v 3.1 and large conductance Ca^{2+} activated K^+ (BK) channels, which contributes to fast firing features, are highly expressed in the basal SGN neurons, whereas K_v 4.2, a subunit that contributes to prolonged AP duration, is mainly expressed in the apical neurons (Chen and Davis 2006; Mo et al., 2002). In addition, SGNs express voltage gated Ca^{2+} channels (Chen et al., 2011; Lv et al., 2012) with predominant expression in the base.

Not all channels expressed in SGN; however, show clear graded expressions. SGN express cohort of various voltage-gated channel (Na^+, Ca^{2+}, and K^+) subtypes (Hossain et al., 2005; Lv et al., 2011; Wang et al., 2013) and other channels, such as ionotropic P2X receptors that are activated by ATP, G-protein–coupled receptors (GPCR), and non-specific cation channels (Dulon et al., 2006), all of which together

thought to contribute to enhanced signal transmission between the IHCs and the higher order auditory neurons. To better understand how each of these channels shapes the complex firing feature of the SGNs, thorough and systematic physiological analyses of SGN conductances are needed.

Significance of SGNs in Auditory Signal Processing

As its bipolar morphology suggests, SGNs are the entry point and the sole bridge that relays the auditory information from the IHCs to higher auditory neurons in the auditory pathway. In mammals, sound energy is amplified and transduced by the hair cells, and the resulting neuronal impulses are carried rapidly to the central nervous system by the function of SGNs. In other words, SGNs are the sensory-neural interface in the auditory system, a critical junction between the electric elements of sound and its neural representation in the brain, together which brings the *perception* of sound. Without SGNs, there will be an instant disconnect between the physical world of sound and its perception, and the consequence of hindered hearing can be quite detrimental. Hence, the importance of SGNs in auditory processing is never questionable.

Given the importance of SGNs in auditory signal processing, this thesis seeks to understand SGN function by examining the firing properties of SGNs using various apporaches. This thesis is a journey from cell to system, and a survey of SGN function as a whole.

Chapter II. Spontaneous Activity in SGNs: Functional Significance and its Origin in SGNs - Past, Present, and Future

It is well established that the SGNs convey signals from the hair cells to the brain in a manner that preserves the frequency and temporal aspects of sound information. Considerable insights and attention have been given to the "sensory-driven", high-fidelity information transfer between the hair cells and the SGNs; however, less is known about the "sensory-independent", spontaneous neural activity that have been documented in SGNs and ascending auditory neurons in various species before the onset of hearing. Previous studies suggest that the spontaneous activity in the developing auditory system contributes to SGN survival, refinement of IHC-SGN synaptic contact, and preservation of the tonotopic maps in the central auditory pathway. However, the exact mechanism that drives this spontaneous activity and its function in SGNs is still debatable. This chapter, thus, attempts to carefully dissect the functional significance and mechanisms of the spontaneous activity in the developing auditory system at the level of SGNs. Together, this information will be of particular interest, as it will provide a better understanding of signal processing in early postnatal SGNs and functional development of the auditory system in general.

I. Spontaneous Activity in the Developing Auditory System

Our ability to perceive sound relies on the highly ordered, topographically arranged neural connections in the auditory system, which is assembled during development. At the periphery, afferent dendrites of spiral ganglion neurons (SGNs) invade the cochlear sensory epithelium very early during embryonic development as soon as the inner hair cells (IHCs) are differentiated (Sher, 1971). Initially, the afferent fibers

make multiple contacts with the IHCs (Perkins and Morest, 1975). Similarly, the central auditory projections also establish their topographic arrangement during embryonic stage before the formation of functional synapses, indicating that early neural circuit formation is initiated by an intrinsic genetic mechanism (Kandler et al., 2009). This initial auditory network undergoes substantial refinement during postnatal development. That is, during this stage, SGNs undergo extensive pruning processes to achieve the mature configuration, in which one SGN contacts one IHC. At the same time, the central projections undergo structural and functional maturation necessary for complex sound signal processing (Cant, 1998).

From a traditional view, general neural circuit development involves two phases: activity-independent and activity-dependent processes (Feller, 1999; Friauf and Lohmann, 1999; Moody, 1998). In activity-independent process, which occurs early in embryonic development, cells acquire their distinct phenotype, migrate to appropriate location, and establish immature early networks, where the wiring is still crude and coarse. This early phase involves expression of genes and molecular guidance markers and depends heavily on preprogramed, intrinsic, genetic mechanisms that do not require neural activity. On the contrary, in the activity-dependent process, which occurs normally later in the development, the immature neural networks undergo extensive refinement to establish intricately connected mature neural system. Although these activity-independent and activity-dependent processes seem to be occurring independently, both processes work in a cooperative manner (Friauf and Lohmann, 1999). That is, both processes are critical and neither one of them can go missing; otherwise the neural development will be incomplete.

A great amount of research has concentrated on the sensory-evoked neural activity and its role on postnatal neural refinement, and thus the general consensus was that the sensory experience-driven neural activity has the most critical role in fine-tuning the immature auditory neural circuits to a mature form. In the auditory system, the sensory-experience dependent refinement of the tonotopic map is a well established phenomenon (Kandler et al., 2009; Rubel and Fritzsch, 2002). When mammals are deprived of auditory stimuli during early postnatal development, it results in abnormal tonotopic map representation in the central auditor pathway (Leake et al., 2006; Zhang et al., 2002). For example, exposure of neonatal mice to repetitive white noise during early postnatal development leads to degradation of tonotopic map in the auditory cortex (Zhang et al., 2002), indicating that sensory-driven neural activity during development has a crucial role for tonotopic map refinement in the central auditory pathway.

However, the traditional view which emphasizes the role of sensory-driven neural activity in auditory neural refinement is being revised by several studies that report the existence of spontaneous neural activity in SGNs and auditory brainstem neurons (Jones and Jones, 2000; Jones et al., 2001; Jones et al., 2007; Lippe, 1994; 1995). At birth, the auditory systems of many altricial animals are very immature and do not respond to airborne sound. Therefore, the existence of spontaneous activity in these animals before the onset of hearing indicates that this neural activity may have a developmental function since the system is not capable of transducing sound-driven information at this stage. Considering that the auditory system undergoes extensive morphological and functional changes before the onset of hearing, it is thought that the spontaneous activity during this period maybe involved in auditory neural development.

Characteristics of Spontaneous Activity before the Onset of Hearing

Hearing onset, in general, refers to the time period in which subjects become responsive to airborne sound or external stimuli. The onset of hearing can be measured by compound action potential recordings in afferent neurons or by behavioral testing (Goodyear et al., 2006). In altricial animals, hearing onset occurs early in development but the exact timing differs slightly between species: [mice and rats: postnatal day (P) 10-12 (Romand, 1983), gerbils: P12 (Romand, 1983), cats: P6 (Moore, 1982), chickens: embryonic day (E) 19 (Saunders, 1973)]. In the context of this thesis, spontaneous activity before the hearing onset refers to neural responses that are autonomous in nature and generated by intrinsic mechanisms that are not driven by inputs from external stimuli.

Spontaneous activity has been found in SGNs and auditory brainstem neurons of mammals and birds, before the onset of hearing (chicken: Jones and Jones, 2000; Jones et al., 2001; Lippe, 1994; 1995; cats: Jones et al., 2007; Tammar Wallabi: Gummer and Mark, 1994). The spontaneous activity found in these prehearing animals share a common feature which consists of rhythmic burst firing followed by a period of quiescence where neurons become "silent" or have a reduced discharge activity (**Fig. 2-1**). This prototypic, patterned, neural discharge indicates that this is not simply an "immature" form of spontaneous activity seen in mature animals.

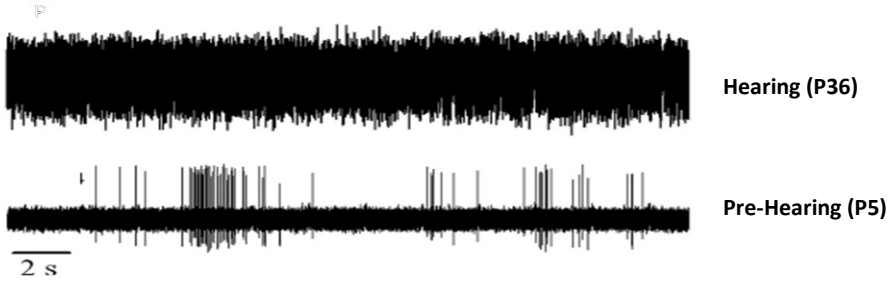

Figure 2-1. **Spontaneous activity in mature and pre-hearing SGNs of postnatal kittens.** Top trace reflects the high frequency, stochastic discharge pattern seen in mature SGNs (Discharge rate: 88 Hz). Bottom trace reflects the prototypical spontaneous discharge pattern seen in SGNs before the onset of hearing. Note the low frequency, rhythmic burst firing that is followed by a long period of "silence" (Discharge rate: 1.8Hz, Bursting: 4.1 bursts/min). Spontaneous activity was obtained using *in-vivo* multi-electrode recordings. Reproduced from Jones et al. (2007), with permission from the American Physiological Society.

It has been shown that the mature auditory nerves also discharge spontaneously in the absence of sound (Romand, 1984; Walsh and McGee, 1987). The spontaneous activity in the mature auditory system is a consequence of tonic release of neurotransmitters from the hair cells. At rest, about 10-15 % of mechano-transduction channels are open (Denk et al., 1995) and the resulting depolarizing current puts the hair cell resting membrane potential in a range that is sufficient to evoke basal transmitter release (Brandt et al., 2005; Farris et al., 2006), thereby driving spontaneous activity in mature auditory nerves. It is thought that this thermally driven, stochastic, random, spontaneous activity in mature auditory nerves allows for low-frequency sound information processing by increasing the sensitivity range of the auditory nerves.

The firing pattern of spontaneous activity in developing animals is fundamentally different from that of mature counterparts, suggesting a difference in function. First, the

spontaneous activity in the developing auditory system has a very low average discharge rate. In all species examined, the discharge patterns of SGNs and auditory brainstem neurons are unimodal, where the distribution of discharge is complete opposite between the prehearing and mature animals. That is, in prehearing auditory neurons, the distribution of discharge rate is skewed towards the lower end (< 10 Hz) while in the mature counterparts the discharge rate is distributed towards the higher end (**Fig. 2-2**). For example, multi-electrode recordings from SGNs of prehearing neonatal cat (P3-9) showed spontaneous activity with a mean discharge rate of 3.1 ± 8.2 Hz (Jones et al., 2007). Similar low discharge rate has also been shown in cochlear ganglion cells of embryonic chick (E13-17), where the mean discharge rate was 4.2 ± 5.0 Hz (Jones and Jones, 2000). The discharge rate increased gradually as the animals reached the onset of hearing; however, the overall discharge rate stayed relatively low, ranging below 10 Hz. In contrast, in mature animals, SGNs and auditory brainstem neurons discharge spontaneously at a rate up to 100Hz (Jones and Jones, 2000; Jones et al., 2001; Müller, 1996; Walsh and McGee, 1978).

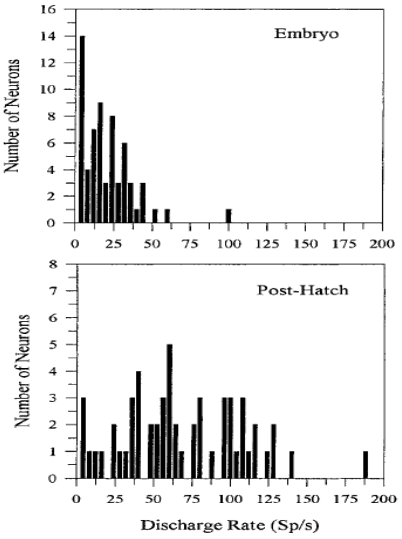

Figure 2-2. **Distribution of afferent discharge rate between embryonic (pre-hearing) and post-hatch (post-hearing) chicks.** Note that the discharge rate of embryonic chicks is skewed toward the lower end, whereas the discharge rate of post-hatch chicks is distributed towards the higher end (n =120). Reproduced from Jones and Jones (2000), with permission from American Physiological Society.

Second, the spontaneous activity in the developing auditory system occurs in rhythmic bursts. The duration of quiet period (i.e., inter-burst interval) differ across species, normally ranging from several milliseconds (ms) to seconds (sec) (Jones and Jones, 2000; Jones et al., 2001; 2007; Lippe, 1994; 1995). As an example, Jones et al. (2007) showed that SGNs in prehearing kittens (P3-9) discharge in rhythmic bursts (4.3 burst/min) with a mean inter-burst interval of 2.7 sec. This stereotypical firing pattern was not evident in the adult SGNs, indicating that the rhythmic burst firing is a feature that is only present before the onset of hearing. Multi-electrode recordings from embryonic chick nucleus magnocellularis (NM, mammalian equivalent of AVCN) and nucleus laminaris (NL, mammalian equivalent of MSO) also support this view, where the inter-burst interval gradually decreased as a function of age (Lippe et al., 1994; 1995). For instance, the mean inter-burst interval of spontaneous activity in preharing chick embryo decreased from 4.9 sec at E14-15 to 2.1 sec at E18, one day prior to onset of hearing. The burst firing was almost non-existent in NM and NL after the onset of hearing (Lippe, 1994).

One valid concern for spontaneous activity observed in the developing auditory system is whether the observed low discharge pattern is an artifact or random discharge resulting from background sounds or physiological response such as heart beat or respiration. The disputing argument against this notion is that, in general, the immature auditory system has a high threshold to sound (Jones et al., 2007; Saunders et al., 1973); therefore it is unlikely that the ambient sound would elicit neural responses in these animals. Second, the heart rate and respiration rate of prehearing animals are normally faster than the spontaneous discharge rate (Lippe, 1994). However, some reports showed

instances where cardiac and respiratory cycles were overlapping with spontaneous firing (Jones and Jones, 2000; Jones et al., 2007). In such case, the investigators noted specifically that those data were not considered for analysis to eliminate possible confounding factors.

Mechanistic concerns regarding the use of multi-electrode recording technique has also been brought to attention. Multi-electrode recording is widely used for *in-vivo* spontaneous activity recordings in the developing auditory system. Multi-electrode recording is performed on anesthetized live animals, and some researchers have questioned whether the use of barbiturate anesthetics (i.e., ketamin, sodium pentobarbital) has any effect on suppressing the spontaneous discharge in immature animals (Rübsamen and Lippe, 1998). However, recent experiment by Jones et al. (2007), which used non-barbiturate general anesthetic, isofluarane, in neonatal kittens, showed spontaneous discharge pattern similar to those obtained using barbiturates (Romand, 1984; Walsh and McGee, 1978), indicating that low spontaneous discharge rate in prehearing animals is an intrinsic phenomenon and is not confounded by experimental approach.

As shown, the prevalence of patterned spontaneous activity in the auditory system before the onset of hearing in many species suggests a fundamental feature of the developing auditory system. Slight differences in discharge rates and burst firing interval rates exist depending on the species examined and the location along the auditory neuraxis; however, the robustness and the stability of the patterned spontaneous activity that persists during the span of prehearing stage implies a functional significance.

A Fundamental Feature of Developing Neural Circuits

From a neurobiological stand point, the finding that the spontaneous neural impulses seen in the immature auditory system has a prototypical pattern that is only present during development raises the possibility that the slow periodicity of spontaneous activity must be carrying some sort of information to the developing system before it transits into a mature system.

Besides the auditory system, spontaneous activity has been found in many developing neural circuits, including the hippocampus, the spinal cord, and the visual system (Feller, 1999). Although the specific function of the spontaneous activity is different in each neural circuit, it shares one common theme, which is neural circuit development. For instance, spontaneous activity in the hippocampus has a role in hippocampal neuronal circuit development (Hanse et al., 1997), whereas in the spinal cord it is involved in motor axon path finding (Hanson and Landmesser, 2004). Spontaneous activity is also observed in the visual system, where it has a role in visual pathway refinement (Galli and Maffei, 1988; Meister et al., 1991; Wong et al., 1993).

The spontaneous activity in various developing neural circuits has a common activity pattern, which is similar to what is found in the developing auditory system. That is, the spontaneous activity consists of rhythmic bursts of action potentials with long inter-burst periods ranging from several hundred milliseconds to seconds (Feller, 1999).

Although numerous studies have indicated that spontaneous activity is important for neural circuit development (Blankenship and Feller, 2010; Moody and Bosma, 2005), to date the precise mechanism of spontaneous activity in developing neural circuits are

not well understood. Likewise, the function and the underlying mechanism of spontaneous activity in the developing auditory system are poorly understood.

II. Role of Spontaneous Activity

Survival and Maintenance of Auditory Neurons

Spontaneous activities observed in SGNs and auditory brainstem neurons of prehearing animals are thought to have a role in survival and maintenance of auditory neural connections. This proposed function mostly comes from cochlear removal or cochlear afferent denervation studies in prehearing animals (Parks, 1997; Russel and Moore, 1995). In embryonic chicks, when the otocyst is removed in early embryonic age (E3), the nucleus magnocellularis (NM) and nucleus laminaris (NL) display abnormal morphology and aberrant projections (Parks, 1997). In a separate study, Parks (1979) also found substantial loss of NM neurons following otocyst ablation in embryonic chicks. Because otocyst ablation completely eliminates neural activity from the cochlea, these findings indicate that cochlear input during development is important for auditory neuron survival.

More direct evidence that spontaneous activity has a role in neural survival and maintenance comes from findings in mammals, in which auditory brainstem neuronal loss is observed following cochlear ablation during the first two postnatal weeks, when spontaneous activity is most prominent in the auditory system (Hashisaki and Rubel, 1989; Mostafapour et al., 2000; Russel and Moore, 1995; Tierney et al., 1997). In gerbils, unilateral cochlear ablation during the prehearing period (P3) resulted in substantial loss

of cochlear nucleus neurons compared to the intact side. However, deafferentation-induced neuronal loss was less severe when the ablation was made right before or after the onset of hearing (Mostafapour et al., 2000; Tierney et al., 1997). These findings, therefore, raised the possibility that spontaneous activity may have a critical role in survival and maintenance of auditory neurons.

Although these cochlear ablation studies provide evidence for the importance of cochlear input during early development, it is difficult to attribute the result as a direct consequence of the absence of spontaneous activity in the system. Since cochlea ablation can cause other abnormal physiological responses resulting from deafferentation, a better experimental approach that can directly pin point the effects of spontaneous activity in neuronal development is strongly needed.

Refinement of Tonotopic Maps in Central Auditory Pathway

In the mature auditory system, tonotopy is preserved from the cochlear sensory epithelium to the auditory cortex in the brain. That is, the frequency arrangement in the cochlea is systemically retained throughout central auditory projections via the precise topographic neural connections at each level along the neuraxis.

Recent studies indicate that the initial tonotopic map that is established during embryonic development undergoes substantial refinement before the onset of hearing, after which functional synapses have formed. The most compelling evidence for tonotopic maps refinement in the auditory brainstem and its possible connection to spontaneous activity is provided by studies utilizing deafness mutant (dn/dn) mice with nonfunctional hair cell, where aberrant synaptic strength and disruption of tonotopic

maps were found in the auditory brainstem neurons as a result of complete lack of spontaneous activity during development (Leo et al., 2006; McCay and Oleskevich 2007).

The cochlear nucleus is the primary auditory brainstem nucleus, wherein the topographically arranged projections formed by the auditory nerves serve the basis for formation of tonotopy in the successive auditory brainstem nuclei, including medial superior olive (MSO), medial nucleus of trapezoid body (MNTB), and lateral superior olive (LSO) (**Fig. 2-3**). Thus, change in synaptic strength in endbulb of Held synapse in the AVCN of dn/dn mice due to the lack of spontaneous activity (McCay and Oleskevich, 2007) could interfere with tonotopic arrangement of ascending auditory neurons, not only in the cochlear nucleus, but also in other brainstem nuclei involved in central auditory processing. As postulated, Leao et al. (2006) demonstrated that the normal gradient of voltage-dependent channel expression, which underlies the topographic arrangement of neurons in MNTB, is lost in these dn/dn mice, indicating that spontaneous activity before the onset of hearing plays an important role in tonotopic maps refinement in central pathway by regulating neuronal membrane properties and voltage-gated channel expression patterns.

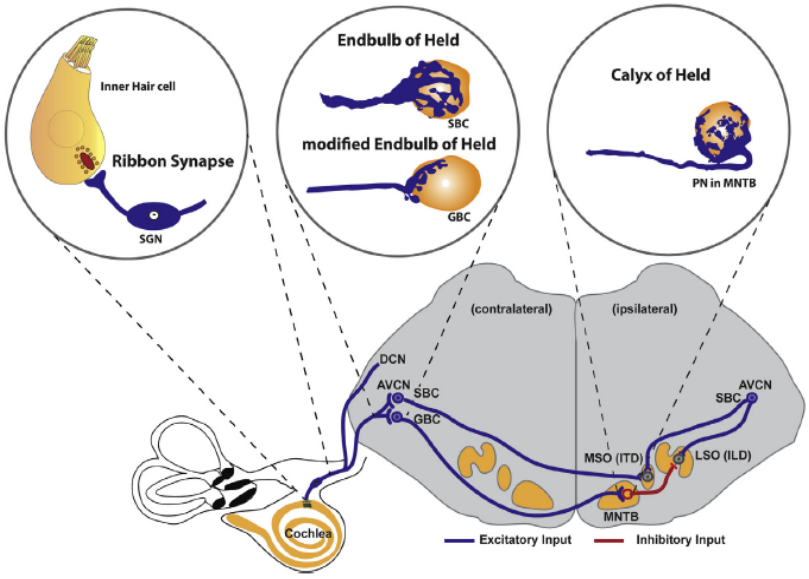

Figure 2-3. **Overview of auditory signal processing along the auditory pathway.** SGN receives input from IHCs via ribbon synapse. The signal is then ascended to the anteroventral cochlear nucleus (AVCN) in the cochlear nucleus and elaborate on Endbulb of Held synapse, an unusually large globular synapse specialized for high frequency signal transmission via AMPA-mediated transmission. Endbulb of Held synapse makes contact on either spherical bushy cells (SBC) or globular bushy cells (GBC). SBC projects bilaterally to medial superior olive (MSO), which is responsible for intraoral time difference (ITD), and GBC sends contralateral projections to medial nucleus of trapezoid body (MNTB) and elaborates on Calyx of Held, which provide inhibitory input to lateral superior olive (LSO) to compute interaural level difference (ILD). DCN: Dorsal Cochlear Nucleus. Reproduced from Yu and Goodrich (2014), with permission from Elsevier.

III. Origin of Spontaneous Activity

General Mechanism of Spontaneous Activity

In order to understand the functional significance of spontaneous activity in the developing auditory system before the onset of hearing, it is critical to study its underlying mechanism. The mechanism by which the spontaneous activity is generated differs in each system, but the general mechanism is largely similar. According to

Blankenship and Feller (2010), the mechanism for spontaneous activity can be summarized as following: In most systems, spontaneous activity is generated by an excitatory network that drives the depolarization across large number of cells, thereby eliciting correlated spontaneous activity. This excitatory network, which controls the periodicity of the spontaneous activity, is transient, only existing during a specific time frame within development. An interesting feature of spontaneous activity in many systems is that it involves a homeostatic mechanism, in which the system ensures that an alternative network is available to drive the spontaneous activity in case of main component failure.

Cochlear-Originated Spontaneous Activity

The fact that patterned spontaneous activity is found in SGNs and subsequent ascending auditory pathway before the onset of hearing suggests that an intrinsic mechanism must be present to drive this activity. However, it is unclear whether this spontaneous activity in SGNs has an intrinsic neural- , or a cochlear-origin.

Earlier evidence suggests that the spontaneous activity in the immature auditory system has a cochlear origin. One of the most compelling lines of evidence for this notion comes from multi-electrode recordings of auditory brainstem neurons of chick embryos (Lippe, 1994; 1995). Lippe (1994) showed that the spontaneous rhythmic discharge in the cochlear nucleus of prehearing embryonic chicks (E14-18) was abolished by application of the sodium channel blocker tetrodotoxin (TTX) to the oval window or removal of the basilar papilla. No change in spontaneous activity was detected following tympanic membrane puncture or columella (chick middle ear bone) removal, indicating

that the spontaneous activity was not resulting from background sound or contraction of the middle ear muscle. Thus, the elimination of spontaneous activity in auditory brainstem neurons following TTX application or cochlear removal strongly demonstrates that the origin of spontaneous activity lies within the cochlear epithelium. Extracellular recordings from ventral cochlear nucleus of prehearing gerbils also supports this view, in which spontaneous discharge is often preceded by prepotentials (Rübsamen and Lippe, 1998). The presence of prepotentials suggests that the spontaneous action potentials are initiated by synaptic activities that most likely originate within the cochlea.

Contribution of Inner Hair Cells (IHCs)

Given that spontaneous activity in developing spiral ganglion neurons (SGNs) and auditory brainstem neurons (Gummer and Mark, 1994; Jones and Jones 2000; Jones et al., 2001; 2006; 2007) has a cochlear origin (Lippe, 1994; 1995); it is plausible that IHCs can provide a mechanism for spontaneous activity in the developing auditory system.

Extensive work by Kros and colleagues has shown that the immature IHCs are able to generate spontaneous recurrent action potentials before the onset of hearing (Kros et al., 1998; Marcotti et al., 2003a; 2003b) (**Fig. 2-4, 2-5**). Whole cell current clamp recordings from immature mouse IHCs (E18-P6) showed spontaneous recurrent Ca^{2+} spikes in response to small depolarizing current injections (Marcotti et al., 2003a). The spontaneous recurrent spiking activity is lost during the second postnatal week as mature IHCs shows graded voltage response to depolarizing current injections (Kros et al., 1998) (**Fig. 2-5**). Similar findings have been also shown in chick hair cells during early

development (E12-15), in which recurrent action potentials can be generated upon current injections (Fuchs and Sokolowski, 1990).

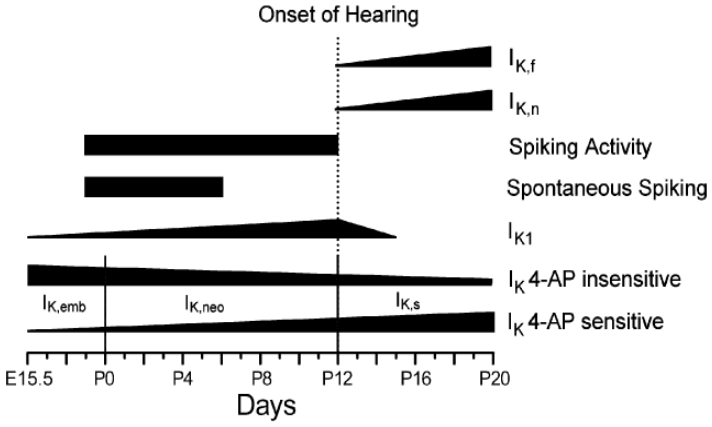

Figure 2-4. **Expression pattern of potassium currents in IHCs during development.** Note that the recurrent spontaneous activity in immature IHCs ceases at P7, before the expression of $I_{K,f}$. Reproduced from Marcotti et al. (2003a), with permission from John Wiley and Sons.

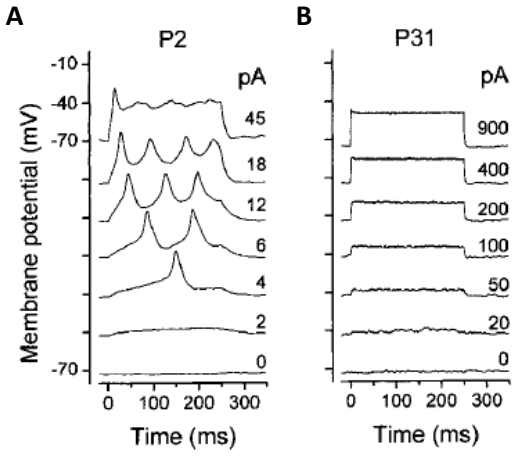

Figure 2-5. **Voltage responses of immature and mature IHCs to depolarizing current injections.** ***A,*** Small depolarizing current injections elicited slow and broad recurrent spiking activity in immature IHCs. ***B,*** Mature IHCs no longer showed recurrent spiking activity in response to depolarizing current injections. Note the rapid graded voltage response in mature IHC. Reproduced from Kros et al. (1998), with permission from Nature Publishing Group.

There are two reasons why spontaneous recurrent spiking activity in IHCs could provide the source for spontaneous activity in the developing SGNs and central auditory neurons. First, the recurrent spiking activity in IHCs is a transient phenomenon, existing only during the first two postnatal weeks and is lost after the onset of hearing (Kros et al., 1998). This developmental timeline of spontaneous recurrent spiking activity in IHCs coincides with the time when spontaneous activity is seen in the SGNs (Jones et al., 2007).

Second, the relatively broad and slow recurrent action potentials seen in IHCs have a very low discharge rate similar to that of developing SGNs neurons which in average fire at a rate smaller than 10 Hz. For example, Kros et al. (1998) showed that immature IHCs (P0-11) can generate spontaneous recurrent spikes at about 2-4 Hz. Similarly, SGNs of prehearing kitten discharge at a rate of 3.1 Hz (Jones et al., 2007). The similarity in discharge rate does not justify IHCs as the source for SGN spontaneous activity until it can be experimentally proven by simultaneous *in-vivo* or *ex-vivo* recordings. However, this comparison is worth noting, as it provides the ground for the possible link that exists between the IHCs and SGNs.

In order for the immature IHCs to transmit spontaneous recurrent action potentials to the ascending auditory pathway, functional synapse must be present between IHCs and SGNs to relay the signal. Previous morphological studies have shown that IHCs are equipped with synaptic machineries at birth. Synaptic contact between IHCs and afferent fibers are observed in early embryonic development (E18) (Sher, 1971), and multiple synaptic ribbons (active zone) are found at birth (Sobcowicz et al., 1982). Near birth,

IHC and SGN acquire almost adult- like innervation patterns, although at this stage the complete one to one relationship between IHC and SGN is not established (Echteler, 1992). Additionally, in situ-mRNA studies indicate that glutamate receptors are expressed on SGN afferent dendrites before birth (Luo et al., 1995). Even though the morphology and the innervation patterns are not as precise as the mature form, the presence of the synaptic machinery suggests that the IHCs are competent for synaptic transmission before the onset of hearing.

The functionality of the IHC-SGN synapse has been confirmed recently by electrophysiological studies (Beutner & Moser, 2001; Johnson et al., 2005). Previously, Marcotti et al. (2003a) showed that IHCs can fire spontaneous recurrent action potentials as early as E17.5, but it was unknown whether this recurrent Ca^{2+} spikes could actually drive neurotransmitter release onto the afferent fibers. Johnson et al. (2005) proved that spontaneous Ca^{2+} action potentials in IHCs can drive exocytosis by showing an increase in capacitance measurement in response to Ca^{2+} action potential waveforms. Moreover, indirect evidence from Glowatkzi and Fuchs (2002) showed that the spontaneous discharge from IHCs can excite SGN afferent terminals via AMPA receptors during early postnatal development. Thus, these morphological and physiological findings indicate that immature IHCs have functional synapses at birth (P0).

The presence of functional IHC-SGN synapse and the coincidental occurrence of spontaneous activity in IHCs and SGNs suggest that spontaneous recurrent spiking activity in immature IHCs can trigger spontaneous activity in SGNs. Recent findings by Tritsch et al. (2010b) provide direct evidence that support this view. In order to confirm whether patterned spontaneous activities in the SGNs and ascending auditory brainstem

neurons are derived from the Ca^{2+} spike activity in IHCs, Tritsch and colleagues took advantage of *in-vitro* simultaneous IHC-SGN recording configuration. In this preparation, evoked depolarization of IHCs triggered Ca^{2+} spikes that coincided with burst of action potentials in synaptically connected SGNs. Similar spike patterns that resembled those in SGNs were also found in the MNTB neurons and inferior colliculus, using *in-vivo* extracellular recordings (Tritsch et al., 2010b), indicating that IHCs act as a pace-maker for patterned spontaneous activities in SGNs and the ascending auditory neurons before the onset of hearing.

Biophysical basis of IHC Recurrent Spiking

The fact that immature IHCs can trigger spontaneous activity in SGNs (Tritsch et al., 2010b) puts IHCs as a possible source for spontaneous activity generation in the developing auditory system. What is unknown, however, is whether IHCs posses the intrinsic mechanism for generating spontaneous activity.

One way to understand how slow and broad spontaneous recurrent action potentials are generated in immature IHCs is to examine the underlying biophysical mechanisms. Well before IHCs becomes fully responsive to sound, IHCs express a complement of ion channels that differ in time and duration of expression (Kros, 2007). Additionally, recent findings have shown changes in the ionic current profile in the basolateral membrane of immature IHCs during embryonic and postnatal development (Kros, et al., 1998; Marcotti et al., 1999; 2003a, 2003b). Together, these findings indicate that IHCs undergo extensive electrophysiological changes that permit recurrent

spiking activity during early development. As such, only the ionic currents pertaining to recurrent spiking activity generation will be explored below.

Spontaneous recurrent spiking activity in immature IHCs (E18-P6) is generated by the interplay between calcium (I_{Ca}) and voltage-dependent, delayed rectifier K^+ currents ($I_{K,\ neo}$) (Beutner and Moser, 2001; Marcotti et al., 2003a; 2003b). The fast inward I_{Ca}, which activates near the resting membrane potential, ensures that IHCs are sufficiently depolarized to fire action potentials, while the slow outward $I_{K,-neo}$, which activates at a more depolarized potential, ensures the repolarizing phase of action potential. Thus the interaction between I_{Ca} and $I_{k\ neo}$ leaves the membrane potential unstable, allowing spontaneous recurrent action potentials to occur. The slow activation kinetics of $I_{K,\ neo}$ is the main contributor of the slow and broad Ca^{2+} action potential waveforms seen during early development. However, at P7, the immature IHCs lose the ability to spontaneously fire recurrent action potentials while still maintaining their ability to spike in response to depolarizing current injections (Marcotti et al., 2003a) (**Fig. 2-5**). This is partly due to the increased conductance of inward rectifier potassium current (I_{K1}), which is expressed in IHCs between E15.5-P12, and a more hyperpolarized activation of outward potassium current, $I_{K,\ neo}$ (Marcotti et al., 2003a).

Spontaneous recurrent spiking activity in immature IHCs is initiated by I_{Ca}, while the contribution of I_{Na} is rather minor. This is different from other excitable cells, including neurons, where I_{Na} is essential for action potential initiation (Royeck et al., 2008; Stuart and Häusser, 1994). When immature IHCs were superfused with Ca^{2+} free external solution, the cells did not generate spontaneous action potentials, indicating I_{Ca} is essential for spontaneous action potential initiation. In the presence of tetrodotoxin (TTX),

IHCs still generated spontaneous action potentials, but the timing to reach the action potential threshold was prolonged (Marcotti et al., 2003b). This indicated that I_{Na} controls the subthreshold timing for action potential, but it is not directly involved in spontaneous action potential initiation process.

At around onset of hearing (P12), IHCs lose the ability to generate either spontaneous-, or evoked recurrent action potentials (Marcotti et al., 2003a) and this is due to the appearance of fast, Ca^{2+}-dependent, outward K^+ current, $I_{K, f}$, (Kros et al., 1998; Marcotti et al, 2003a). $I_{k,f}$ is mediated by the expression of Ca^{2+} activated K^+ (BK) channels (Kros et al., 1998; Langer et al., 2003; Marcotti et al., 2003a). The time course of $I_{K, f}$ expression correlates with cessation of spontaneous activity in SGNs (Jones et al., 2007). $I_{K, f}$, which was originally identified in guinea pig IHCs (Kros and Crawford, 1990), has fast kinetics, activates at hyperpolarized potentials, and has a larger conductance compared to $I_{K, neo}$ (Marcotti et al., 2003b). Thus, fast activating $I_{K,f}$ prevents the generation of recurrent action potential by shortening the membrane time constant (**Fig. 2-5)**. This in turn enables the cell to respond to sound with fast graded receptor potentials at the onset of hearing, which is critical for precise sound information coding (Kros and Crawford, 1990).

Role of IHC Recurrent Spiking: IHC Maturation

One of the interesting aspects of the spontaneous Ca^{2+} spiking activity in the immature IHCs is that it not only can trigger spontaneous activity in SGNs (Tritsch et al., 2010b), but also contributes to maturation of IHC itself by regulating the expression of $I_{k,f}$ (Brandt et al., 2003; Platzer, 2000).

Using mice that lack Ca_v 1.3, which is an L-type Ca^{2+} channel that mediates I_{Ca} in IHCs, Brandt et al. (2003) showed morphological abnormality and lack of $I_{K,f}$ in the IHCs. The Ca_v 1.3 knockout mice do not generate spontaneous Ca^{2+} action potentials in IHCs during development, and their absence is attributed to the failure of $I_{K,f}$ expression. The absence of $I_{K,f}$ was not due to a defect in the Ca^{2+}-activated K^+ (BK) channel gene expression. Rather, it was speculated that intracellular Ca^{2+} oscillations that result from spontaneous Ca^{2+} action potentials regulate the expression of functional BK channels to the plasma membrane of IHCs (Brandt et al., 2003). As shown, these results indicate that Ca^{2+} action potentials have a critical role in functional maturation of IHCs by expression of mature channels.

The above findings and studies from other systems (Moody and Bosma, 2005), suggest that the activity-dependent channel maturation is a widespread concept that developing systems use. In the IHCs, immature channels are expressed to elicit spontaneous recurrent spiking activity, and in turn this electrical activity regulates the expression of mature channels to meet the demands of sensory input at the onset of hearing. This paradigm seems counter intuitive at first, considering the extra metabolic cost imposed on the developing IHCs could be bypassed by direct expression of mature channels. Instead, it seems that spontaneous activity in the immature IHCs acts as check point in a positive feedback system that ensures maturation of IHC electrical activity and proper development by modulating channel properties and densities. Taken together, the tight relationship between spontaneous activity and mature channel expression in IHCs shows that IHC recurrent spiking activity has an indispensible role in IHC maturation.

Role of IHC Recurrent Spiking: IHC-SGN Synapse Refinement

Provided that immature IHCs are capable of exocytosis in response to spontaneous Ca^{2+} action potential and able to excite SGN afferent dendrites (Beutner and Moser, 2001; Glowatkzi and Fuchs, 2002; Johson et al., 2005; Tritsch et al., 2010b), it raises the possibility that spontaneous recurrent spiking in IHCs has a role in IHC-SGNs synapse refinement.

Although not directly tested, studies that observed morphological changes of IHC afferent terminals during postnatal development seem to offer an explanation. During the first postnatal week, multiple synaptic ribbons (active zone) appear in IHCs, peaking at the end of the first week (Sobcowicz et al., 1982). Afterwards the number of synaptic ribbons gradually decreases to one synaptic ribbon per IHCs (Liberman, 1980). This reduction in the number of synaptic ribbons is attributed to afferent dendrite pruning process, which occurs postnatally (Echteler et al., 1992; Simmons et al., 1991). At birth SGN afferents innervate multiple IHCs. However, by the end of the first postnatal week, a substantial reorganization occurs in SGNs' dendritic arbor, thereby establishing the mature IHC-SGN innervation pattern (Simmons et al., 1991). This afferent synaptic configuration preserves precise sound information transfer between the IHCs and SGNs.

The fact that afferent synapse maturation coincides with spontaneous recurrent Ca^{2+} spikes in IHCs suggests that the spontaneous action potentials in immature IHCs may have a critical role in afferent terminal maturation and development. In other developing systems, such in retina and hippocampus, the increase in intracellular Ca^{2+} as a result of spontaneous activity is often linked to exocytosis, gene expression, neurotrophin release, and synaptogenesis (Moody and Bosma, 2005). Extrapolating that

same principle to the auditory system, the morphological maturation seen in IHCs afferent synapse during postnatal development can be attributed as a secondary effect of increased intracellular Ca^{2+}. Thus, based on morphological studies, it is possible that the spontaneous Ca^{2+} action potentials in immature IHCs are involved in maturation of the IHC afferent synapse.

Contribution of Efferent System

According to Moody and Bosma (2005), in many developing cells, if not all, spontaneous activity is mediated by expression and optimization of appropriate sets of ion channels during early development. These ion channels generate patterned spontaneous Ca^{2+} action potentials that can be synchronized among other cells and activate appropriate developmental programs. Once the system reaches maturation, the spontaneous activity self-terminates via expression of other types of ion channels that can generate electrical signals compatible for the mature system. Consistent with this notion, immature IHCs follow a similar scenario, where the recurrent Ca^{2+} spikes are initiated by the interplay between I_{Ca} and transiently expressed $I_{K,\ neo,}$ and terminated by the expression of $I_{K,f}$ at the onset of hearing.

It has been debated whether the efferent feedback has a role in modulating the spontaneous activity in the immature IHCs (Glowatzki and Fuchs, 2000; Kros, 2007; Walsh and McGee, 1988). In mature auditory system, efferent nerve fibers that project down from the lateral superior olive (LSO) in the auditory brainstem make contact with afferent SGNs (Liberman, 1980). However, during the first postnatal week, a great number of efferent fibers make transient axosomatic contact on the basolateral membrane

of the immature IHCs (Pujol et al., 1998). This transient contact is thought to disappear after the onset of hearing (Katz et al., 2004). Because of this transient innervation pattern, it is postulated that the efferent fibers may have an effect on recurrent spontaneous activity in immature IHCs.

Previous studies show that efferent fibers, which release acetylcholine (ACh), exert inhibitory effect on immature IHCs via nicotinic acetylcholine receptors (nAChRs) that contain α9α10 subunits (Glowatzki and Fuchs, 2000; Goutman et al., 2005; Katz et al., 2004). α9α10 nAChRs are non-selective cation channels present in IHCs that exhibit high permeability to extracellular Ca^{2+} (Elgoyhen et al., 2001). Studies indicate that Ca^{2+} influx via the α9α10 nAChRs activates small conductance, Ca^{2+}- activated K^{+} (SK2) channels, whose outward potassium current hyperpolarizes immature IHCs (Glowatzki and Fuchs, 2000; Katz et al., 2004). This ACh mediated inhibitory response is most prominent during P3-14 in immature IHCs (Katz et al., 2004).

Because IHCs show maximum response to ACh during the postnatal development, it is conceivable that the efferent system plays a role in modulating recurrent spontaneous spiking in immature IHCs. Previous electrophysiological studies are in agreement with this notion. Glowatzki and Fuchs (2000) showed that when ACh is superfused to the immature IHCs (P7-13), the number of evoked Ca^{2+} action potential decreases. Similarly, when the efferent fibers are repeatedly stimulated *in-vitro*, the resulting inhibitory postsynaptic current (IPSC) inhibits the recurrent action potentials in immature rat IHCs (P7-11) (Goutman et al., 2005). Recently, Jonson et al. (2011) also reported efferent modulation via α9α10 nAChRs in early postnatal IHCs in mice, rat, and gerbil, where it had a more pronounced effect in the apical IHCs cells than in basal cells.

Therefore, it is clear that efferent system has a position-dependent modulatory effect on IHCs during development. At present, however, it is unknown to what extent efferent fibers exert inhibitory effects in the immature IHCs *in-vivo*, since the available studies so far have been solely based on *in-vitro* preparation. Thus, it would be necessary to test these questions *in-vivo*.

Contribution of Supporting Cells: Kölliker's Organ

Recently, Tritsch et al. (2007) have shown that Kölliker's organ, non-neuronal supporting cells found adjacent to the inner hair cells (IHCs), can be the source for spontaneous activity in the developing auditory system before the onset of hearing. Kölliker's organ is a transient columnar structure found in the inner sulcus, or inner supporting cells, of the developing mammalian cochlea, and spans the entire length of the organ of Corti (Hinojosa, 1977; Forsythe, 2007; Kelley, 2007) (**Fig. 2-6**). Its exact function, however; is largely unknown.

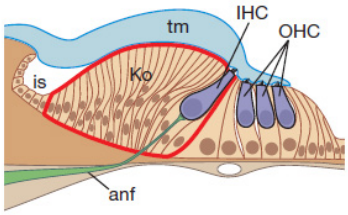

Figure 2-6. **Cross section of Kölliker's organ in rat organ of Corti.** Ko: Kölliker's organ; IHC: Inner Hair Cell; OHC: Outer Hair Cell; tm: tectorial membrane; anf: auditory nerve fiber; is: inner sulcus. Reproduced from Tritsch et al. (2007), with permission from Nature Publishing Group.

Using the whole cell, voltage- , and current-clamp techniques in acutely excised rat (P7-10) cochlea *in-vitro*, Tritsch and their colleagues (2007) found ATP-mediated spontaneous activity in Kölliker's organ can trigger spontaneous activity in the immature IHCs and auditory nerve fibers. Tritsch et al. (2007) showed that the spontaneous activity in Kölliker's organ coincided with recurrent Ca^{2+} spikes in IHCs, suggesting Kölliker's organ as the source for spontaneous activity in the immature IHCs. In addition, exogenous application of ATP also triggered spontaneous activity in spiral ganglion neurons (SGNs) (P7-10). The ATP-induced spontaneous discharge in SGNs was reduced when the AMPA receptor blocker was applied, suggesting that the spontaneous activity in SGNs is mostly mediated through the activity of IHCs, which are depolarized by Kölliker's organ. However, considering that postnatal SGN afferent dendrites also express purinergic receptors (Ito and Dulon, 2002) and that ATP is a potential neuromodulator for SGNs (Salih et al., 1999), it has to be tested whether ATP released from Kölliker's organ can directly initiate spontaneous activity in SGNs *in-vivo.*

One of the features of the spontaneous activity in the developing system is that it is a transient phenomenon that exists only during a specific time point in development. The transiency is established by the appearance of local circuits or receptor channels that are not supported by the mature system (Blankenship and Feller, 2010). Spontaneous activity in the developing SGNs and auditory brainstem neurons is most prominent before the onset of hearing (P10-12). This implies that the source for spontaneous activity, if present, should also follow this developmental time line. In agreement to this notion, the spontaneous activity in Kölliker's organ ceases after the onset of hearing. Tritsch et al, (2007, 2010a) showed that the ATP- mediated spontaneous activity in Kölliker's organ

and spontaneous inward currents in IHCs gradually diminish with development and are completely abolished after onset of hearing.

It is unknown how transiency is established in the Kölliker's organ, but one possible explanation is the reduction of channels that release ATP, similar to the developing visual system, where the number of nicotinic acetylcholine receptors (nAChRs) decreases before the cholinergic retinal waves disappear in starburst amacrine cell (SAC) network (Zheng et al., 2004).

Studies have indicated that gap junctions are present in the supporting cells of the mammalian inner ear (Forge et al., 2003). Connexin 26 and 30 are the predominant isoforms in the organ of Corti (Forge et al., 2003; Kikuchi et al., 1995), and they permeate ATP (Goldberg et al., 2002). Tritsch et al. (2007) showed that the ATP-mediated spontaneous activity in Kölliker's organ is blocked by gap junction inhibitors, indicating that Kölliker's organ releases ATP via the gap junctions. Hence, it is plausible that reduction of gap junctions is the cause for cessation of spontaneous activity in Kölliker's organ after the onset of hearing. However, this is a weak argument, since connexin 26 and 30 remain highly expressed in mammalian adult organ of Corti (Forge et al., 2003), although other types of gap junction isoforms could be involved in purinergic signaling in Kölliker's organ.

Another possible mechanism that can account for Kölliker's organ's transiency is the transformation or autophagocytosis of Kölliker's organ itself (Hinojosa, 1977; Kamiya et al., 2001). Hinojosa et al. (1977) found that Kölliker's organ undergoes autophagocytosis, progressing from base to apex along the cochlear axis in kittens before the onset of hearing. Recent findings by Kamiya et al. (2001) further support this view,

by showing that cells in the greater epithelial ridge, which includes Kölliker's organ, undergo apoptosis around P12-14. Considering that ATP-mediated spontaneous activity in Kölliker's organ ceases around P12, these findings show that the regression of Kölliker's organ contributes to decline of spontaneous activity after the onset of hearing.

Given that spontaneous activity in the developing auditory system originates in Kölliker's organ, how does this support the idea of cochlear-originated spontaneous activity? Two important points need to be considered. First, it appears that the local release of ATP in Kölliker's organ synchronizes the activity of neighboring IHCs. Tritsch et al. (2007) showed that the percentage of synchronized spontaneous activity is higher in IHCs that are in close proximity, compared to those that are further apart (**Fig. 2-7**). IHCs encode different frequencies of sound along the tonotopic axis of the cochlea. Thus, it is likely that the spontaneous activity in Kölliker's organ synchronizes the activity of groups of IHCs along the cochlea, which would ultimately help establish the tonotopic map in the auditory system. Similar functions have been found in the retina, in which spontaneous retinal waves in the retinal ganglion cells (RGCs) synchronize the activity of neighboring cells, thereby providing spatio-temporal information necessary for eye-specific layer segregation in lateral geniculate nucleus (LGN) during development (Meister et al., 1991).

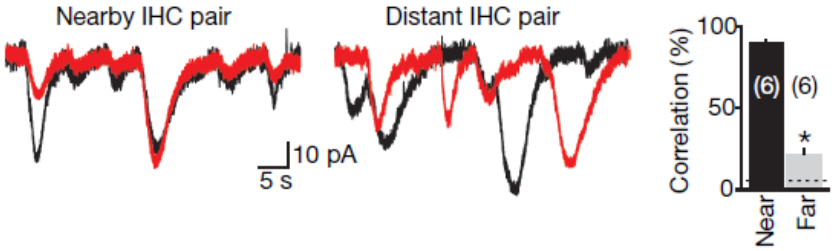

Figure 2-7. **Local release of ATP synchronizes the activity of neighboring IHCs. a**. Spontaneous inward currents recorded simultaneously from two IHCs that are located near or far from each other in response to local ATP release from Kölliker's organ. **b.** Percentage of correlation of spontaneous inward currents in IHCs as a function of location. * $P< 0.0001$. Reproduced from Tritsch et al. (2007), with permission from Nature Publishing Group.

Second, ATP-mediated spontaneous activity in Kölliker's organ may play a critical role in maintaining spontaneous recurrent action potentials in immature IHCs. Tritsch et al. (2010a) showed that the IHCs become most responsive to extracellular ATP at P8. Based on these results, it is possible that spontaneous activity in the auditory system is mediated by tight coordination between IHC channel activity and purinergic signaling from Kölliker's organ. That is, during the first postnatal week, the expression I_{Ca} and $I_{K,\,neo}$, enables IHCs to spontaneously fire recurrent action potentials, while during the second postnatal week they become gradually more responsive to ATP. The increase in sensitivity to ATP may be a result of the increased number of purinergic channels in IHCs. Previous findings show that ionotropic P2X and metobaotropic P2Y receptors that bind ATP are present in the developing mammalian IHCs, with their expression peaking between P8-12 (Housley, 2000). As a result, IHCs can fire Ca^{2+} action potentials, without causing an avert change in spontaneous activity in the IHCs before the onset of hearing. Although this hypothesis sounds plausible, whether the IHCs and Kölliker's

organ actually work in concert to generate spontaneous activity in auditory neurons during postnatal development requires further testing.

A similar developmental switch in spontaneous activity generation has been also observed in the visual system. During early development, retinal waves are mediated by cholinergic input from the starburst amacrine cells (Zheng et al., 2006). Right before the onset of vision, the cholinergic retinal waves are replaced by glutamatergic waves mediated by bipolar cells (Zheng et al., 2004). This transition occurs without apparent changes in the overall spontaneous activity in the retina.

Taken together, the findings by Tristsch et al. (2007, 2010a) provide new evidence for the involvement of purinergic signaling in auditory system development. These results offer compelling grounds for Kölliker's organ as the origin for spontaneous activity in the developing auditory system. At this point, it is difficult to conclude if Kölliker's organ is the only source for spontaneous activity in the developing auditory system, or whether it has a compensatory function to maintain spontaneous activity in the case of IHC failure. Compensatory homeostatic mechanisms for spontaneous activity generation have not been observed in the auditory system. Whether it exists or not is still an open question.

IV. Endogenous Spontaneous Activity in Spiral Ganglion Neurons (SGNs)

The question regarding the origin of spontaneous activity in the developing higher auditory pathways still remains elusive. The current understanding that spontaneous activity in the developing SGNs and auditory brain stem neurons has a cochlear origin

comes from studies that used *in-vivo* extracellular microelectrode recordings, where cochlear function was blocked by TTX or where the entire organ was surgically removed (Lippe, 1994; 1995). Although this experimental approach provided *in-vivo* evidence for the importance of cochlear activity in spontaneous activity generation; it has its own limitations because it cannot rule out the possible contribution of SGNs. Here, two aspects of the previous experimental methods will be revisited. First, the use of TTX is not adequate because it not only blocks activity of IHCs but also SGNs, since both cells express voltage-activated, TTX-sensitive sodium channels. Second, surgical ablation of cochlea can damage neurons in the cochlear nucleus, thus it is possible that the results seen after cochlear ablation may reflect the pathological responses from denervation rather than the absence of cochlear activity. As such, the argument that spontaneous activity originates from the cochlea awaits definitive proof from further studies that can address the specific role of SGNs in spontaneous activity using other approaches.

The very first attempt to show that SGNs can endogenously generate spontaneous action potentials in the absence of IHCs was reported in a study by Lin and Chen (2000). Because the findings by Lin and Chen (2000) are the only existing data that show the presence of intrinsic spontaneous activity in developing SGNs, a careful analysis of the data is required. Lin and Chen (2000) took several experimental conditions into consideration to circumvent the problems mentioned above and to prove that the spontaneous activity in developing mouse SGNs are "endogenously" derived. First, the recordings of cultured neurons were made in special bath solution which contained 6,7-Dinitroquinoxaline-2,3-dione (DNQX) to block glutamatergic transmission via AMPA receptors. Second, the recording was obtained using non-invasive extracellular patch

method to eliminate possible confounding factors arising from the use of whole-cell, tight-seal patch technique, which can perturb the ionic content and electrical properties of the neurons.

Cultured SGNs (P0-5) recorded in these conditions, displayed stable, random, spontaneous action potentials with relatively short inter-spike-intervals (Lin & Chen, 2000). The overall low discharge rate (4spikes/sec) was similar to the recordings obtained from the SGNs of neonatal kitten in-vivo (3.1spikes/sec) (Jones et al., 2007). However, burst firing that is typically seen in developing auditory system were not present.

The study by Lin and Chen (2000) allow two opposing interpretations. One interpretation is that the low frequency, random spiking that lacks burst firing could be a general feature of endogenously generated spontaneous activity in developing SGNs, while the burst firing component is most likely a feature derived from IHC input activity. The burst firing might be a consequence of unique IHC-SGN innervation pattern (Liberman 1980), where single IHC can drive activity in multiple, synaptically connected SGNs.

If intrinsic spontaneous activity is present in SGNs, there are several mechanistic routes that may lead to its activation, based on general features of spontaneous activity seen in other systems: 1) Contribution of transient network, 2) pacemaker -like activity, 3) intrinsic membrane properties. The first possibility could not be tested because of the use of cultured neuronal preparation.

One mechanism by which immature SGNs can generate endogenous spontaneous action potential is by having a pacemaker-like system or ion channels that intrinsically

oscillate. Lin and Chen (2000) showed that when the resting membrane potential is manipulated by injecting hyperpolarizing currents, the frequency of action potential firing decreased and the average cell resting membrane potential was biased towards a more depolarized potential at the end of the hyperpolarizing current injection, suggesting that there must be a mechanism that can drive the membrane potentials to a depolarized direction. Although the specific ion channels that activate near the resting membrane potential of SGNs were not tested in their study, one possible candidate is the HCN channels that mediate hyperpoarization activated current (I_h). I_h acts as a pacemaker current that sets the membrane properties and firing behaviors of many excitable cells by providing depolarizing current in response to membrane hyperpolarization (Robinson and Siegelbaum, 2003). For instance, in postnatal hippocampal neurons, I_h is shown to drive spontaneous activity by membrane oscillations (Strata et al., 1997). Heterogenous expression of I_h has been found in neonatal spiral ganglion neurons *in-vitro* (Mo and Davis, 1997), however; the link between I_h and SGN endogenous spontaneous activity has not been determined. Therefore, future study is necessary to discern the role of I_h in endogenous spontaneous activity generation in developing SGNs.

The presence of intrinsic spontaneous activity indicates that it must be arising due to instability of membrane properties. In response to suprathreshold current injection, immature SGNs (P3) fired regenerative action potential traces, while adult SGNs only fired one action potential (Lin and Chen, 2000), showing the presence of different membrane properties between immature and mature SGNs. This difference was attributed to the differential expression of voltage-gated delayed rectifier potassium ($K_V3.1$) channels that constitute for delayed rectifier potassium current (I_K) in SGNs.

The current density of I_K increases about 3.6 fold during the postnatal development, and this increase in I_K are thought to contribute to absence of spontaneous firing in adult SGNs (Lin & Chen, 2000). The change in potassium channel expression during development is analogous to the change seen in immature IHCs. In mammalian IHCs, the recurrent Ca^{2+} action potentials are ceased with the expression of fast-activating, potassium outward current ($I_{K,f}$) at the end of second postnatal week (Kros et al., 1998, Marcotti et al., 2003a). If SGNs were a mere "conveyer belt" that relays the information from the IHCs to the brain, it is uncertain why this redundancy is necessary.

One explanation that could account for this redundancy is homeostatic regulation of spontaneous activity in which in the absence or failure of a main component the remaining circuitry compensates for the loss (Blankenship & Feller, 2010). Homeostatic regulation of spontaneous activity has been observed in the developing visual system. For example, in the developing retina, the output of retinal waves is preserved even when cholinergic waves are blocked (Stacy et al., 2005). Using a conditional knockout mouse that lacks choline acetyltransferase (ChAT), an enzyme critical for acetylcholine (ACh) synthesis, Stacy et al. (2005) showed that these mice exhibit ACh-independent, gap junction-mediated waves. This study indicates that a homeostatic mechanism is involved to ensure that developmentally important retinal waves persist during development.

It is unknown if homeostatic mechanisms for spontaneous activity are present in the developing auditory system. Whether endogenously generated spontaneous activity in SGNs serves this purpose or not requires further studies. And if so, what mechanism controls the periodicity of spontaneous activity in SGNs? Many critical questions remain

to be answered to better understand the contribution of SGNs in spontaneous activity in the developing auditory system.

The opposing interpretation of the findings by Lin and Chen (2000) is that the endogenously elicited spontaneous activity may not reflect the actual response *in-vivo*. The recordings by Lin and Chen (2000) were acquired from cultured SGNs, in which SGNs are no longer in contact with the IHCs. Because the tonotopic arrangement of SGNs is lost in the culture preparation, it is difficult to rule out whether the endogenous SGN spontaneous activity from *in-vitro* system would be the same *in-vivo*.

In summary, previous reports put forward the possibility that developing SGNs can endogenously generate spontaneous activity in the absence of input from the IHCs before the onset of hearing. However, the use of *in-vitro* culture preparation confines the extent to which the result can be generalized. Regardless, the attempt for verifying the role of SGNs in spontaneous activity generation is worthwhile, since it opens up a new horizon to better understand the functional significance of SGN spontaneous activity in the developing auditory system. Nonetheless these findings are in agreement with the role of the cochlea for spontaneous activity generation, but *in-vivo* studies are needed to identify the precise role of SGNs in the generation of spontaneous activity in the developing auditory system.

V. Functional Relevance of Spontaneous Activity

Although questions regarding the mechanism of spontaneous activity still exist in the field, it appears that the spontaneous activity before the onset of hearing has

functional significance both at microscopic and macroscopic level. As discussed previously, spontaneous activity in the developing auditory system before the onset of hearing occurs in a distinct pattern, in which low frequency (10 Hz), rhythmic burst firing is followed by a period of quiescence that ranges from several milliseconds to seconds. The immediate question then becomes what functional significance does the pattern of neural impulse have in the developing auditory system at the cellular level?

Spontaneous activity in the developing auditory system involves transient intracellular Ca^{2+} oscillations. Spontaneous recurrent Ca^{2+} action potentials in immature IHCs trigger exocytosis and glutamate release onto afferent boutons of developing spiral ganglion neurons (Beutner and Moser, 2001; Glowatzki and Fuchs, 2002). Since SGNs express AMPA, NMDA receptors (Chen et al., 2007; Niedzielski et al., 1995) and voltage dependent L-type calcium channels (Han et al., 1994), postsynaptic depolarization of SGNs can lead to elevation of intracellular Ca^{2+}. Previous *in-vitro* SGN culture studies showed that electrical stimulation-induced depolarization of SGN results in increase of intracellular Ca^{2+} and subsequent elevation of cyclic AMP (cAMP), whose downstream targets include pro-survival intracellular signaling pathways, such as cAMP-dependent protein kinase (PKA) (Bok et al., 2003; Hegarty et al., 1997) and Ca^{2+}-calmodulin dependent protein kinase (CaMK) (Hansen et al., 2003) (**Fig. 2-8**). Both PKA and CaMK phosphorylate cAMP-responsive element binding protein (CREB), which initiates gene transcriptions critical for neuronal survival, maintenance, and synaptic refinement. For example, under depolarizing conditions, the presence of CaMK inhibitor (Hansen et al., 2003), or a dominant-negative mutation of CREB (Bok et al, 2003), resulted in marked decrease in SGN (P5) survival, suggesting that activation of a Ca^{2+}-dependent

intracellular signaling pathway is critical for SGN survival and maintenance. Therefore, Ca^{2+} oscillations in auditory neurons during patterned spontaneous activity can mediate developmental functions such as survival and maintenance of auditory neurons by activation of Ca^{2+}-dependent prosurvival intracellular pathways.

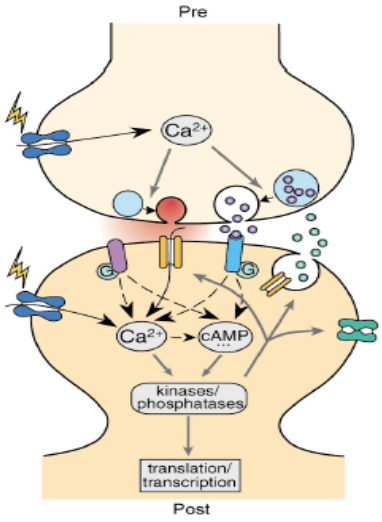

Figure 2-8. **Potential cellular pathway mediated by spontaneous Ca^{2+} action potentials in developing auditory neurons.** Adapted from Zhang and Poo (2001), with permission from Nature Publishing Group.

One may argue that the low discharge rate of spontaneous activity would not allow sufficient amount of Ca^{2+} to enter the cell and trigger Ca^{2+}-dependent developmental events in auditory neurons. However, previous study by Kotak and Sanes (1995) showed that the immature auditory neurons display prolonged depolarization in response to afferent stimulation that mimics the patterned spontaneous activity. This finding suggests that the immature auditory neural circuits are tuned to respond efficiently to low discharge rate stimulation. Hence, at the microscopic level, the slow periodicity of the patterned spontaneous activity may ensure enough time for appropriate Ca^{2+}-dependent developmental changes to take effect in the developing SGNs and central auditory neurons.

If the spontaneous activity in the developing auditory system initiates local synaptic developmental programs, at macroscopic level, the rhythmic burst activity may promote the refinement of tonotopic maps in the central projections. Previously, Tritsch et al. (2007, 2010a) have shown that Kölliker's organ synchronizes the activity of groups of IHCs along the cochlear tonotopic axis. That is, the synchronization of activity is higher between the cells that are located close to each other than those that are further apart. Thus, the rhythmic burst activity ensures that the activity of IHCs within a given frequency range are synchronized at the same time, therefore enabling the tonotopic map refinement along the auditory neuraxis.

In addition, the rhythmic burst activity might be efficient in formation and consolidation of the tonotopic map in central projections. It is suggested that the patterned burst activity seen in the developing auditory system is similar to theta burst which effectively induces long term potentiaion (LTP) in the hippocampus (Tao et al., 2001). This reflects the idea of Hebb, in which synaptic strengthening between two neurons is achieved by repetitive stimulation that is coincident in time. The repetitive pre-synaptic input to converging postsynaptic target, however; should occur in specific time window; otherwise it will result in LTP failure (Zhang et al., 1998). If the repetitive presynaptic stimulation occurs with high frequency at a constant rate, it can also lead to synaptic depression. For instance, in the endbulb of Held synapse in the cochlear nucleus of the prehearing animals, sustatined high frequency (200 Hz) stimulation results in synaptic depression (Brenowitz and Trussell, 2001). Therefore, considering the importance of temporal patterns of presynaptic input activity for neural consolidation, the

rhythmic burst activity that is tightly correlated in time and space might be more efficient in consolidating and maintaining tonotopic maps in the developing auditory system.

VI. Spontaneous Activity in Spiral Ganglion Neurons (SGNs) and its Implication

Most forms of the hearing impairment result from the loss or degeneration of cochlear hair cells. Currently, the most widely used and most effective clinical intervention for these types of hearing loss is the cochlear implants (Moore and Shannon, 2009). By providing direct electrical stimulation onto the SGNs, the cochlear implant restores substantial hearing function in the absence of normally functioning hair cells.

One factor that determines the beneficial outcome of cochlear implant is the integrity and the survival of the remaining SGNs, which show marked degeneration after IHC loss, as evidenced in animal models of deafness and in human studies (Leake et al., 2008). The rate of SGN degeneration depends on the age of onset at which deafness occurred and the time since deafness. However, the general trend is that SGNs undergo rapid degeneration immediately following IHC loss and thereafter the rate of degeneration becomes gradual (Leake et al., 2007). The degeneration of SGNs and auditory nerves are much more profound and severe if the deafness occurred early in development (Lustig et al., 1994; Stakhovskaya et al., 2008), suggesting that disturbance of the critical period of auditory development has a significant impact on severity of deafness.

Since SGNs receive both electrical input and trophic support from the IHCs *in-vivo*, exogenous neurotrophine delivery and electrical stimulation of SGNs have been

tested in culture systems as a potential method to prevent SGN degeneration after deafness (Roehm et al., 2005). A growing body of literature indicates that these potential SGN survival factors work in an additive manner to attenuate SGN degeneration. However, some researchers suggested that SGN depolarization by electrical stimulation may have a more potent effect on survival than neurotrophin replacement alone (Hegarty et al., 1997). The reason that electrical stimulation is a much stronger effector for SGN survival can be attributed to parallel activation of several Ca^{2+}- dependent, intracellular pro-survival signaling pathways, such as those mediated by cAMP, PKA, CaMK, following depolarization of SGN *in-vitro* (Bok et al., 2003; Hansen et al., 2003; Hegarty et al., 1997).

The pro-survival effect of electrical stimulation shown in a reduced culture system has been also demonstrated *in-vivo*, using animal models of deafness. Chronic electrical stimulation of SGNs for an extended period of time following neonatal deafness results in higher SGN density compared to unstimulated controls (Leake et al., 1991). Additionally, 3-month electrical stimulation by implant devices in congenitally deaf cats resulted in restoration of cochlear nucleus synapses (Ryugo et al., 2005). However, not all chronic stimulation resulted in pro-survival effect in deafened animal models (Araki et al., 1998; Li et al., 1999), suggesting the importance for finding the specific aspects of electrical stimulation, such as duration, intensity, and rate, that can enhance SGN survival.

Based on findings that show the possibility that spontaneous activity in auditory neurons before the onset of hearing might provide instructional cues for synaptogenesis and refinement of tonotopic maps in the central auditory pathway, it is possible to

hypothesize that the same stimulus if provided to the SGNs would enhance their survival in deafened subjects, especially those who have congenital deafness.

At present, no direct mechanism is available that can explain the developmental effects mediated by spontaneous activity during early auditory development. Specifically, it is unknown whether spontaneous activity in SGNs activates the pro-survival signaling pathway (**Fig. 2-8**) and induces the proposed developmental effect *in-vivo*. It is also unknown whether SGNs themselves possess the intrinsic spontaneous activity during early development, and whether the endogenously derived spontaneous activity has a different functional role than the IHC derived spontaneous activity.

Dissecting out the precise mechanism of spontaneous activity in SGNs during early development is very critical as it can provide a new avenue for better understanding normal auditory development and may further provide valuable insights for clinical interventions for deafness and cochlear implant technology development.

Chapter III. Functional Contributions of HCN Channels in Spiral Ganglion Neurons of Mouse Inner Ear[1]

[1] The text in this chapter is a reproduction of earlier publication by © Kim Y-H & Holt JR, 2013. Originally published in *JOURNAL OF GENERAL PHYSIOLOGY*. doi: 10.1085/jgp.201311019. Authors retain copyright to their own work and its reuse has been granted by the Rockefeller University Press. Portion of the text has been reformatted to match the terminology and style of this thesis.

Chapter III

SGNs express various voltage-gated ion channels to tailor their firing properties to meet the demand of high-fidelity signal transfer from the IHCs (Chapter I). Hence, examination of ionic conductance and its underlying channel function is fundamental for understanding SGN function in auditory signal processing.

The hyperpolarization-activated, cationic current, I_h has been found in various organs, including the auditory system (Bal and Oertel, 2000; Banks et al. 1993; Koch and Groethe 2003). I_h is carried by the *Hcn* channel family, *Hcn1-4*, which can form homo- or hetero- tetrameric channels. Unlike other channels which activate upon depolarization, I_h activates in response to membrane hyperpolarization negative to -50 mV and passes inward current which depolarizes the cell membrane. Owing to its unique biophysical properties, I_h has been shown to regulate resting membrane potential and modulate firing properties in many different cell types (Biel et al. 2009). Previous studies had shown the presence of I_h in SGN somata (Chen 1997; Mo and Davis 1997), however; its molecular correlates and functional significance in SGNs had not been fully explored.

Thus, the aim of the study was to investigate the molecular composition and the functional contribution of HCN channels in SGNs.

ABSTRACT

The hyperpolarization-activated current, I_h, is carried by members of the *Hcn* channel family and contributes to resting potential and firing properties in excitable cells of various systems, including the auditory system. I_h has been identified in spiral ganglion neurons (SGNs), however, its molecular correlates and their functional contributions have not been well characterized. To investigate the molecular composition of the channels that carry I_h in SGNs, we examined *Hcn* mRNA harvested from spiral ganglia of neonatal and adult mice using quantitative RT-PCR. The data indicate expression of *Hcn1*, *2*, and *4* subunits in SGNs, with *Hcn1* being the most highly expressed at both stages. To investigate the functional contributions of HCN subunits we used the whole-cell, tight-seal technique to record from wild-type SGNs and those deficient in *Hcn1*, *Hcn2* or both. We found that HCN1 is the most prominent subunit contributing to I_h in SGNs. Deletion of *Hcn1* resulted in reduced conductance (G_h), slower activation kinetics (τ_{fast}) and hyperpolarized half-activation ($V_{1/2}$) potentials. We demonstrate that I_h contributes to SGN function with depolarized resting potentials, depolarized sag and rebound potentials, accelerated rebound spikes following hyperpolarization and minimized jitter in spike latency for small depolarizing stimuli. Auditory brainstem responses (ABR) of *Hcn1*-deficient mice showed longer latencies, suggesting that HCN1-mediated I_h is critical for synchronized spike timing in SGNs. Together, our data indicate I_h contributes to SGN membrane properties and plays a role in temporal aspects of signal transmission between the cochlea and the brain, which are critical for normal auditory function.

INTRODUCTION

Spiral ganglion neurons (SGNs) are the first-order sensory neurons of the auditory system, which provide afferent innervation of hair cells in the mammalian cochlea. SGNs convey signals from hair cells to the brain in a manner that preserves the amplitude, frequency, and temporal aspects of sound information (Geisler, 1998; Meyer and Moser, 2010; Taberner and Liberman, 2005). This high-fidelity signal transmission between the hair cells and the SGNs is critical for normal auditory processing and sound localization.

To perform these functions spiral ganglion neurons express a variety of voltage-gated ion channels which allow efficient signal transfer from inner hair cells (Davis, 2003). The expression of specific voltage-gated ion channels in SGNs allows them the ability to precisely encode graded membrane potentials of hair cells into trains of action potentials. For example, SGNs express voltage-gated calcium and potassium channels along the cochlear tonotopic axis in a graded manner that reflects the tonotopic specialization of hair cells (Adamson et al., 2002; Chen et al., 2011; Davis 2003; Lv et al., 2012).

The hyperpolarization-activated cationic current, I_h, has been identified in neurons of the auditory system (Bal and Oertel, 2000; Banks et al., 1993; Koch and Groethe, 2003) including SGNs (Chen, 1997; Mo and Davis, 1997; Yi et al., 2010) but the molecular composition of the channels that carry I_h and their precise function have not been clarified. I_h is carried by subunits of the HCN channel family, HCN1-4, which form homo- and hetero- tetrameric channels (Ishii et al., 1999; Ludwig et al., 1998). Unlike other channels which activate upon depolarization, I_h activates in response to membrane hyperpolarization negative to −50 mV and passes inward current which depolarizes the

cell membrane. Thus, the unusual biophysical properties of I_h contribute to resting membrane potential and firing properties in many different cell types (Biel et al., 2009; Robinson & Siegelbaum, 2003).

Recently, Yi et al. (2010) characterized I_h at the hair cell afferent synapse, however, the molecular correlates of I_h and their functional contributions in SGN cell bodies were not examined. To identify which *Hcn* genes are expressed in neonatal and adult SGNs, we harvested SGN mRNA for quantitative RT-PCR (qPCR) analysis. To examine the contributions of *Hcn* gene expression to I_h we recorded from SGNs of wild-type mice and mice that lacked *Hcn1*, *Hcn2*, or both. Our qPCR and electrophysiology data indicate expression of HCN1, 2, and 4 subunits in neonatal SGNs, with HCN1 being the most highly expressed subunit. Deletion of *Hcn1* resulted in reduced conductance, hyperpolarized half-activation voltage and slower activation kinetics. We recorded from SGNs in current-clamp mode to investigate the functional contributions of I_h to SGN membrane and firing properties. We show that I_h depolarizes SGN resting membrane potentials, regulates rebound spike timing, and synchronizes action potential (AP) firing in response to small depolarizing stimuli. In addition, auditory brainstem responses indicate possible auditory deficits in *Hcn1*$^{-/-}$ animals. *Hcn1*$^{-/-}$ mice had delayed ABR latencies, suggesting a contribution to spike timing in the 8th cranial nerve. Taken together, the present study provides evidence that I_h, HCN1 in particular, contributes to the membrane properties of SGNs and plays a role in the temporal aspects of auditory signal transmission required for normal auditory function.

MATERIALS AND METHODS

Animals All animal protocols used in this study were approved by the Institutional Animal Use and Care Committee (IACUC) at the University of Virginia (protocol # 3123) and Boston Children's Hospital (protocol # 11-04-1959). Experiments were performed in strict accordance to the guidelines therein. *Hcn1* deficient (*Hcn1*$^{-/-}$) mice (strain: B6.129S-*Hcn1*^{tm2Kndl}/J; Nolan et al., 2003) were obtained from The Jackson Laboratories (Bar Harbor, ME) and *Hcn2* deficient (*Hcn2*$^{-/-}$) mice were obtained originally from Ludwig et al. (2003). Mice deficient in *Hcn1* and *2* (*Hcn1/2* $^{-/-}$) mice were generated by crossing *Hcn1*$^{+/-}$ and *Hcn2*$^{+/-}$ mice, as previously described (Horwitz et al*.,* 2011). Both sexes of animals were used in non- discriminatory fashion. Wild-type (WT) control data were obtained from three different strains, Swiss Webster (Charles River, Wilmington, MA; n = 11 SGNs), WT littermates (n = 5) obtained from *Hcn1*$^{+/-}$ and *Hcn1*$^{+/-}$ crosses and WT littermates (n = 9) obtained from *Hcn2*$^{+/-}$ and *Hcn2*$^{+/-}$ crosses. We found no statistical difference in any of the analyzed parameters and have pooled the WT data.

Neonatal SGN preparation Spiral ganglion neurons (SGNs) were acutely dissected from neonatal mice, age ranging between postnatal day (P) 1-8. Following rapid decapitation, cochleae from both sides of the inner ear were excised from the temporal bone, and bathed in sterile MEM with glutamax (Gibco # 41090, Grand Island, NY) supplemented with 10 mM HEPES (Sigma, St. Louis, MO) and 25 mg ampicillin (Sigma), pH 7.4. The bony labyrinth encapsulating the cochlea was chipped away to gain access to whole cochlear turn, and the spiral ligament and stria vascularies were peeled

off. Spiral ganglion neurons were isolated carefully from the cochlear modiolus, by severing the central fiber tracts that connect to the cochlear nucleus. No enzyme was used for SGN dissection. Care was given so that the SGN peripheral fibers and the Organ of Corti were left relatively intact. SGN explants were divided into halves as base and apex in relation to the cochlear tonotopic axis and mounted flat on glass cover slips (Fisher Scientific, # 12-546, Waltham, MA), with Organ of Corti facing down to gain better access to SGN cell bodies. The sections were secured in place under two thin glass fibers glued to the coverslip with Sylgard® 184 (Dow Corning, Midland, MI). SGN organotypic explants were incubated at 37 °C in a humidified incubator (5% CO_2) for 1-2 hours, after which were used for acute electrophysiological studies. All SGN explants were used within 4-5 hours after dissection.

Type I SGNs SGNs can be categorized into type I and type II neurons based on their innervation pattern and morphology. Type I neurons, which constitute 90-95% of the entire SGN population, innervate inner hair cells (IHCs) and are responsible for sound information transfer (Liberman, 1982). Type I neurons are highly myelinated (Romand and Romand, 1987) and in general have relatively large cell body size compared to type II neurons (Rusznák and Szűcs, 2009). The myelin sheath tightly covers the axon fibers and loosely wraps around the cell bodies of SGNs, ensuring high velocity signal conduction to the central pathway. Type II neurons, which compose the remaining ~5% of SGNs, on the other hand, innervate the outer hair cells (Perkins and Morest, 1975). Type II neurons are unmyelinated and have smaller cell bodies than type I neurons (Rusznák and Szűcs, 2009). The different morphology and abundance in number allowed

for easy detection of neonatal type I SGNs for electrophysiological recordings. All neonatal SGN data presented in this paper were obtained from type I cells.

Adult SGN culture Adult mouse SGN culture technique was performed in accordance to the method previously described (Lv et al*.,* 2010). Adult mouse was sacrificed and decapitated rapidly. For each culture, 3-4 animals were pooled. Temporal bones were removed from the skull and bathed in ice-cold minimum essential medium (MEM) with Hank's salt (Gibco # 11575) supplemented with 0.2 mg/mL Kynurenic acid (Sigma), 10 mM $MgCl_2$, 2% Fetal Bovine Serum (FBS; Gibco # 16000, v/v), and D-glucose (6 g/L, Sigma). The bony shell encapsulating the cochlea was chipped off using a scalpel, and the organ of Corti was removed from the central core. The modiolus, which contained the SGNs was isolated in above dissecting media that contained 2% FBS (v/v) was replaced with 2% B27 (Gibco # 17504, v/v), and split into apical and basal sections. The sections were subsequently digested in enzyme solution containing collagenase type 1 (1 mg/mL, Sigma) and DNase (1 mg/mL, Sigma) at 37 °C for 15 min. Following enzyme treatment, trypsin (0.25%, Gibco # 15090) was added to the solution and incubated for an additional 10 min at 37 °C. The reaction was quenched with equal volume FBS (v/v). After gentle trituration, the cell solution was transferred to Hank's balanced salt solution (HBSS) containing 0.45 M sucrose (Sigma) and centrifuged at 2000 rpm for 5 min. The cell pellets were reconstituted in Neurobasal A ^{TM} (Gibco # 10888) supplemented with 2% B27, 0.5 mM L-glutamine (Sigma), and penicillin (100 u/mL, Sigma). The freshly isolated SGN cells were filtered through a 40 μm cell strainer and plated onto glass cover slips, pretreated with poly-D-lysine (0.5 mg/mL, Sigma) and

laminin (1 mg/mL, Sigma). The SGN culture was supplied with 10% FBS, kynurenic acid (0.2 mg/mL, Sigma), NT3 (10 ng/ul, Sigma) and BDNF (10 ng/ul, Sigma), and incubated at 37 °C in humidified incubator (5% CO_2) for 24-48 hours prior to electrophysiological recordings. To ensure quality recording and minimize space-clamp errors, only spherical SGNs with one or two neurites were selected for voltage-clamp recordings.

Electrophysiology The whole-cell, tight-seal patch clamp technique was used in voltage- and current-clamp modes to record I_h from SGN cell bodies. All electrophysiological recordings were performed at room temperature (22-24 °C). SGN explants were placed into a custom-made recording chamber and viewed under Zeiss Axioskop FS upright microscope (Oberkochen, Germany) equipped with 63× water-immersion lens and differential interface contrast (DIC) optics. SGN explants were bathed in a standard external solution that contained (in mM): 137 NaCl, 0.7 NaH_2PO_4, 5.8 KCl, 1.3 $CaCl_2$, 0.9 $MgCl_2$, 5.6 D-glucose, 10 HEPES, amino acids (1:50, Gibco # 11130), vitamins (1:100, Gibco #11120). The pH was adjusted to 7.4 with NaOH and the measured osmolarity was 303 mOsmol/kg. Recording pipettes (3-5 MΩ) were pulled from R-6 soda lime capillaries (King Precision Glass, Claremont, CA), using a two-stage vertical pipette puller (PC-10; Narishige, Tokyo, Japan). To minimize pipette capacitance, tips were coated with Ski wax. Recording pipettes were filled with standard internal solution that contained (in mM): 135 KCl, 2.5 $MgCl_2$, 2.5 K_2-ATP, 5.0 HEPES, 5.0 EGTA, 0.1 $CaCl_2$; pH 7.4 (KOH), 283 mOsmol/kg. All reagents for electrophysiology solution were purchased from Sigma, unless otherwise noted. I_h was

recorded immediately after the cell membrane was broken through at giga-ohm (GΩ) seal. Series resistance (R_s) and membrane capacitance (C_m) were corrected. Both parameters were continuously monitored, in order to ensure stable recording. Compensated residual R_s was below 7 MΩ on average.

For pharmacology experiments, the following drugs were applied to the external bath: 100 μM ZD7288 (Tocris Bioscience, Ellisville, MO); 100 μM Ni_2Cl (Sigma), 200 μM 8-br-cAMP (Sigma). Chemicals were dissolved in deionized water (dH_2O) to appropriate stock concentrations, stored at –20 °C, and applied directly to the external solution at the desired final concentrations.

Electrophysiological data from SGNs was recorded using Axopatch200B (Molecular Devices, Palo Alto, CA) amplifier. Signals were filtered at 1 kHz with a low pass Bessel filter and digitized at ≥ 20 kHz using 12-bit acquisition system, Digidata 1332 (Axon Instruments, Union City, CA), and pClamp 9.0 (Molecular Devices, Sunnyvale, CA). All stimulus protocols were generated using pClamp 9.0 and data were stored on a PC.

SGN micro-dissection and quantitative-PCR Neonatal SGN tissue was harvested from P3 Swiss Webster mice in ice-cold MEM with Glutamax (Gibco # 41090), supplemented with 10 mM HEPES (Sigma) and 25 mg ampicillin (Sigma), pH 7.4. SGNs were gently isolated from cochlear modiolus by severing the central processes. In order to prevent cross contamination from cochlear hair cells, organ of Corti was trimmed away along the cochlear turn using a microblade so that the SGN isolates only contained cell

bodies. Micro-dissected SGNs were rinsed in fresh MEM, transferred into microcentrifuge tubes, and rapidly frozen on dry ice. Two preparations of SGN tissue were pooled from 10 (5 mice) and 14 (7 mice) cochleas respectively and were processed in parallel for RNA isolation and q-PCR experiments.

Adult SGNs were harvested from Swiss Webster mice P ≥ 40 or older. Temporal bones were removed from the skull and bathed in ice-cold minimum essential medium (MEM) with Hank's salt (Gibco # 11575) supplemented with 0.2 mg/mL Kynurenic acid (Sigma). The bony shell encapsulating the cochlea was chipped away using a scalpel. SGNs were excised from the central core and processes were sectioned where the cochlear nerve joins the vestibular nerve to prevent contamination from vestibular neurons. Dissected SGN tissue was rapidly frozen in dry ice. Two samples of adult SGN tissue were pooled from 6 (3 mice) and 10 (5 mice) cochleas, respectively, and were processed in parallel for RNA isolation and subsequent q-PCR experiments.

The frozen SGN micro-isolates were thawed, spun down in a centrifuge to remove excess media, and processed for RNA isolation. Total SGN RNA was prepared with RNAqueous® micro kit (Ambion # 1931, Austin, TX) according to the manufacturer's instruction. The isolated RNA was then purified with DNA-free RNA kit ™ (Zymo Research # R1013, Irvine, CA) and stored in –80 °C. RNA concentration was measured on a spectrophotometer (Nanodrop ND-1000, Thermo Fisher Scientific, Pittsburgh, PA). For RNA quality control, the samples were analyzed with a Bioanalyzer (Agilent Technologies, Santa Clara, CA) and found to have RNA integrity number of > 9.0. One hundred ng of RNA was reverse transcribed into cDNA using QauntiTect

Reverse Transcription Kit (Qiagen # 205311, Germantown, MD). Q-PCR was carried out in triplicates using SYBR Green ER™ qPCR Supermix (Invitrogen # 56470, Grand Island, NY) according to the manufacturer's instructions, and processed on a CFx Real-Time PCR Detection System (BioRad, Hercules, CA). Each reaction (25 µl) included primers at 0.2-0.4 picoM and cDNA generated from 5 ng of RNA. Q-PCR parameters were set for 40 cycles and amplicon purity was confirmed with melt curve analysis. Q-PCR primers had melting temperatures ranging from 58- 61° C and the sequences were as following: *Hcn1*: ACA TGC TGT GCA TTG GTT ATG GCG and AAC AAA CAT TGC GTA GCA GGT GGC; *Hcn2*: ACT TCC GCA CCG GCA TTG TTA TTG and TCG ATT CCC TTC TCC ACT ATG AGG; *Hcn3*: CCT CAT CCG CTA CAT ACA CCA GT and GAC ACA GCA GCA ACA TC; *Hcn4*: ACT TTA ACT GCC GAA AGC TGG TGG and GAA ACG CAA CTT GGT CAT GGA. Q-PCR primer sets were designed to amplify specific regions of HCN amplicons produced by RT- PCR (Horwitz et al., 2010).

Expression levels and possible genomic DNA contamination were tested with ribosomal 29S as housekeeping gene by running reverse transcribed cDNA samples and no-reverse transcript controls simultaneously. Cochlear hair cell contamination was determined with cochlear hair cell specific gene, prestin as a control. The sequences of ribosomal 29S and prestin primers (Lelli et al., 2009) were as following: *29S*: GGA GTC ACC CAC GGA AGT TCG and GGA AGC ACT GGC GGC ACA TG; *prestin*: TTA CGG CTC GAT TTG GAG GGT GAA and GTG CAA GAG GCC TGT TAA TCT TTG.

Auditory brainstem responses *Hcn1*$^{-/-}$ mice (n = 7) and their wild type littermates (n = 5) were used for the auditory brainstem response (ABR) recording. Due to mixed genetic background (C57BL/6 and 129S) of the strain, mice were tested at 6-7 weeks of age, to minimize confounding factor from age-related hearing loss that these strains exhibit around 3 months of age (Kane et al., 2012; Zheng et al., 1999).

ABRs were performed in sound-proof chamber. Before ABR measurements, mice were anesthetized with 100 mg/Kg Ketamine and 20 mg/Kg Xylazine via intraperitoneal injection, and placed on a heating pad to maintain body temperature. Needle electrodes were placed subdermally at the vertex and below the pinna, and a ground electrode was placed near the tail. Tone pips (5 msec, 40 Hz) at varying frequencies (5.6, 8, 11.3, 16, 22.6 and 32 kHz) were delivered to the right ear via a sound system, in which dual sound source was coupled to a microphone and positioned near the ear canal. Each stimulus was presented with alternating polarities and the responses were recorded with increasing sound pressure levels, from 10 dB to 80 dB with 5 dB intervals. For each level, waveforms were amplified (Gain 10,000), filtered (0.1-3 kHz), and averaged across 1024 presentations. Threshold was determined with visual inspection of the waveforms. Amplitude and latencies of the ABR waveforms were analyzed using ABR Peak Analysis software.

Data analysis Offline data analysis was performed using OriginPro 7.5 (Origin Lab, Northampton, MA). Liquid junction potentials (4 mV) were adjusted offline for all membrane potentials. Voltage-dependent steady state I_h activation was analyzed by using the following Boltzmann equation:

$$G\,(Vm) = Gmin + \frac{Gmax - Gmin}{1 + e^{(V - V½)/s}} \quad (1)$$

where G_{max} and G_{min} are the maximum and minimum conductance, $V_{½}$ is the voltage at half maximum activation and s is the slope factor.

I_h activation kinetics were examined by fitting the current evoked by a step to -144 mV potential with double exponential function:

$$Ih(t) = Iss + I_f \exp(t/\tau fast) + I_s \exp(t/\tau slow) \quad (3)$$

where I_{ss} is the steady state current at a given potential, I_s and I_f denote the amplitude of the slow and fast current components and τ_{slow} and τ_{fast} are the corresponding time constants for I_h activation.

Statistical analysis was performed using OriginPro 7.5. All results were reported as means ± standard deviation (SD) unless otherwise specified. Statistical analysis for I_h conductance (G_h), half-activation voltage ($V_{1/2}$), slope factor (s), and activation kinetics (τ_{fast}) were made using independent *Student t-test.* If comparison involved multiple genotypes, analysis of variance (ANOVA) was used followed by Dunnett's post -*hoc* test. 8-Br- cAMP effect on I_h activation was analyzed using independent samples *Student t-test*. The effects of ZD7288, Ni_2Cl and Mibefradil on SGN firing properties were determined using paired *Student t-test*. Difference in means were considered significant if $p < 0.05$. Degree of scatter in spike time variation in response to small depolarizing current injection was quantified using confidence interval (CI) at 95 %.

RESULTS

Spatiotemporal development of I_h in Spiral Ganglion Neurons

To examine the contributions of HCN subunits to I_h in spiral ganglion neurons (SGN) we began with a quantitative RT-PCR (qPCR) analysis using primers that were selective for *Hcn1-4* and mRNA harvested from P3 WT SGN tissue. As shown in **Fig 3-1*A***, the qPCR analysis indicated expression of *Hcn1*, *2*, and *4* in early postnatal SGNs. The total mRNA expression for *Hcn1*, *Hcn2*, and *Hcn4* per cochlea was 700,000: 200,000: 400,000 respectively, with little expression of *Hcn*3. When normalized to *Hcn3* mRNA copy number, the relative expression was as follows: *Hcn1*:*Hcn2*:*Hcn3*:*Hcn4:* 21:6:1:12. Based on the expression ratio, it is evident that *Hcn1* was the most highly expressed in neonatal SNGs followed by *Hcn4* and *Hcn2*. We speculate that the *Hcn3* expression in SGNs is minimal or nonexistent based on the low mRNA copy number, thus, its functional contributions in neonatal SGNs are likely to be negligible.

In adult SGNs our qPCR analysis of *Hcn* mRNA revealed expression of *Hcn1*, *2*, and *4* (**Fig. 3-1*B***). *Hcn1* was again the most highly expressed, with a significant increase in mRNA copy number relative to neonatal stages (**Fig. 3-1*A, B***). When normalized to *Hcn3*, the relative expression ratio was: *Hcn1:Hcn2:Hcn3:Hcn4*: 1000:300:1:100. The data suggest that HCN1 is the principle subunit at both neonatal and adult stages.

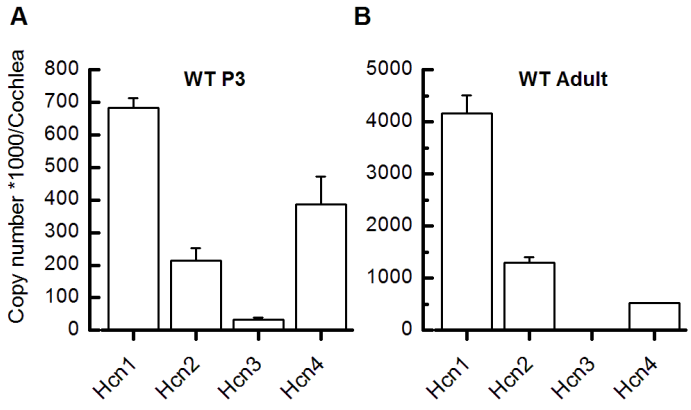

Figure 3-1. **Expression of *Hcn* mRNA in mouse SGNs.** Expression of *Hcn1-4* in neonatal (***A***) and adult (***B***) WT mouse SGNs. Quantitative RT-PCR was used to estimate the total mRNA copy number of *Hcn* genes present in both neonatal (P3) and adult stages (P ≥40). Neonatal SGN samples were collected from a pool of 24 whole cochleas. Adult SGN samples were obtained from a pool of 16 whole cochleas. Each preparation was run in triplicate. Results are shown as average total copies in thousands of *Hcn* mRNA transcripts per cochlea. Error bars represent standard error of the mean (SEM).

To examine I_h in spiral ganglion neuron (SGN) cell bodies, we used the whole-cell, tight-seal technique in the voltage-clamp configuration to record from organotypic SGN explants acutely excised from neonatal mouse cochlea (P1-8). In response to 4-sec hyperpolarizing voltage injections stepped from −74 mV to −144 mV in 10 mV increments from a holding potential of −84 mV, wild type (WT) SGNs exhibited slowly activating inward currents. A representative family of current traces is shown in **Fig. 3-2*A***, in which the slowly activating inward current was detected at potentials negative to −84 mV and was fully activated at potentials negative to −124 mV. This current profile

is characteristic of I_h in other neurons including SGNs (Chen, 1997; Mo and Davis, 1997; Yi et al., 2010) and was observed in every WT SGN we examined (n = 143).

To analyze the voltage-dependence of I_h in WT SGNs, activation curves were generated by fitting a Boltzmann function (equation 1) to tail currents plotted as a function of step potential (**Fig. 3-2*B***). Tail currents were measured at the instant of a step to −84 mV, very close to potassium equilibrium potential (E_K). At −84 mV, contamination from potassium currents was minimal and other voltage-dependent currents were deactivated. WT SGNs (n = 25) had a mean maximum conductance (G_h) of 2.3 ± 0.8 nS and half-activation voltage ($V_{1/2}$) of −97.1 ± 4.1 mV (range: −91.2 mV to −106.0 mV) with a slope factor (s) of 5.9 ± 0.6 mV (range: 5.0 to 7.2 mV). These activation parameters were similar to those previously reported for I_h activation in SGNs of various species (Chen, 1997; Szabó et al., 2002; Mo and Davis, 1997; Yi et al., 2010).

WT SGNs showed a developmental increase in the amplitude of I_h during the first postnatal week (**Fig. 3-2*D***). We measured G_h between P1 and P8 and found a gradual increase as a function of age. This developmental increase in G_h in WT SGNs also reflected graded expression of I_h along the cochlear tonotopic axis (**Fig. 3-2*C, D***). Comparison of G_h from apical and basal cells within same age groups (P1 to P4) revealed significantly larger G_h in basal than apical SGNs (**Fig. 3-2*D***). By the end of the first postnatal week the tonotopic gradient had diminished.

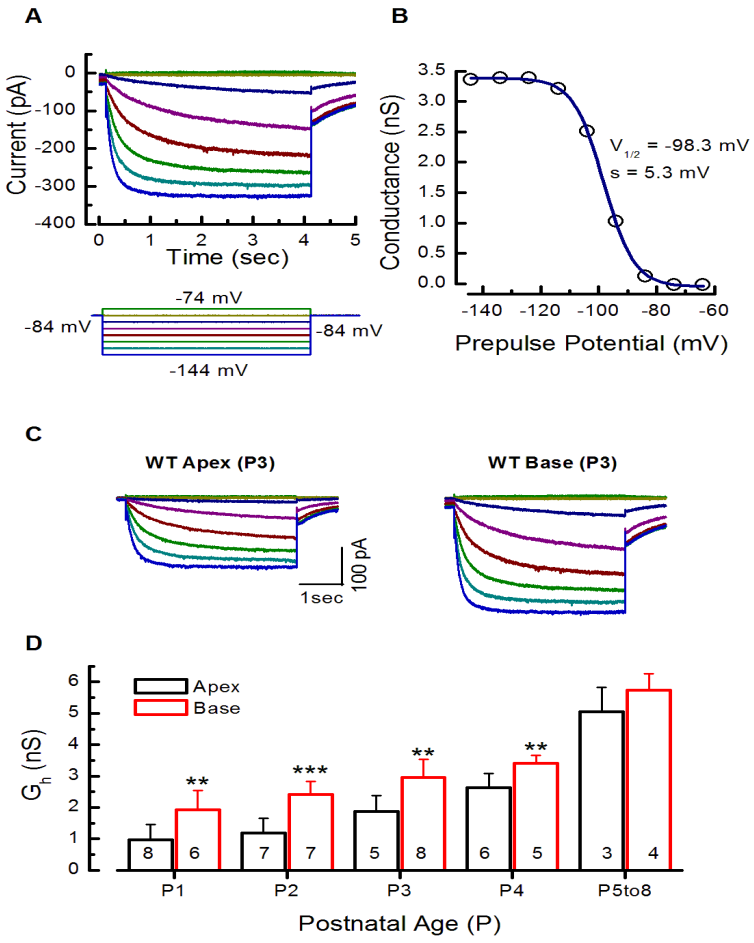

Figure 3-2. **I_h in spiral ganglion neurons.** ***A,*** Representative current traces recorded from a wild type (WT) spiral ganglion neuron (SGN) cell body (P3, base) in response to 4-sec voltage steps from a holding potential of −84 mV to potentials between −144 and −74 in 10 mV increments. The lower panel shows the voltage-clamp protocol. ***B,*** A representative activation curve for G_h generated from the tails currents shown in panel ***A***. Tails currents were divided by driving force (40 mV) and fitted with a Boltzmann function (black line, Eq. 1): $V_{1/2}$= −98.3 mV, s = 5.3 mV, and G_h = 3.4 nS. ***C***, Representative I_h traces of from apical and basal SGNs (P3) from the same cochlear explant. The scale bar applies to both current families. ***D,*** Mean maximal conductance (G_h) plotted as a function of postnatal (P) age and cochlear location (apex vs. base). Statistically significant differences (** $p < 0.01$; *** $p < 0.001$) indicated a tonotopic gradient (apex vs base) during the first postnatal week. There was also a gradual, yet significant ($p < 0.001$), increase in G_h during the first postnatal week (mean of P0-P4 relative to P5-P8). Number of samples is for each group is shown at the bottom.

I_h in neonatal SGNs is carried by HCN1, 2 and 4

To verify that the hyperpolarization-activated inward currents in WT SGN cell bodies were carried by HCN channels, we applied the HCN blocker ZD7288 during voltage-clamp recordings and measured the change in I_h. We applied either 10 or 100 μM ZD7288 in the external bath and found that 10 μM blocked 47 ± 16% (n = 4) of the current at −124 mV, while 100 μM blocked 92 ± 4% (n = 6; **Fig. 3-3**). Complete I_h block was achieved 15 min post 100 μM ZD7288 treatment and the effect was irreversible. To confirm that the ZD7288 effect was selective for I_h, we subtracted a family of currents recorded in the presence of 100 μM ZD7288 (**Fig. 3-3*B***) from control currents (**Fig. 3-3*A***) recorded prior to application of the drug. The subtracted currents (**Fig. 3-3*C***) revealed that the ZD7288-sensitive currents were nearly identical in amplitude and activation kinetics to the control currents. Importantly, the subtracted currents did not include properties of any other current, suggesting that 100 μM ZD7288 is specific for I_h in SGNs. Although we have shown ZD7288 to be an I_h-specific antagonist (BoSmith et al., 1993; Harris and Constanti, 1995), it does not distinguish amongst the four HCN subunits. Thus, we wondered which HCN subunits contribute to the biophysical properties of I_h in WT SGNs. A previous study indicated localization of HCN1 and 4 subunits in rat SGN cell bodies at P9-10 (Yi et al., 2010), however, functional evidence implicating specific HCN subunits was not reported. Another study reported the presence of all four HCN subunits in adult guinea pig SGN cell bodies (Bakondi et al., 2009) raising the possibility that all four HCN subunits may be present in WT mouse SGNs.

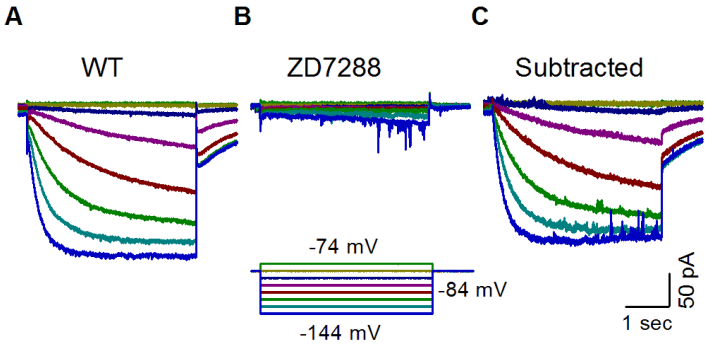

Figure 3-3. **I_h in SGNs is carried by HCN channels.** ***A, B,*** Representative currents recorded from a WT, P2, basal SGN in response to hyperpolarizing voltage steps before (***A***) and after (***B***) 100 µM ZD7288 bath application. Voltage-clamp protocol shown below. ***C***, Subtracted currents from data sets ***A*** and ***B*** show characteristics of I_h. The scale bar applies to all current families.

To determine whether the *Hcn* mRNA expression patterns (**Fig. 3-1**) were translated into physiological expression of I_h we recorded from SGNs excised from mice deficient in *Hcn1*, *Hcn2* or both. Since our data and several *in-situ* hybridization studies indicate very low expression levels of *Hcn3* mRNA (Ludwig et al., 1998; Moosmang et al., 1999), *Hcn3*$^{-/-}$ mice were not investigated. *Hcn4* is expressed in SGNs, however, *Hcn4*$^{-/-}$ mice are embryonic lethal (Stieber et al., 2003) and conditional *Hcn4*$^{-/-}$ mice are not available. Representative families of I_h recorded from SGNs of WT, *Hcn1*$^{-/-}$, *Hcn2*$^{-/-}$, and *Hcn1,2*$^{-/-}$ mice are shown in **Figure 3-4*A***. Inward currents indicative of I_h were present in SGNs harvested from mice of all four genotypes. Current amplitudes and activation kinetics were noticeably diminished in *Hcn1*$^{-/-}$ SGNs relative to WT. *Hcn2*$^{-/-}$

SGNs showed reduced current amplitudes, however, their current activation kinetics were not significantly different from WT. In *Hcn1,2*$^{-/-}$ SGNs, in which both *Hcn1* and *Hcn2* were deficient, I_h was significantly reduced.

Representative activation curves are shown in **Fig. 3-4*B***. Relative to WT controls, the mean G_h was significantly ($p < 0.01$) reduced in both *Hcn1*$^{-/-}$ and *Hcn2*$^{-/-}$ SGNs, indicating expression of both HCN1 and HCN2 subunits contribute to I_h at early postnatal stages. Reduction of G_h was most prominent in *Hcn1,2*$^{-/-}$ SGNs ($p < 0.001$). We suggest the larger reduction of G_h in *Hcn1,2*$^{-/-}$ SGNs is a consequence of simultaneous deletion of HCN1 and 2 subunits. The small residual I_h in *Hcn1,2*$^{-/-}$ was blocked by ZD7288, indicating the presence of other HCN subunits, most likely HCN4 (**Fig. 3-4*A***). In summary (**Fig. 3-4*C***), the data suggest a prominent role for HCN1 with minor contributions from HCN2 and perhaps HCN4.

Analysis of G_h activation curves from *Hcn* mutant mice revealed additional evidence suggesting involvement of HCN1, HCN2 and HCN4 subunits in neonatal SGNs (**Fig. 3-4*C* - *E***). The mean voltage of half-activation was shifted in the negative direction in both *Hcn1*$^{-/-}$ and *Hcn1,2*$^{-/-}$ SGNs relative to WT ($p < 0.001$). *Hcn2*$^{-/-}$ SGNs also showed a slight but significant ($p < 0.05$) negative shift in $V_{1/2}$, raising the possibility that HCN2 makes a minor functional contribution in neonatal SGNs. (**Fig. 3-4*D***). There were significant differences in the mean slope factors of *Hcn1*$^{-/-}$, *Hcn2*$^{-/-}$ and *Hcn1,2* $^{-/-}$ SGNs relative to WT further supporting involvement of both HCN1 and HCN2 in neonatal SGNs (**Fig. 3-4*E***).

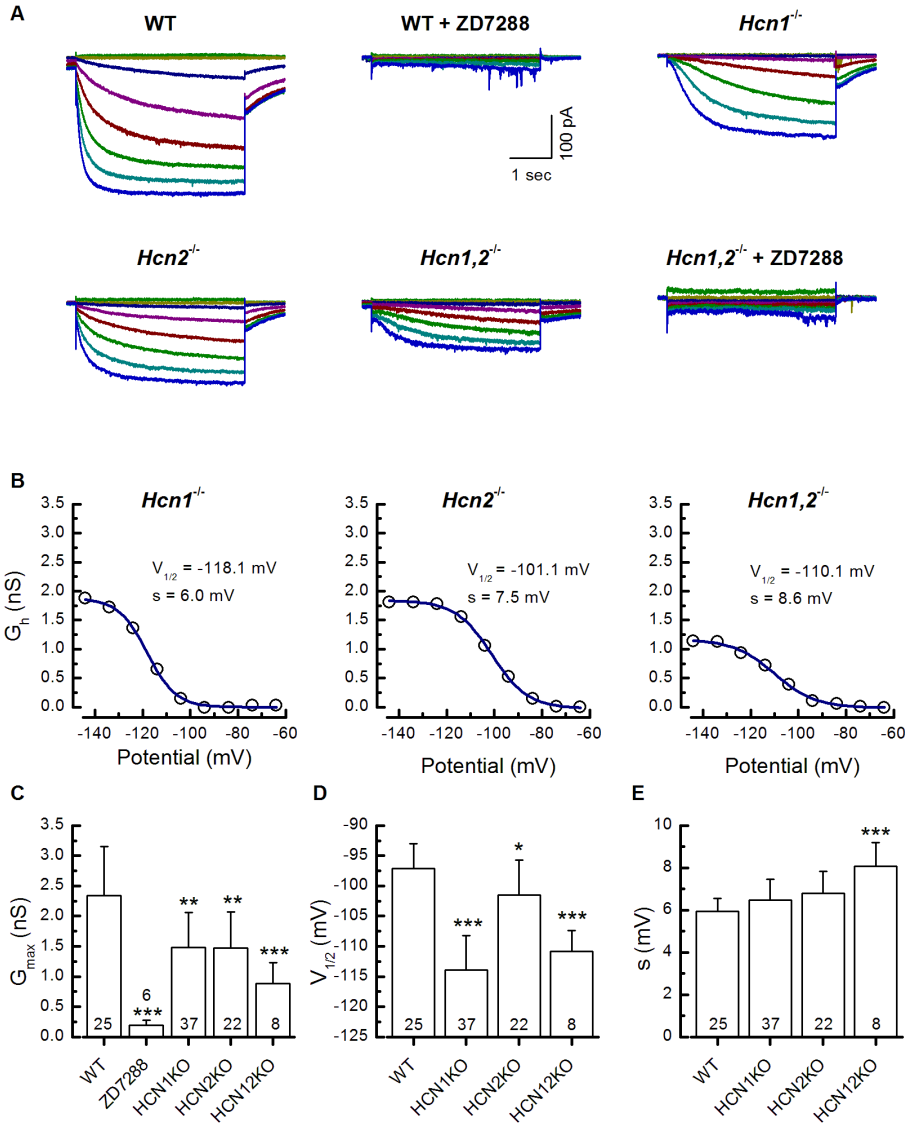

Figure 3-4. **Biophysical characterization of I_h in neonatal (P1-P4) WT and Hcn-deficient SGNs.** ***A***, Family of representative I_h from WT, WT + 100 µM ZD7288, *Hcn1*$^{-/-}$, *Hcn2*$^{-/-}$, and *Hcn1,2*$^{-/-}$ SGNs as indicated. Currents were evoked using the same voltage-clamp protocol shown in **Fig. 3-2**. Residual currents in *Hcn1,2*$^{-/-}$ SGNs was blocked by 100µM ZD7288. ***B,*** Representative G_h activation curves for *Hcn1*$^{-/-}$, *Hcn2*$^{-/-}$ and *Hcn1,2*$^{-/-}$ SGNs fitted with Boltzmann equations. $V_{½}$ and *s* are indicated on the graphs. ***C,*** Summary of mean maximal G_h. ***D,*** Summary of mean half-activation voltage and ***E,*** mean slope factor. Number of samples and genotype are indicated below. * $p < 0.05$; ** $p < 0.01$; *** $p < 0.001$.

The kinetics of I_h activation were measured from double exponential fits to currents evoked by steps to −144 mV (**Fig. 3-5*A***). Fast time constants (τ_{fast}) were significantly ($p < 0.001$) slower in both *Hcn1*$^{-/-}$ (393 ± 123 msec, n = 18) and *Hcn1,2*$^{-/-}$ (522 ± 99 msec, n = 8) SGNs, compared to WT (127 ±47 msec, n = 18) and *Hcn2*$^{-/-}$ (134 ± 57 msec, n = 19) SGNs (**Fig. 3-5*B***). Similarly, slow time constants (τ_{slow}) were significantly ($p < 0.05$) slower in both *Hcn1*$^{-/-}$ (2922 ± 2168 msec, n = 18) and *Hcn1,2*$^{-/-}$ (2993 ± 1970 msec, n = 8) compared to WT (799 ± 901; n = 7) and *Hcn2*$^{-/-}$ (951 ± 670 msec, n = 19).

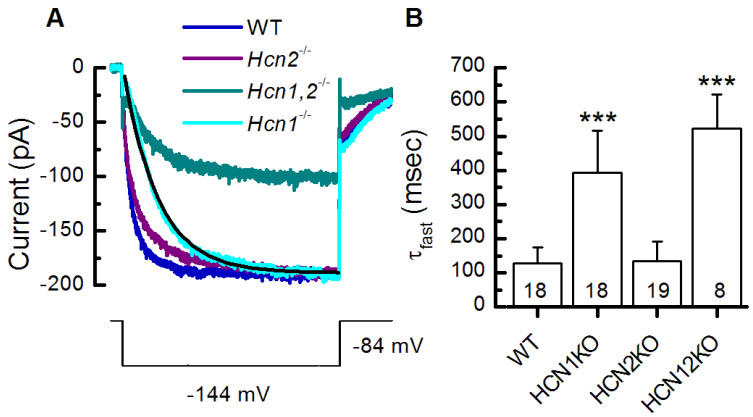

Figure 3-5. **I_h activation kinetics (τ_{fast}) comparison in WT vs. Hcn deficient SGNs (P1-P3).** ***A,*** Representative currents in WT, *Hcn1*$^{-/-}$, *Hcn2*$^{-/-}$, and *Hcn1,2*$^{-/-}$ in response to −144 mV voltage steps. I_h activation kinetics were measured by fitting a double exponential equation (Eq. 2, black lines). ***B,*** Summary of mean fast activation time constants for Number of samples and genotype are indicated below. *** $p < 0.001$.

In summary, the data from *Hcn*-deficient mice revealed I_h had significantly different biophysical properties in SGNs that lacked *Hcn1*. The differences included reduced current and conductance amplitudes, more negative $V_{1/2}$ values and slower activation kinetics. These differences suggest that HCN1 subunits contribute to the properties of I_h in SGNs. Interestingly, we found some differences in the properties of I_h in *Hcn2* $^{-/-}$ SGNs compared to WT, including reduction in G_h, a small negative shift in $V_{1/2}$ and a slight broadening of the activation curve, but no difference in kinetics, suggesting that the functional contributions of HCN2 to I_h in SGNs during early postnatal stages are minor relative to HCN1. Lastly, we suggest that small residual I_h in *Hcn1,2*$^{-/-}$ SGNs implies the presence of another HCN subunit. As *Hcn3* expression was shown to be minimal (**Fig. 3-1*A***), the small residual I_h is mostly likely due to expression of *Hcn4*.

I_h is modulated by cAMP

HCN channel activity can be modulated by intracellular cyclic nucleotides (DiFrancesco, 1986; DiFrancesco and Tortora, 1991). Previous work in auditory brainstem neurons has shown that cAMP shifts I_h activation towards more depolarized potentials and speeds up activation kinetics (Banks et al., 1993; Yamada et al., 2005). To examine cAMP modulation of I_h in SGNs we measured I_h activation following application of a membrane permeable cAMP analog, 8-Br-cAMP (200 μM), to the external bath (**Fig. 3-6*A***). In the presence of 8-Br-cAMP, the I_h activation range was shifted ($p < 0.001$) toward more depolarized potentials ($V_{1/2} = -88.5 \pm 0.6$ mV, n = 4) compared to control ($V_{1/2} = -95.3 \pm 0.3$ mV, n = 4) (**Fig. 3-6*B***), with no increase in the maximal conductance. The +7mV shift in $V_{1/2}$ in the presence of cAMP accounted for a

20% increase in I_h active at rest (~ −80 mV). Similar results were found in rat SGN afferent dendrites, in which application of 8-Br-cAMP (200 µM) resulted in 12 mV positive shift in $V_{1/2}$ (Yi et al., 2010).

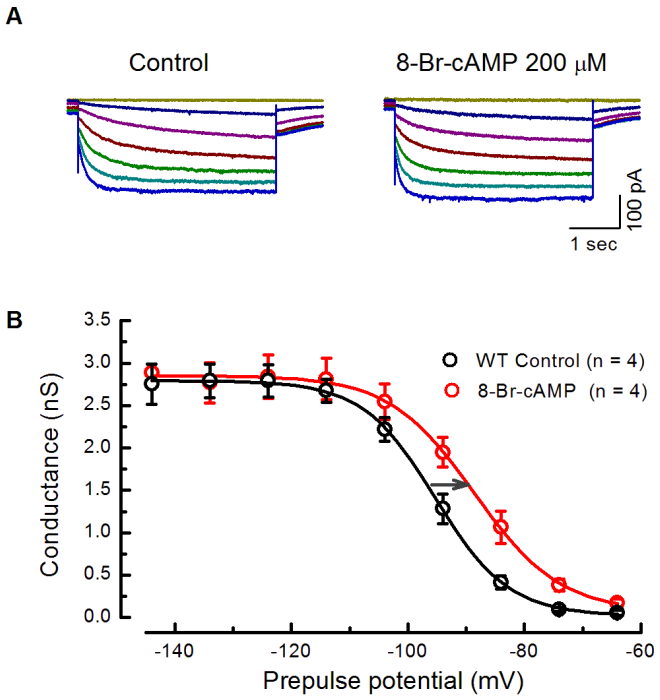

Figure 3-6. **Modulation of I_h voltage dependence by cAMP.** ***A,*** Representative I_h traces from WT SGNs (P4, apex) in control (left) and after bath application of 200 µM 8-Br-cAMP (right). Recordings were made in two different cells from the same SGN explant tissue. Currents were evoked using the same voltage-clamp protocol shown in **Fig. 3-2**. ***B,*** Mean voltage-dependent G_h activation curve from P3-P4 SGNs. Control (black line, n = 4); 200 µM 8-Br-cAMP (red line, n = 4). Data were fitted by a Boltzmann function. Note the shift in $V_{1/2}$ toward depolarized potentials with 8-Br-cAMP.

I_h in adult SGNs

We found a significant increase in the amplitude of I_h at adult stages, indicating developmental regulation (**Fig. 3-7*A***). Cultured WT SGNs (n = 11; Apex: n = 5; Base: n = 6) from adult mice P40 or older had a mean conductance of 13.4 ± 4.2 nS which represented a 6-fold increase in G_h compared to neonatal SGNs (P1-4, G_h = 2.3 ± 0.8 nS; n = 25). The tonotopic gradient in G_h expression during first postnatal week (**Fig. 3-2*D***) was absent at adult stages (apex: 15.1 ± 5.8 nS, base: 12.0 ± 1.9 nS, $p = 0.24$), $V_{1/2}$ (apex: −94.9 ± 3.8 mV, base: −92.3 ± 6.3 mV, $p = 0.44$), and s (apex: 7.8 ±1.8 mV, base: 7.8 ± 2.8 mV, $p = 0.93$).

Representative activation curves for adult WT and *Hcn* deficient SGNs are shown in **Fig. 3-7*B***. Relative to adult WT SGNs, adult *Hcn1*$^{-/-}$ SGNs had significantly ($p < 0.001$) reduced mean G_h (**Fig. 3-7*C***), while *Hcn2*$^{-/-}$ SGNs had G_h values similar to WT. The $V_{1/2}$ values of adult *Hcn1*$^{-/-}$ were also significantly ($p < 0.001$) hyperpolarized compared WT, while *Hcn2*$^{-/-}$ SGNs were not (**Fig. 3-7*B, D***). The slope factors were not significantly different between the three genotypes (data not shown). Activation kinetics of adult I_h were analyzed as described for neonatal I_h. Mean fast time constants (τ_{fast}) for WT, *Hcn1*$^{-/-}$ and *Hcn2*$^{-/-}$ SGNs are presented in **Fig. 3-7*E***. Interestingly, the activation kinetics (τ_{fast}) were significantly ($p < 0.01$) faster in adult WT neurons (57.3 ± 17.7 msec, n = 11) than in early postnatal neurons (127 ± 47 msec, n = 18). Yet, like the early postnatal cells, deletion of HCN1 subunits resulted in a significant slowing of I_h activation in adult SGNs (255.6 ± 67.3 msec, n = 6, $p < 0.01$), while deletion of HCN2 subunits did not have a significant effect on fast activation kinetics (43.2 ± 16.4 msec, n =

11) compared to WT. Likewise, mean slow activation time constants (τ_{slow}) were significantly ($p < 0.001$) prolonged in *Hcn1*$^{-/-}$ (2209 ± 1408 msec, n = 6) compared to WT (870 ± 699 msec, n= 11) and *Hcn2*$^{-/-}$ (611± 335 msec, n = 11). *Hcn1,2*$^{-/-}$ mice do not survive into adulthood and thus were not examined.

The adult qPCR data (**Fig. 3-1*B***) are consistent with the voltage-clamp data (**Fig. 3-7**) which showed significant reduction (~6-fold) of G_h in *Hcn1*$^{-/-}$ SGNs, supporting the notion that HCN1 is the principal subunit contributing to I_h function in WT adult SGNs.

In summary, genetic deletion of *Hcn1* had qualitatively similar effects in neonatal and adult SGNs, indicating that HCN1 subunits are major components of I_h channels in both early postnatal and adult SGNs. Deletion of *Hcn2* was without significant effect at adult stages, raising the possibility that HCN2 contributions to SGN cell bodies may be transient. Doubly deficient *Hcn1,2*$^{-/-}$ mice did not live to adult stages, yet the similarity between residual I_h in neonatal *Hcn1,2*$^{-/-}$ SGNs and the small residual I_h in adult *Hcn1*$^{-/-}$ SGNs suggests the presence of additional HCN subunits, mostly likely HCN4 based on the qPCR analysis. The faster I_h activation kinetics at adult stages suggests that additional factors, perhaps intrinsic differences in endogenous cAMP levels, may also contribute to I_h function in adult SGNs.

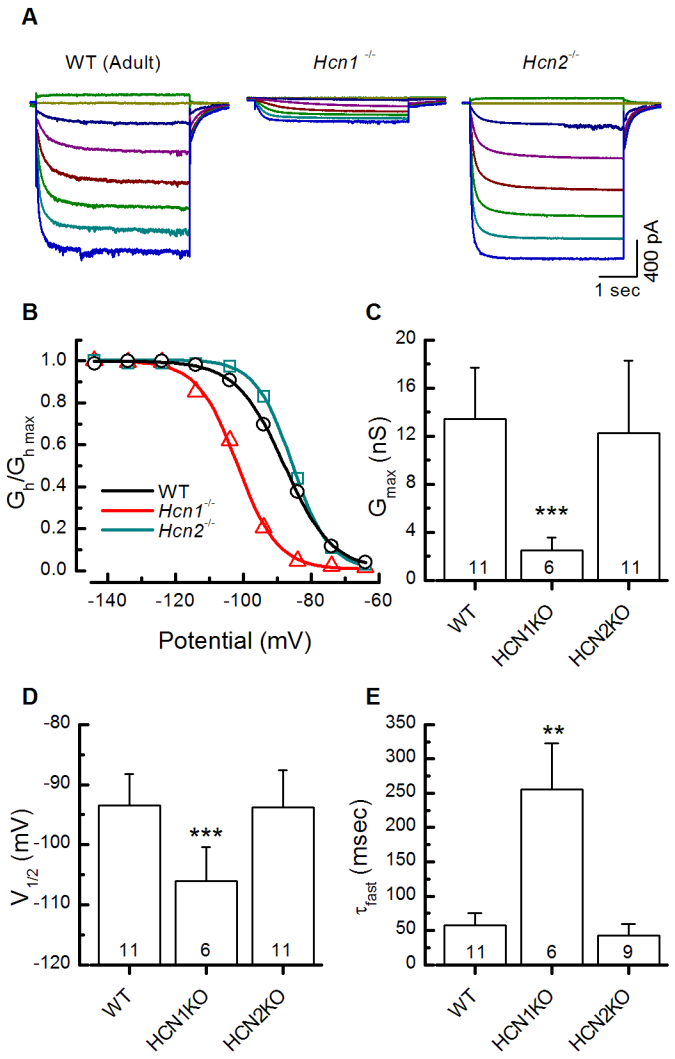

Figure 3-7. **I_h expression in cultured adult SGNs.** ***A***, Family of representative I_h traces from adult (P ≥ 40, base) WT, *Hcn1*$^{-/-}$, and *Hcn2*$^{-/-}$ SGNs. ***B,*** Normalized I_h activation curves generated by fitting a Boltzmann function to tail currents shown in ***A***. Note the hyperpolarized half-activation voltage shift in *Hcn1*$^{-/-}$ SGNs (red trace) compared to WT (black trace) and *Hcn2*$^{-/-}$(green trace). ***C***, Summary of conductances and half-activation voltages (***D***) for 11 WT, 6 *Hcn1*$^{-/-}$, and 11 *Hcn2*$^{-/-}$ SGNs. ***E***, Summary of I_h fast activation time constants. ** $p < 0.01$; *** $p < 0.001$

I_h contributes to resting potential

To examine the functional contributions of I_h to SGN membrane responses, we recorded from neonatal SGNs (P1-8) in current-clamp mode. Application of ZD7288 resulted in significant ($p < 0.05$) hyperpolarization of WT SGN resting membrane potentials (**Fig. 3-8*A, B***). The mean resting membrane potentials before and after bath application of 100 μM ZD7288 revealed a 6 mV hyperpolarization. The hyperpolarized resting membrane potential following ZD7288 treatment was similar to that of *Hcn1*$^{-/-}$ SGN resting membrane potentials (**Fig. 3-8*A***), while there was no significant difference in *Hcn2*$^{-/-}$ or *Hcn1,2*$^{-/-}$ SGNs. The data suggest that HCN1 subunits contribute depolarizing current that shifts the WT SGN resting membrane potential in the excitatory direction. The lack of resting potential effect in the *Hcn1,2*$^{-/-}$ SGNs was unexpected, but may be a result of compensatory upregulation of HCN4 subunits or some other depolarizing current as a consequence of genetic deletion of both *Hcn1* and *Hcn2* .

I_h contributes to sag and rebound potentials

To examine the contributions of I_h to membrane responses evoked by small input currents we injected 5 pA hyperpolarizing currents for 2 seconds in WT SGNs. The membrane responded with a small fast hyperpolarization followed by a depolarizing "sag", which returned the membrane potential toward the resting level (**Fig. 3-8*B***). The 5-pA current injections were sufficient to produce prominent sag, while ensuring that the cell did not hyperpolarize negative to the physiological range, ~ −100 mV. The depolarization sag developed over ~150 msec, which reflected the slow activation

kinetics (τ_{fast}) of WT I_h (**Fig. 3-5**). At the termination of the hyperpolarizing current step, a prominent rebound potential (10-15 mV, n = 11) was evident (**Fig.3-8*B***, black trace).

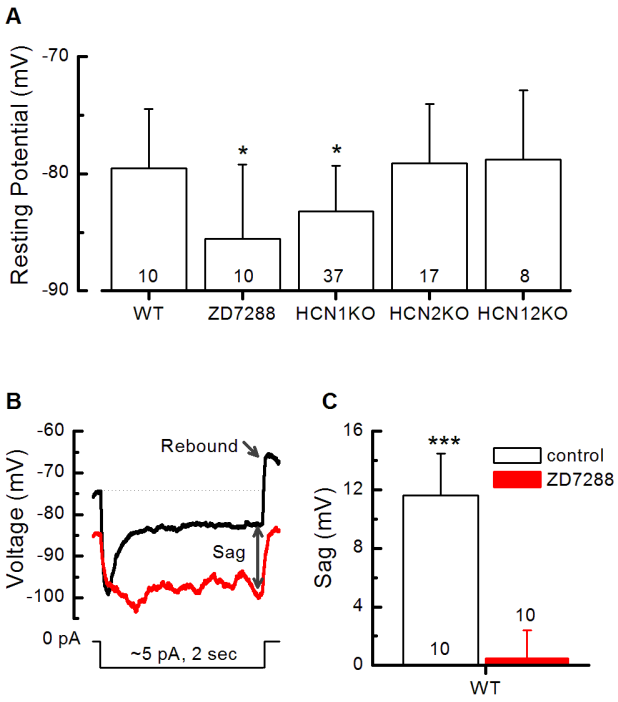

Figure 3-8. **I_h contributes to neonatal (P1-P4) SGN membrane responses.** ***A,*** Comparison of resting membrane potential (V_{rest}) before and after treatment with 100 µM ZD7288 in WT SGNs. Note that ZD7288 hyperpolarizes WT SGN V_{rest} to potentials comparable to that of *Hcn1*$^{-/-}$ SGNs. ***B,*** Representative current-clamp recordings in WT SGNs (P3) in response to 2-sec hyperpolarizing current (5 pA) injections. Note the depolarizing sag and rebound potential at the end of hyperpolarizing current step in the control condition (black trace). In the presence of 100 µM ZD7288, the depolarization sag and rebound potential are abolished (red trace). ***C,*** Quantification of sag amplitude before and after treatment with 100 µM ZD7288 from the same cells. Sag amplitude was measured as the difference between the peak hyperpolarization and the steady-state potential near the end of the current step. * $p < 0.05$; *** $p < 0.001$.

In order to confirm whether these membrane responses were the result of I_h, we blocked I_h with bath application of 100 μM ZD7288 (**Fig. 3-8*B***). ZD7288 hyperpolarized the resting potential and abolished the depolarization sag (**Fig. 3-8*B*,** red trace) with a difference of 11.6 ± 2.8 mV (n = 10) relative to control (**Fig. 3-8*C***). The sag was measured as the difference between the peak hyperpolarization and the steady-state potential near the end of the current step (**Fig. 3-8*B***). The rebound potential was also abolished in the presence of ZD7288, indicating the contribution of I_h at the offset of the current step (**Fig. 3-8*B***, red trace).

I_h contributes to SGN firing properties

The preceding data showed the involvement of I_h in shaping membrane responses to small current injections. Next, we investigated the functional contributions of I_h to action potential (AP) firing in WT cells and in cells exposed to ZD7288. We used two different current-clamp conditions. In the first condition, APs were evoked from rest (I=0) by injection of depolarizing currents in 2 pA increments. In the second condition, APs were evoked at the termination of 2-sec membrane hyperpolarization to physiological levels (i.e. not exceeding −100 mV). In both conditions, AP threshold and latency were measured in the same cell before and after ZD7288 treatment. The current-clamp protocols were designed to allow systematic comparison of I_h contributions to SGN firing properties at rest where HCN channels are partially active, and following hyperpolarization when HCN channels are maximally activated within the physiological range.

As shown in **Figure 3-9*A* & *B***, an initial spike (at the onset of a depolarizing step) and a rebound spike (at the offset of a hyperpolarizing step) were evoked both before and after ZD7288 treatment. We found no significant difference in threshold for either the initial spike or the rebound spike, although the current required to evoke rebound spikes was less than that required for the initial spike (data not shown).

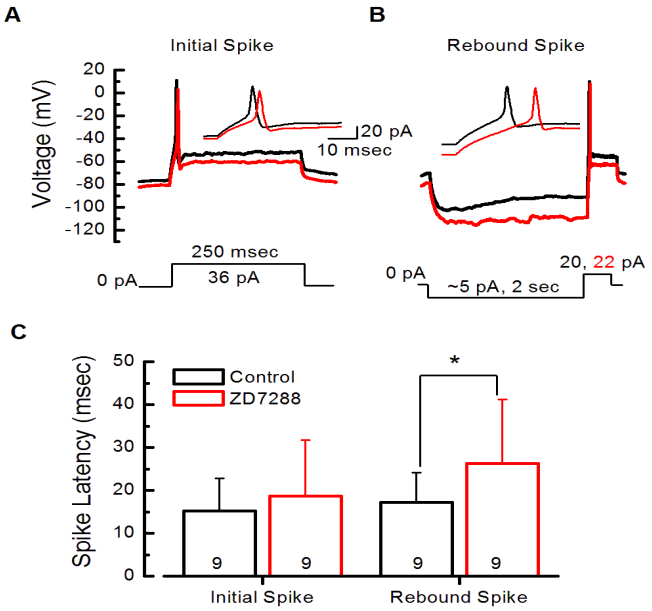

Figure 3-9. **I_h modulates firing properties in SGNs.** ***A,*** Representative traces (P1, apex) showing AP firing in WT SGNs in two different conditions. An initial spike was evoked from resting membrane potential (I=0) by injecting depolarizing currents in 2-pA increments until threshold was reached (current-clamp protocol below). ***B,*** Representative rebound spikes (P1, apex) were evoked after hyperpolarization of the membrane to potentials within the physiological range (≥ -100 mV). Both initial spikes and rebound spikes were examined in the same cell. For each condition, representative recordings obtained in control (black trace) and in the presence of 100 µM ZD7288 (red trace) were superimposed for comparison. The inset shows the same spike pairs on an expanded time scale. ***C,*** Comparison of spike latency for initial spikes and rebound spikes (P1-P3), before (white column) and after 100 µM ZD7288 application (red column). * $p < 0.05$.

Spike latency, however, was significantly delayed for the rebound spike following treatment with ZD7288. Latency was measured as the time from the current step to the peak of first spike. There was a slight delay in the initial spike following ZD7288 exposure, but the latency difference post ZD7288 treatment (16.5 ± 7.7 msec, n = 9) was not statistically significant compared to control (15.2 ± 7.6 msec, n = 9; $p = 0.08$) (**Fig. 3-9*A*** inset, ***B*, *C***). On the other hand, there was a significant delay in the rebound spike in ZD7288 treated cells ($p = 0.02$) compared to control (**Fig. 3-9*A*** inset, **3-*B, C***). Blockage of I_h delayed the rebound spikes on average by 9.1 ± 9.6 msec.

To investigate the possibility that the delay in the rebound spike may have been affected by activation of low-voltage-activated calcium channels we used bath application of the calcium channel blockers, nickel (100 μM) or Mibefradil (2 μM), either alone or together with 100 μM ZD7288. Neither nickel nor Mibefradil alone affected rebound spike latency, as no difference was found before (control) and after treatment (**Fig. 3-10*A*-*C***). However, when ZD7288 was added subsequently, there was a significant ($p < 0.01$) delay in the rebound spike, again indicating that I_h and not low-voltage-activated calcium channels, is a significant contributor for rebound spike timing in SGNs (**Fig. 3-10*A*-*C***).

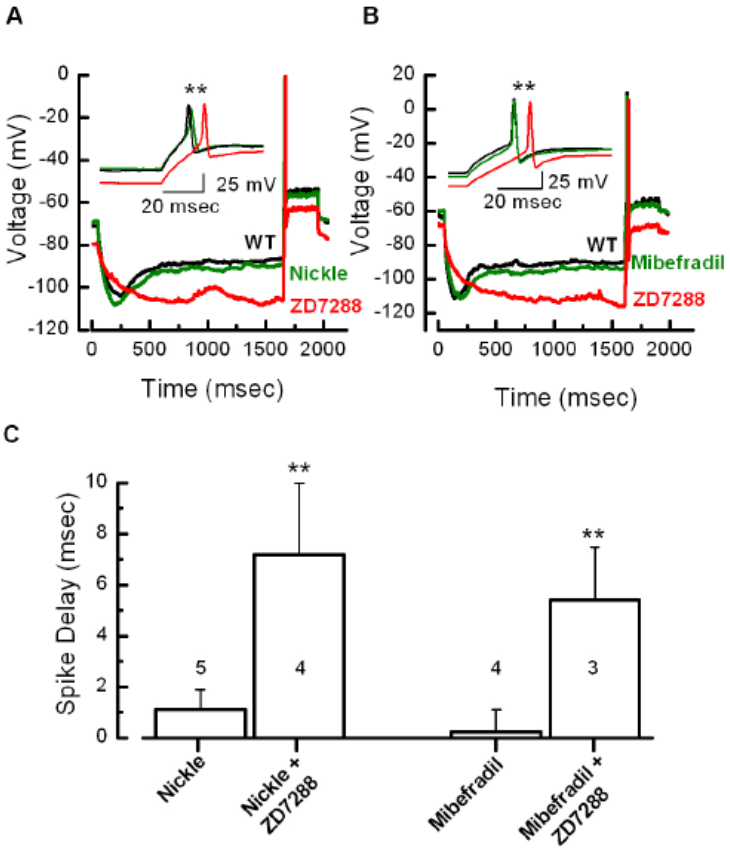

Figure 3-10. **I_h regulates rebound spike latency.** ***A,*** Representative traces of rebound spikes recorded from a WT SGN (P3, base) in three different conditions, control, 100 µM nickel and both nickel and 100 µM ZD7288. Note that calcium channel blocker, nickel, had little effect on resting membrane potential, sag potential and rebound spike latency (inset). Subsequent block of I_h by ZD7288, however, abolished the depolarizing sag and delayed the rebound spike (inset). ***B,*** Representative traces of rebound spikes recorded in WT control conditions, with 2 µM Mibefradil and with Mibefradil and 100 µM ZD7288. Here again, the T-type calcium channel blocker had little effect on resting membrane potential, sag potential and rebound spike latency (inset), while ZD7288 hyperpolarized the cell, blocked the sag potential and delayed the rebound spike. **C**, Spike delay was measured as the difference between spike peaks in WT control conditions and after application of the drugs indicated below. Number of cells is indicated on the bar graph. ** $p < 0.01$.

To investigate whether the I_h effect on resting potential, sag potential and spike latency were due to HCN1 or HCN2 we examined adult SGNs of WT, *Hcn1*$^{-/-}$ and *Hcn2*$^{-/-}$ mice. SGNs from adult *Hcn1*$^{-/-}$ mice had resting potentials that were significantly more hyperpolarized than both WT and *Hcn2*$^{-/-}$ SGNs (**Fig. 3-11*A***). Hyperpolarizing current steps evoked a prominent sag (**Fig. 3-11*B***) that decayed more quickly than the sag recorded from neonatal SGNs (**Fig. 3-8*B***), consistent with the faster I_h activation kinetics in adult SGNs (**Fig. 3-7*E***). The amplitude of the sag potential was also significantly reduced in adult *Hcn1*$^{-/-}$ SGNs relative to WT and *Hcn2*$^{-/-}$ SGNs (**Fig. 3-11*C***). Lastly, we noted a delay in rebound spike latency in adult *Hcn1*$^{-/-}$ SGNs (**Fig. 3-11*B, D***), which confirms a prominent role for HCN1 in spike timing in adult SGNs.

I_h contributes to synchronized firing

To address the extent to which tonically active I_h contributes to action potential (AP) firing, we delivered a series of 20 AP threshold current steps in WT SGN cell bodies before and after bath application of 100 μM ZD7288. Before ZD7288 treatment, SGNs exhibited little variation in spike latency for a threshold stimulus (**Fig. 3-12*A***, black traces). After application of ZD7288, we found both an AP delay and a larger distribution in spike latency (**Fig. 3-12*A***, red traces), suggesting that I_h active at rest contributes to the regularity of spike timing. To examine the contributions of I_h to the action potential wave form, the spikes shown in **Fig. 3-12*A*** were aligned with their peaks at time zero and averaged. The averaged spikes before and after application of ZD7288 (**Fig. 3-12*B***) revealed that I_h functions to speed the depolarization to threshold and depolarize the membrane during the after hyperpolarization, but does not affect the peak

or rising/falling phases of the AP. Spike latency was also delayed and with greater distribution for small superthreshold stimuli of 30 to 40 pA (**Fig. 3-12*C***) but the effect was absent for larger stimuli (≥ 50pA). The data support the notion that I_h helps shape the membrane response to small current steps, has significant impact on AP latency, and functions to enhance synchronized firing in response to small depolarizing stimuli.

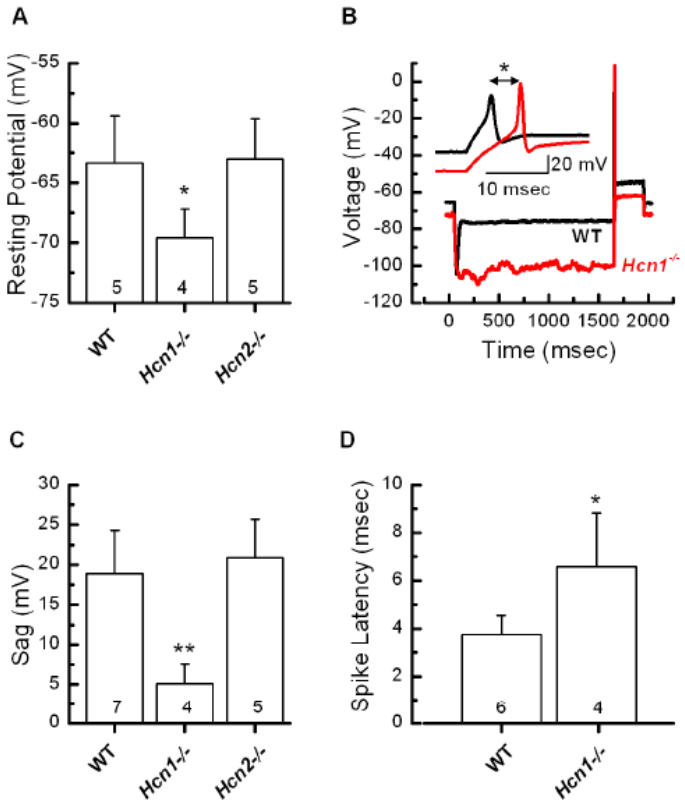

Figure 3-11. **HCN1 contributes to membrane properties in adult SGNs.** ***A,*** Mean resting potentials recorded from 14 adult SGNs of the indicated genotypes. Number of cells for each genotype is indicated below. * $p < 0.05$. ***B,*** Representative membrane responses to hyperpolarizing currents steps recorded from adult WT (black trace) and *Hcn1*$^{-/-}$ (red trace) SGNs. The inset shows the rebound spike on an expanded time scale. ***C***, Sag potential was significantly (** $p < 0.01$) diminished in adult *Hcn1*$^{-/-}$ SGNs. ***D,*** Mean rebound spike latency for adult *Hcn1*$^{-/-}$ SGNs showed a significant delay relative to WT SGNs (* $p < 0.05$).

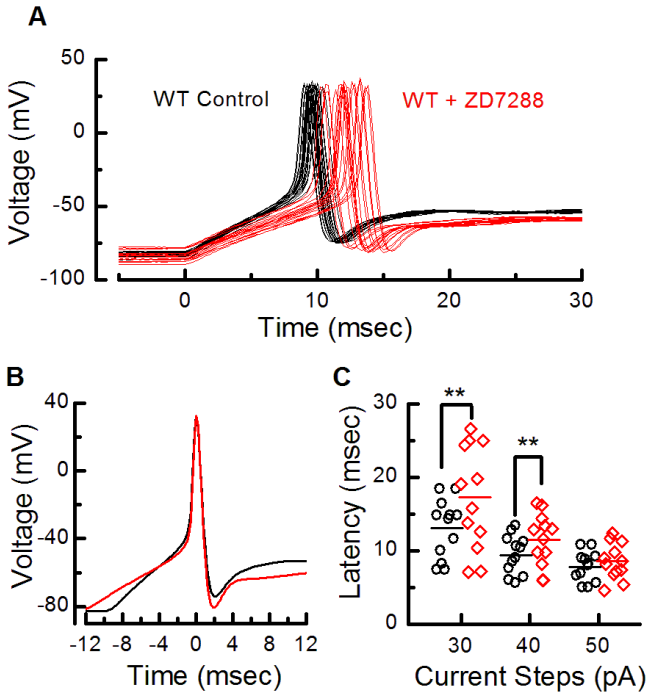

Figure 3-12. **I_h contributes to synchronized AP firing in response to small depolarizing currents.** ***A***, Representative action potentials measured from the same WT SGN (P4, apex) before (black traces) and after treatment with 100 µM ZD7288 (red traces). For each condition, a series of 20 action potentials were evoked using threshold current steps. Note the delay and larger distribution in spike latency after application of ZD7288. ***B,*** Representative averaged (P4, apex) spike waveforms before (black trace) and after ZD7288 (red trace). Spikes were aligned with their peaks at time zero and averaged. ***C,*** Scatter plot showing spike latency for three different current injections from the same 12 cells (P1-P4), before (black symbols) and after treatment with 100 µM ZD7288 (red symbols). The mean latency is indicated by horizontal lines. Note the variation in spike latency is significantly increased for small depolarizing current steps (30 & 40 pA) in the presence of 100 µM ZD7288 but is minimal for larger steps (≥ 50pA). Confidence interval (CI 95 %) of mean difference was used to quantify the degree of variation in spike latency before and after treatment with ZD7288. 30 pA: 1.55 < CI 95 % < 6.83 msec; 40 pA: 0.93 < CI 95 % < 3.18 msec; 50 pA: 0.28 < CI 95 % < 1.70 msec.

I_h contributes ABR latency

Given that the results presented in the previous sections show HCN1 subunits carry a significant fraction of I_h in both neonatal and adult SGNs and that I_h contributes to resting membrane potential, spike latency and synchrony, we wondered whether I_h may contributed to auditory processing. Behavioral deficits in auditory function have not been reported in previous studies of *Hcn* deficient mice (Herrmann et al., 2007; Ludwig et al., 2003; Nolan et al., 2003; 2004). As none of these prior studies focused on auditory function, we decided to measure auditory brainstem responses (ABR) to sound stimuli in adult *Hcn1*$^{-/-}$ mice and their WT littermate controls. We restricted our analysis to the first peak of the ABR waveform which represents the summed activity of the 8th cranial nerve. Relative to WT littermate controls, *Hcn1*$^{-/-}$ mice showed no difference in threshold (**Fig. 3-13*A***) or amplitude (**Fig. 3-13*B***) indicating that auditory sensitivity and the number of responsive SGNs was unaffected. However, we did notice that *Hcn1*$^{-/-}$ mice showed longer compound AP latencies at several stimulus intensities (**Fig. 3-13*C***). As temporal fidelity is a critical parameter for auditory processing, we suggest that differences in latency at the level of the single SGN action potential and in the ABR waveform may have significant consequences for normal sound processing.

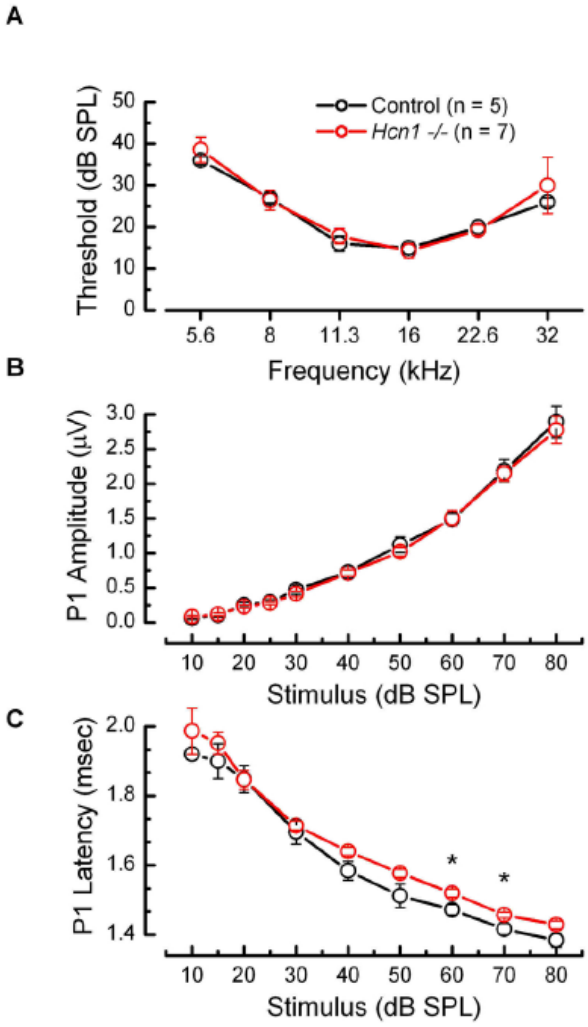

Figure 3-13. Hcn1*$^{-/-}$ animals have delayed ABR latency.** ***A, Mean auditory brainstem response (ABR) thresholds for control and *Hcn1*$^{-/-}$ animals at 6-7 weeks of age. ***B,*** Mean wave 1 (P1) amplitude and ***C***, mean wave 1 (P1) latency responses evoked by 16 kHz tone pips delivered across increasing sound stimulus intensity. Note that *Hcn1*$^{-/-}$ mice show delayed P1 latency relative to controls, while no significant difference was found in threshold (***A***) or amplitude (***B***).

DISCUSSION

We characterized I_h in SGN cell bodies harvested from neonatal (P1-8) and adult (≥ P40) mice, using whole-cell, tight-seal technique. Biophysical analysis of I_h in WT and *Hcn*-deficient mice indicated a prominent role for HCN1 subunits as major carriers of I_h in SGNs. *Hcn1*$^{-/-}$ SGNs exhibited significantly reduced conductances (G_h), hyperpolarized half-activation voltages ($V_{1/2}$), and slow activation kinetics (τ_{fast}). qPCR analysis of *Hcn* mRNA revealed strong expression of *Hcn1* in both neonatal and adult SGNs, strengthening the notion that HCN1 is a major functional subunit underlying I_h in SGNs. I_h in SGNs is partially active at the cell's resting membrane potential and its activation increases with hyperpolarization. Here we present evidence that I_h contributes to SGN resting membrane potentials and firing properties, as blockage of I_h hyperpolarized the resting potential, abolished depolarization sag potentials, delayed rebound spikes and increased variance in spike latencies. Furthermore, *Hcn1*$^{-/-}$ mice showed longer ABR latencies, further supporting the view that HCN1 subunits contribute to action potential firing patterns and high fidelity auditory information transfer between the periphery and the brain.

SGN I_h is developmentally regulated

Spiral ganglion neurons express various voltage-dependent currents (Adamson et al., 2002; Chen et al., 2011) in a manner that may serve to enhance developmental mechanisms throughout the first postnatal week until the onset of hearing, P10-P12 (Romand, 1983). Consistent with this notion, we found that I_h in SGNs is developmentally regulated. Whole-cell voltage-clamp recordings from WT SGN cell

bodies revealed a gradual increase in G_h over the first postnatal week. Due to myelination of SGN cell bodies (Echteler, 1992; Romand and Romand, 1987), which presents a technical limitation for whole-cell electrophysiological recordings, we did not attempt to record from SGNs beyond postnatal day 8, a time point after which myelination becomes prohibitively thick and the bony labyrinth encapsulating SGNs becomes fully calcified. While our recording time frame (P1-8) does not provide the full view of SGN I_h development, it did reveal a clear pattern leading up to the onset of hearing. Because synaptogenesis and mature innervation patterns between IHCs and SGNs are nearly complete by the end of the first postnatal week (Pujol et al., 1998; Simmons et al., 1991), it is likely that early postnatal development of I_h in SGNs impacts maturation of the auditory system prior to the onset of hearing.

The lack of I_h data around the onset of hearing raises the possibility that the developmental trend we noted is a transient phenomenon. However, our data from cultured adult SGNs indicate that I_h expression is sustained into adulthood. Previous studies, which showed the presence of I_h in dissociated adult guinea pig SGN culture (Chen, 1997; Szabó et al., 2002) support this view.

Tonotopic expression of I_h in SGNs

An important task of the auditory system is decomposing complex sound into constituent frequencies along the tonotopic axis of the organ of Corti. Inner hair cells (IHCs) located in the basal part of the cochlea encode high frequency sound, whereas those located in the apical region encode low frequency sound. The tonotopic specialization is retained at each level along the ascending auditory pathway, including

spiral ganglion neurons which are organized to reflect the tonotopic arrangement of IHCs (Rubel and Fritzsch, 2002). To enable this tonotopic arrangement, SGNs are equipped with morphological and electrophysiological specializations, including graded expression of voltage-gated channels (Adamson et al., 2002; Chen et al., 2011; Lv et al., 2010; 2012).

In the present study, we found that I_h in neonatal WT SGNs is also graded along the cochlear tonotopic axis, with greater I_h amplitudes in neurons from the basal end of the cochlea. Considering the graded expression of other voltage-gated channels in neonatal SGNs (Adamson et al., 2002; Chen et al., 2011), it seems I_h follows this trend. However, because the cochlea develops from base to apex, we cannot exclude the possibility that the graded I_h expression we report here for neonatal SGNs might be a transient phenomenon reflecting the developmental lag between the cochlear base and apex. Indeed, at adult stages we noted little difference between I_h of basal and apical SGNs. Nonetheless, if larger I_h in SGNs from the basal, high frequency end persists in the interval between P8 and more mature stages, we predict it will contribute to enhanced spike timing. Similar trends have been shown in neurons of the medial nucleus of trapezoid body (MNTB), higher order auditory neurons in the brainstem, in which graded I_h expression with high to low expression along the medio-lateral (high to low frequency) axis results in a gradient of time delays in neuronal firing (Leao et al., 2006).

Characterization of I_h in mouse spiral ganglion neurons

The biophysical properties of I_h in WT SGNs in the present study are consistent with those previously reported for I_h in the auditory system, including SGNs (Chen, 1997; Mo and Davis, 1997; Szabó et al., 2002; Yi et al., 2010) and auditory brainstem neurons

(Bal and Oertel, 2000; Banks et al., 1993). WT SGN I_h was a ZD7288-sensitive, slowly-activating, non-inactivating inward current evoked by hyperpolarizing voltage steps. SGN I_h was active at the cell's resting potential and its activation range was well fit by Boltzmann functions with parameters ($V_{1/2}$ = –97 mV, s = 6 mV) similar to those reported for SGN I_h in previous studies of various rodent species (guinea pig: $V_{1/2}$ = −101 mV, s = 9 mV, Chen, 1997; $V_{1/2}$ = −104 mV, s = 6 mV, Szabó et al., 2002; mice: $V_{1/2}$ range= −83 to −109, s range = 7.6 to 13.1 mV, Mo and Davis, 1997; rat: $V_{1/2}$ = −104 mV, s = 11 mV, Yi et al., 2010). These biophysical and pharmacology properties are consistent with the notion that I_h in SGNs is carried by HCN subunits. Although one prior study presented immunolocalization data suggesting the presence of HCN1, HCN2 and HCN4 subunits in rat SGNs (Yi et al., 2010), none presented definitive physiological evidence identifying the precise HCN subunits involved.

Expression of HCN1, 2 and 4 in neonatal SGNs

Given their complex heterogeneous biophysical properties, identification of HCN subunits mediating SGN I_h is challenging, yet critical for a comprehensive understanding of their functional relevance. Through q-PCR analysis and examination of biophysical properties of I_h in *Hcn*-deficient animals, we demonstrated that I_h in neonatal SGNs is carried by HCN1, 2 and 4 subunits, with HCN1 being the most prominent subunit. Deletion of *Hcn1* resulted in significant reduction in I_h, hyperpolarized half-activation voltage and slower activation kinetics. The biophysical differences we noted in neonatal *Hcn1*-deficient SGNs are consistent with those of HCNs expressed in various heterologous systems. Homomeric HCN1 channels have the fastest activation kinetics

and most depolarized half-activation range (Altomare et al., 2003; Ishii et al., 2001; Santoro et al., 2000), while homomeric HCN4 channels show the slowest activation kinetics (Ishii et al., 2001; Ludwig et al., 1999). Homomeric HCN2 channels exhibit activation kinetics intermediate to HCN1 and HCN4 (Ludwig et al., 1999). In our study, I_h in *Hcn2*$^{-/-}$ SGNs had reduced amplitudes and a negative shift in the half-activation voltage, however, the differences were not as striking as those between *Hcn1*$^{-/-}$ and WT SGNs, suggesting that the functional contributions of HCN2 subunits are minor. The low expression levels of *Hcn2* mRNA in neonatal SGNs also suggested a small contribution from *Hcn2*. Previous immunolocalization work (Yi et al., 2010) demonstrated HCN2 immunoreactivty in P20 rat SGNs, but earlier time points were not examined. Thus, it is unclear whether there are actual differences in the temporal expression pattern of HCN2 or differences between rodent species. Yi et al. (2010) also reported robust expression of HCN1 and HCN4 in rat SGN cell bodies at P9-10. Their HCN1 and HCN4 localization data are consistent with our qPCR and electrophysiolgical data and both studies suggest contributions from HCN1 and HCN4 prior to the onset of hearing at P10-P12.

HCN1 contributes to I_h in adult SGNs

Analysis of mRNA expression in neonatal SGNs indicated that *Hcn1* is most abundantly expressed subunit followed by *Hcn4* and *2*. Strong *Hcn1* expression persisted into adult stages, suggesting HCN1 as the major subunit in adult SGNs. Our qPCR data are in agreement with *Hcn1* gene expression results from the SHIELD database (Shared Harvard Inner-Ear Laboratory Database, https://shield.hms.harvard.edu; Lu et al., 2011). This database incorporates RNA gene chip sequencing information from SGNs harvested

from mice expressing GFP under an SGN-specific MafB promoter at several developmental time points (E16, P0, P4, P7, P16). Among the three *Hcn* genes (*Hcn1*, *Hcn2*, and *Hcn3*) examined, *Hcn1* showed the strongest signal with a gradual developmental increase, consistent with our findings.

The strongest evidence supporting a prominent role for HCN1 in adult SGNs is derived from our voltage-clamp data which showed a ~80% reduction in G_h in SGNs from adult *Hcn1*$^{-/-}$ mice relative to WT. There was also significant difference in half-activation voltage and activation kinetics (τ_{fast}) relative to WT, strengthening the notion that HCN1 is indeed a major subunit contributing to I_h function in adult SGNs. There was no difference in I_h of adult SGNs from *Hcn2*$^{-/-}$ mice relative to WT, suggesting HCN2 does not contribute at adult stages. The qPCR data suggested expression of *Hcn4* at adult stages, however, in the absence of electrophysiological data supporting this result we are reluctant to draw conclusions about functional contributions of *Hcn4* in adult SGNs.

I_h contributes to SGN membrane potential

I_h has been shown to contribute to resting membrane potentials by providing inward current at rest. We demonstrated I_h has a similar role in resting membrane potentials in SGN cell bodies, as acute block of I_h with ZD7288 resulted in significant resting potential hyperpolarization (−6 mV) in WT SGNs. Similar results were reported for postnatal rat SGN dendrites, which had a −4 mV hyperpolarization after ZD7288 treatment (Yi et al., 2010). I_h contribution to resting potential has been also observed in higher order auditory neurons, such as cochlear nucleus and inferior colliculus, where

inhibition of I_h resulted in similar resting membrane potential hyperpolarization (Bal and Oertel, 2000; Koch and Grothe, 2003; Nagtegaal and Borst, 2010).

In WT neurons depolarization of the resting membrane potential is due to tonic activation of I_h at rest. Based on the SGN I_h activation curve, we estimate that ~5% of I_h is active at rest at neonatal stages and ~20% at adult stages, suggesting an I_h contribution may be greater at adult stages. Because the reversal potential of I_h in SGNs is more positive than the cell's resting membrane potential (Chen, 1997: −36 mV; Mo and Davis, 1997: −41 mV; Yi et al., 2010: −45 mV) the resulting inward current drives the membrane toward more depolarized voltages. The tonic inward current produced by I_h in SGNs is most likely mediated through HCN1 subunits, as *Hcn1*$^{-/-}$ SGNs exhibited hyperpolarized resting membrane potential similar to WT cells treated with ZD7288.

Given that SGNs are critical for high fidelity information transfer between IHC and central neurons in the auditory pathway, the functional significance of I_h in SGNs is clear. Because action potentials are generated at the spike initiation zone close to the IHC-SGN afferent synapse, it could be argued that the role of the cell body may be minor for auditory signal propagation. Recently, Yi et al. (2010) showed the presence of I_h in SGN afferent dendrites, and its contribution to shortening the EPSP waveform at the IHC-SGN synapse. We suggest I_h in SGN cell bodies may also contribute to signal propagation from afferent terminals to central axons. SGNs are bipolar with large cell bodies positioned between dendrites and axons, which may present a problem for signal propagation (Hossain et al., 2005). The large SGN cell body may behave as an electrical sink, where the electric load may cause impedance mismatch, which in turn could

interfere with rapid and efficient signal propagation from dendrite to axon. One mechanism for overcoming this electrical challenge in SGNs is expression of ion channels at peripheral and central initial segments flanking SGN cell bodies (Hossain et al., 2005). Indeed, SGNs express several varieties of voltage-gated channels (Santos-Sachi, 1993; Szabó et al., 2002) that may help enhance current density in the cell bodies. Given that HCN channels are also expressed in SGN cell bodies, it is plausible that the tonic activation of I_h at rest may provide an extra "boost" by depolarizing the resting membrane potential and thereby enhancing auditory signal transmission.

I_h contributes to spike timing

We found that I_h activation modulates SGN firing properties. Here we show that activation of I_h by physiologically relevant hyperpolarizing currents induced depolarizing sag potentials and enhanced rebound potentials in SGNs. The depolarization sag, with a time course that reflects I_h activation kinetics, slowly restored membrane potentials toward the resting potential. The rebound potentials at the end of hyperpolarizing steps enhanced membrane depolarization, bringing the cell closer to threshold for action potential generation. During ZD7288 inhibition of I_h, the depolarizing sag and rebound potentials were completely abolished, suggesting that activation of I_h provides subthreshold inward currents that enhance SGN excitability. We have extended this observation in adult SGNs to show that HCN1, in particular, contributes to depolarizing sag potentials, enhanced rebound potentials and shorter rebound spike latencies.

Previous studies indicated that additional factors may contribute to rebound spikes such as low-voltage activated T-type calcium channels (Aizenman and Linden, 1999

Lüthi and McCormick, 1998). Upon hyperpolarization, T-type calcium channels can recover from inactivation, making them available to open and enhance rebound potentials. Recent studies demonstrated I_h and low-voltage-activated T-type calcium channels act in concert to enhance rebound spike timing in auditory brainstem neurons (Felix II et al., 2011; Kopp-Scheinpflug et al., 2011). As T-type calcium channels have been identified in murine SGNs (Chen et al., 2011; Lv et al., 2012), we wondered whether rebound spike timing in SGNs is due to I_h alone or functions in concert with T-type calcium channels. We found that neither nickel, a broad spectrum calcium channel inhibitor, nor mibefradil, a T-type channel blocker, affected the depolarization sag or rebound spike timing. Thus, we conclude that I_h is a prominent contributor to rebound spike timing in SGNs with little contribution from calcium channels.

I_h also contributes to synchronized AP firing in response to small depolarizing stimuli. In the presence of ZD7288, the scatter in AP spike timing increased significantly for small depolarizing stimuli. The effect became less pronounced for larger depolarizing stimuli. We reason that synchronous firing in response to small depolarization is a direct consequence of tonic I_h activation at rest, which provides additional inward current, thereby driving membrane potentials toward the AP threshold more quickly. For larger depolarizing stimuli, I_h is reduced as membrane potential is driven closer to the I_h reversal potential and the relative contribution of I_h is diminished due to enhanced activation of voltage-gated sodium channels. Thus, I_h is most influential for small membrane potential deviations around the SGN resting potential.

Given the slow activation kinetics, it is unlikely that I_h can follow rapid membrane potential changes at auditory frequencies. Rather than following hair cell

receptor potentials on a cycle by cycle basis, it is more likely that the tonic activation of I_h helps shape the DC component of auditory signal processing by depolarizing the resting SGN membrane potential, leading to synchronized AP firing.

During development, however, the slow activation kinetics of I_h may suit the system. Before the onset of hearing (P12) IHCs fire recurrent Ca^{2+} APs at a very low discharge rates (2-4 HZ, Kros et al., 1998), which are hypothesized to drive spontaneous activity in SGNs during development (Tritsch et al., 2007; 2010). Considering the tonotopic and developmental regulation of I_h in SGNs as shown in the present study, it is possible that I_h primes SGNs to faithfully follow the recurrent Ca^{2+} spikes from IHCs during development (Johnson et al., 2011; Tritsch et al., 2007; 2010).

Contributions of SGN I_h to auditory function

Our results indicate that I_h contributes to SGN firing properties by regulating rebound spike timing and enhancing synchronized AP firing in response to small depolarizing stimuli. If so, what is the functional significance of I_h for auditory processing? Since SGNs relay auditory information from the IHCs to higher order auditory neurons via the 8th cranial nerve, our ABR data from *Hcn1*$^{-/-}$ mice, which indicate measureable delays in the latency of auditory signals, suggest that HCN1 helps preserve temporal fidelity in the 8th cranial nerve.

Accurate and precise transmission of IHC signals with high temporal fidelity is critical for normal auditory information processing. Thus, we propose I_h has a role in ensuring temporal precision, particularly for faint auditory signals. Although we did not detect differences in ABR threshold in *Hcn1*$^{-/-}$ mice, I_h may serve to boost sensitivity to

faint auditory stimuli. In the mature auditory system, SGNs innervate IHCs in a one to one ratio (*i.e.,* each SGN contacts only one IHC), while each IHC is innervated by groups of 20 to 30 SGNs (Liberman, 1982). This IHC-SGN innervation pattern ensures the activity of each SGN is strictly dependent on the activity of just one presynaptic hair cell and that each hair cell can drive the activity of multiple SGNs. Our findings suggest that I_h enhances synchronized AP firing to small depolarizing stimuli both within a single neuron and across a population of neurons. Thus, in response to slight changes in the membrane potential of a single IHC, SGN I_h enhances the likelihood of triggering synchronous APs in populations of SGNs. Synchronous firing, with reduced temporal jitter, across a population of neurons can help preserve temporal fidelity and enhance signal to noise ratios, particularly for small stimuli. Preservation of these signals may allow higher order auditory centers to extract relevant faint signals from a noisy background. Thus, I_h in SGNs may serve to enhance temporal fidelity and boost sensitivity to soft sounds.

Yi et al. (2010) showed that I_h in the postsynaptic SGN dendrites can boost EPSP speed, particularly for small signals. Here we extend those observations and show that I_h carried mostly by HCN1, contributes to processing and transmission of auditory information in SGN cell bodies as well. Whether preservation of I_h-dependent temporal information is critical for behaviorally relevant auditory tasks such as sound localization remains to be determined.

Acknowledgements: We thank the members of the Holt/Géléoc laboratory for helpful discussions and review of previous versions of the manuscript. We thank Dr. Andreas Ludwig for kindly providing *Hcn2* deficient mice. This work was supported by the National Institutes of Health (NIH)/ National Institute on Deafness and Other Communication Disorders (NIDCD) grants DC05439 to J.R.H.

Chapter IV. Position Dependent Spontaneous Activity in Postnatal Spiral Ganglion Neurons

Chapter IV

Previous studies suggest that the spontaneous activity in the developing auditory system is required for SGN neuronal survival, refinement of IHC-SGN synaptic contact, and preservation of the tonotopic maps in the central auditory pathway. However, the exact mechanism that drives this spontaneous activity in SGNs is still debatable, let alone the exact origin of this activity in cochlea has not been resolved (Chapter II).

This chapter provides recent experimental data from early postnatal SGNs, showing position-dependent spiking activity that mirrors the spontaneous activity pattern of the immature IHCs. These findings expand the current knowledge of spontaneous activity in SGNs and raise the possibility that spontaneous activity in postnatal SGNs is IHC driven.

INTRODUCTION

Spontaneous activity refers to cell autonomous neural manifestation that is generated by intrinsic intra- or inter-cellular mechanisms that are not triggered by external stimuli. The general agreement is that the spontaneous activity in the developing auditory system before the onset of hearing has a cochlear IHC origin (Chapter II). Several previous studies have identified likely candidates that contribute to the spontaneous activity in the cochlea, such as efferent system (Glowatzki and Fuchs, 2000; Goutman et al., 2005) and Kölliker's organ (Tritsch et al., 2007; 2010a), however, the question regarding the origin of its activity still remains elusive. Recently, another factor, the IHC mechanotransduction current has been added to the growing list of sources for spontaneous activity in the cochlea, where the resting transducer current is shown to depolarize the IHCs cells near to AP threshold, thus enabling sustained spontaneous activity (Johnson et al., 2012).

While most of the studies that investigated spontaneous activity in IHC have focused on identifying the source for the activity, one very recent study by Johnson et al. (2011) showed position-dependent spontaneous firing in IHCs along the cochlear tonotopic axis, where burst-like spontaneous activity is much pronounced in the apical IHCs compared to basal IHCs. The difference in firing pattern along the cochlear location was largely due to efferent modulation through α9α10 nicotinic ACh receptors (nAChRs), which subsequently activates Ca^{2+}activated K^{+} (SK2) channels, thereby hyperpolarizing the cell. The effect of efferent modulation was more prominent in the apex compared to base, thus giving rise to burst-like spontaneous activity pattern in the apical region.

In this study, we sought to assay spontaneous activity pattern in postnatal SGNs. Although previously one study indicated the possibility of endogenous activity in SGNs (Lin and Chen, 2000), however; it remains inconclusive whether the spiking activity detected in SGNs are purely endogenously driven or whether it is a random thermal activity of unknown origin as the spiking pattern was markedly different from prototypic spontaneous neural firing patterns found in many other developing cells including the IHCs.

There are several reasons we reason that the spontaneous spiking activity in SGNs can be IHC dependent during early postnatal development. First, regenerating Ca^{2+} spikes or action potential have been shown in IHCs during the first postnatal week (Kros et al, 1998; Marcotti et al. 2003; 2004). Second, these spontaneous Ca^{2+} spikes trigger exocytosis onto the afferent dendrite (Beutner et al., 2001). Third, postnatal SGNs are capable of firing action potentials that synchronizes with IHCs spiking activity (Tritsch et al., 2010b). In this regard, it is plausible to hypothesize that SGNs will fire spontaneous action potentials that mirror the IHCs spiking activity, under the assumption that SGNs make functional contact onto IHCs.

MATERIALS AND METHODS

Animals All animal experiments and procedures in this study were performed in strict accordance to the protocol approved by the Animal Research Children's Hospital (ARCH) of Boston Children's Hospital (Protocol # 11-04-1959).

IHC-SGN Intact Preparation Swiss Webster mice (Taconic Farms, Germantown, NY), age ranging between postnatal day (P) 1-3, were used as wild-type. Following rapid decapitation, temporal bones were removed from both sides of the skull and bathed in ice-cold Minimum Essential Medium (MEM) with glutamax (Gibco # 41090, Grand Island, NY), supplemented with 10 mM hydroxy-ethyl piperazineethanesulfonic acid (HEPES; Sigma, St. Louis, MO) and 0.05 mg/mL ampicillin (Sigma) at pH 7.4. The bony labrynth encapsulating the cochlea was chipped away and the whole cochlear turn was isolated from the core, by severing the SGN central fiber tract at the level of modiolus. Stria vascularis and tectorial membrane were gently peeled off, while leaving the rest of the Organ of Corti and SGNs intact. Special care was given to minimize damage to the hair bundle and to preserve afferent fiber connection between the organ of Corti and SGN cell bodies. Freshly dissected cochlear tissue were divided into base and apex and mounted flat on glass cover slips such that IHC sterocillia bundles were facing in an upright direction. The tissues were secured in place beneath a pair of thin class fibers glued to the cover slips with Sylgard ®184 (Dow Corning, Midland, MI). Cochlear organotypic explants were maintained *in vitro* at 37°C in a humidified incubator (5% CO_2) for 1-2 hours, after which were used for acute electrophysiological recording. All explants were used within 4-5 hours after dissection.

Electrophysiology All electrophysiological recordings were made at room temperature (22-24 °C; 73-76 °F). Cochlear organotypic explants were placed into a custom-made recording chamber and viewed under Zeiss Axioskop FS upright microscope (Oberkochen, Germany) equipped with 63× water-immersion lens, differential interface contrast (DIC), and epifluorescence optics. Explants were bathed in a standard external solution that contained (in mM): 137 NaCl, 0.7 NaH_2PO_4, 5.8 KCl, 1.3 $CaCl_2$, 0.9 $MgCl_2$, 5.6 D-glucose, 10 HEPES, amino acids (1:50, Gibco # 11130), vitamins (1:100, Gibco #11120). The pH was adjusted to 7.4 with NaOH and the measured osmolarity was 308 mOsmol/kg. Recording pipettes (3.5-4.5 MΩ) were pulled from R-6 soda lime capillaries (King Precision Glass, Claremont, CA), using a two-stage vertical pipette puller (PC-10; Narishige, Tokyo, Japan). To minimize pipette capacitance, tips were coated with Ski wax, and filled with standard internal solution that contained (in mM): 135 KCl, 2.5 $MgCl_2$, 2.5 K_2-ATP, 5.0 HEPES, 5.0 EGTA, 0.1 $CaCl_2$; pH 7.4 (KOH), 288 mOsmol/kg. 1.5 mM (< 2%) Lucifer Yellow CH dipotassium salt (Sigma # L0114) was added to the internal solution for retrograde labeling of SGN afferent fibers to their innervating IHCs via diffusion. All electrophysiological reagents were purchased from Sigma, unless otherwise noted.

Currents in SGNs was recorded in whole-cell, tight-seal technique in both voltage-, and current-clamp configurations, using Axopatch 200B (Molecular Devices, Palo Alto, CA) amplifier. SGN somas were held at a holing potential of –84 mV. Spontaneous activity was recorded in current clamp configuration (I=0), with no current injection. Currents were recorded immediately after the cell membrane was broken

through at giga-ohm (GΩ) seal. Series resistance (R_s) and membrane capacitance (C_m) were corrected. Both parameters were continuously monitored, in order to ensure stable recording. Compensated residual R_s was below 7 MΩ on average. Signals were filtered at 1 kHz with a low pass Bessel filter and digitized at ≥ 20 kHz using 12-bit low-noise acquisition system, Digidata 1332 (Axon Instruments, Union City, CA), and recorded using pClamp 9.0 (Molecular Devices, Sunnyvale, CA). Calculated liquid junction potential of –4mV was corrected for voltage. All stimulus protocol was generated using pClamp 9.0 and acquired data were stored on a PC for offline analyses.

Data analysis Spontaneous spikes were analyzed by calculating the following parameters: firing rate (total number of spike/total time period), inter-spike intervals (ISI), and coefficient of variation (CV). The CV was used as a quantitative measure for spike discharge regularity (Jones and Jones, 2000; Jones et al., 2007; Sonntag et al., 2009), and is defined as the ratio of standard deviation (SD) of ISI and mean ISI ($CV = SD_{ISI}/Mean_{ISI}$). CV < 1 indicates regular, and CV > 1 indicates irregular discharge activity. The CV for random Poisson process is 1 (Jones and Jones, 2000; Jones et al., 2007). Cells were considered spontaneous if firing rate was larger than 0.1 spikes/sec. Spontaneous recording was calculated from traces ranging from 40s to 280 s. For statistical analysis, independent *Student t-test* was used. Difference in means were considered significant if $p < 0.05$. All data is represented as mean ± SEM, unless otherwise noted.

RESULTS

Spontaneous activity in SGNs (P1-3) was recorded in whole-cell, tight-seal, current clamp mode without any current injection (I=0) from acutely dissected explant in which IHC and SGN were intact. While cell-attached recording paradigm is favored over whole-cell tight seal technique for recording spontaneous activity by some researchers as it does not perturbate internal milieu of the cell (Perkins, 1996), previous study indicated there is no difference in the quality or characteristics of spontaneous activity recorded using the two methods (Johnson et al., 2011). Therefore, we are confident that our result is not confounded by other extrinsic factors and that the spontaneous activity recorded from SGNs are reflection of cells autonomous activity. Among 69 recordings, 39 cells were spontaneous, and of those 39, total of 19 cells that showed stable spontaneous firing for the duration of recording were used for analysis. Each age group comprised of roughly equal number of cells from both apex and base.

As the representative current traces shows (**Fig. 4-1, Fig. 4-2**) postnatal SGNs (P1-3) showed position dependent spontaneous activity. While both apical (CV = 1.4 ± 0.1, n = 11) and basal (CV= 1.1 ± 0.1, n = 8) SGNs showed irregular firing based on the the CV value, where CV value larger than 1 indicates irregular discharge (Jones et al., 2001; 2007) (**Fig. 4-3*A***), difference in firing pattern between the cochlear tonotopic axis was evident. The firing pattern of apical SGN had a burst-like pattern (**Fig. 4-1**), compared to basal SGNs, which showed sustained firing (**Fig 4-2, Fig. 4-3*A***). Basal SGNs had significantly ($p < 0.01$) higher firing rate (mean: 1.4 ± 0.2 Hz, median 1.32, n = 8) compared to apical SGNs (mean: 0.6 ± 0.1 Hz, median 0.6, n = 11) (**Fig. 4-3*B***). A

general trend of increase in firing frequency was noticed as a function of postnatal day in both apical and basal cells; however, the difference was not statistically significant (data not shown). The inter-spike interval was significantly longer in apical cells (mean: 3519.8 ± 836.7 msec; median: 2165.4 msec, n = 11) compared to basal cells (mean: 999.6 ± 285 msec, median 785.8 msec; n = 8), which is thought to contribute to "burst like" firing pattern in the apical SGNs (**Fig. 4-1, Fig. 4-3*C***).

Previous studies showed resting mechanotransducer current contributes to Ca^{2+} spikes immature IHCs (Jonhson et al., 2012) and that spontaneous spike rate in mature SGN can be determined by the synapse location on IHC circumference (Lieberman 1982), in which SGNs contacting the pillar side (close to OHCs) have high spontaneous discharge rate while those contacting the modioular side have low discharge rate (0.05 spikes/sec). In order to verify that the cochlear position-dependent spike activity seen in postnatal SGNs is not confounded by these factors, we recorded spontaneous activity from explants with four different configurations (**Fig. 4-4**). We reasoned if spontaneous activity in SGNs is modulated by IHC resting mechanotransducer current, the presence or absence of tectorial membrane (*Tect ON/ Tect Off*) can make a difference in spontaneous rate, as it can introduce bias to the IHC hair bundle position. In our preparation, the explants were secured onto coverslips with pairs of thin glass fibers; therefore it is possible that the glass fibers can press the tectorial membrane against the hair bundle in a negative direction, thus closing the mechanotransduction current at the tip of the stereocillia and suppressing spontaneous activity. We also reasoned the orientation of the explants, in which IHCs were facing upward or downward (*HC up/ HC down*) depending on the explant orientation, may bias the population of SGNs accessible for recording. It is

not known whether immature SGNs exhibit difference in spontaneous spiking depending on IHC –SGN synapse location on IHC, as it is evident in their mature counterparts. Regardless, we hypothesized in upward configuration (HC up), we may have higher chance of recording from SGN facing the modiolar side (low-spontaneous SGNs), and in downward configuration (HC down) we may have higher incidence of recording SGNs from the pillar side (high-spontaneous SGNs). We reasoned that, if early postnatal SGNs exhibit similar spontaneous firing features similar to those in mature stages, there will be higher chance of recording from spontaneously firing cells from the downward configuration.

Our finding shows that there is no significant difference in spiking activity in terms of explants orientation or the presence or absence of tectorial membrane (**Fig. 4-4**). While the *HC up, Tect Off* configuration has the highest percentage of spontaneously spiking SGNs, however the fraction of spontaneously spiking cells was not as significantly different from the rest, indicating that the spontaneous activity in postnatal SGNs is not confounded by SGN cell type (high spontaneous vs. low spontaneous firing cells) or orientation of the hair bundle.

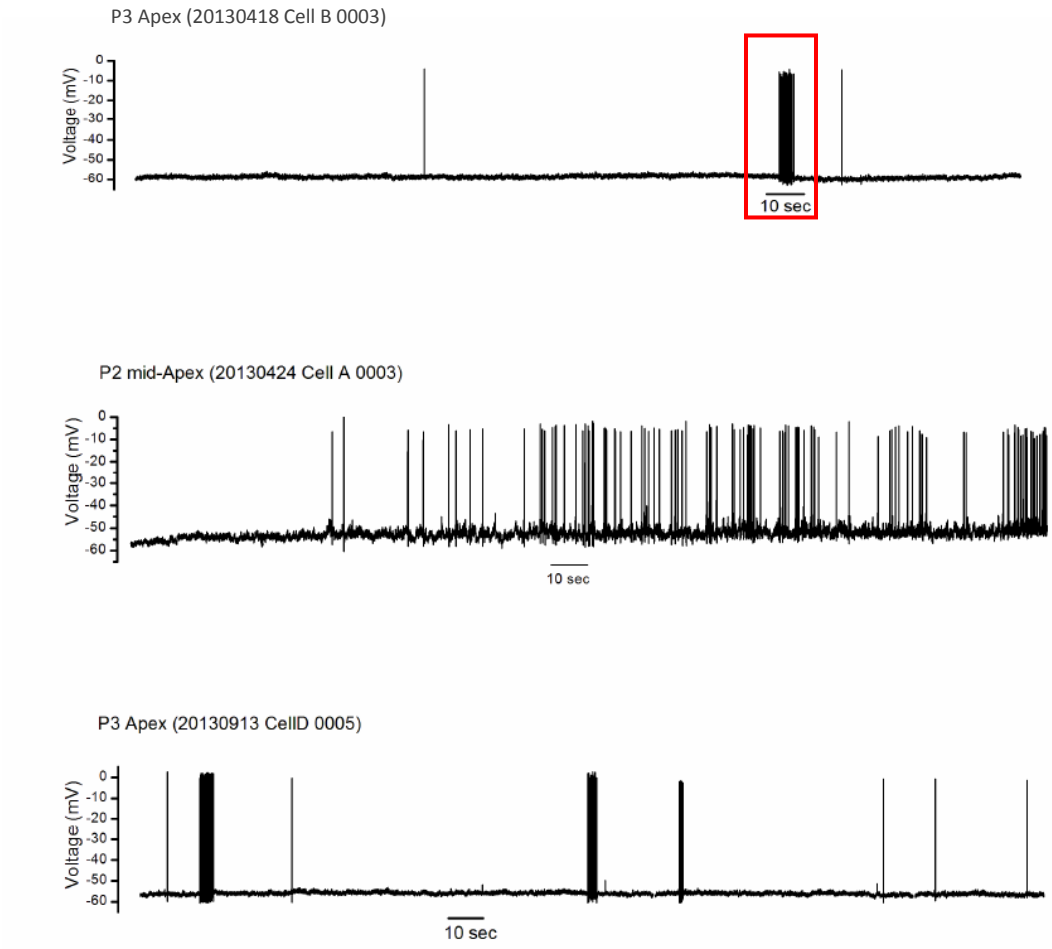

Figure 4-1. **Burst-like spontaneous firing pattern in apical SGNs.** Representative current traces showing spontaneous activity recorded from individual apical SGNs (P2-3, base) from three different cochleas in whole-cell, tight-seal technique. The spontaneous activity was measured for the duration of 280 sec in current clamp mode at I= 0. In general, apical cells showed tendency for burst-like firing, characterized by intermittent high frequency burst firings that are followed by quiescent periods. 3 out of 14 cells (21 %) recorded showed very low spiking high burst firing as shown in the top and bottom traces. The rest of the cells firing pattern is represented by the middle trace (11/14 cells). The 3 cells, that exhibited very low spiking were not included for ISI and CV analysis in **Fig. 4-3** as it will skew the data, but shown here to show heterogeneity in spiking pattern found in apical cells. Note that the top cell show a very long inactive period, however, due to its high burst period (red rectangle: ISI: 586 msec, CV 0.58) the mean ISI for this cell is 1128 msec, while the middle trace ISI is 2503 msec. Top: ISI: 1128 msec, CV: 1.2, 0.04 Hz; Middle: ISI: 2503msec, CV 1.2, 0.4 Hz; Bottom: ISI: 7456 msec, CV: 1.48, 0.18Hz.

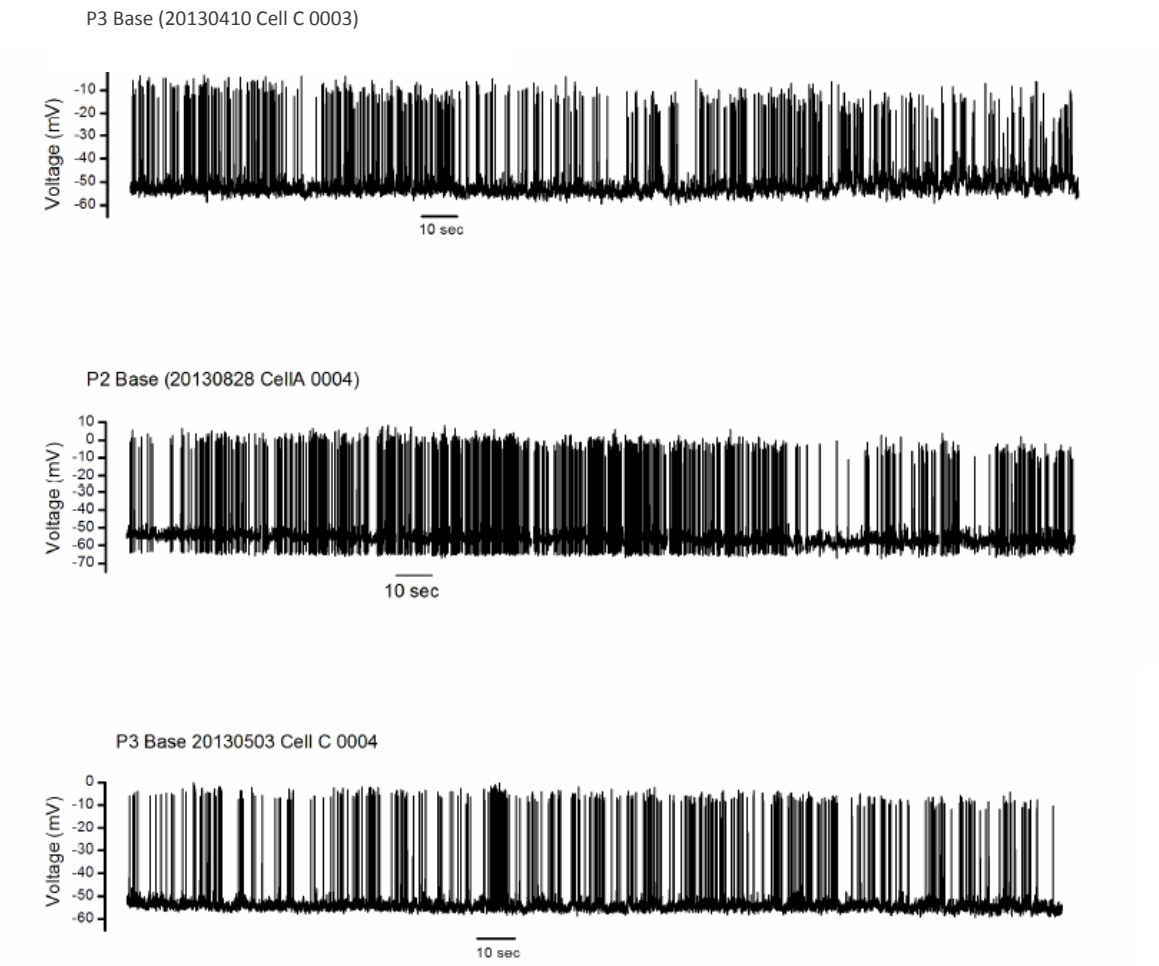

Figure 4-2. **Sustained spontaneous firing pattern in basal SGNs.** Representative current traces showing spontaneous activity recorded from individual basal SGNs (P2-3, base) from three different cochleas in whole-cell, tight-seal technique. The spontaneous activity was measured for the duration of 280 sec in current clamp mode at I=0. Basal cells showed sustained and robust spiking activity. Top: ISI: 595 msec; CV: 0.97; Hz: 1.7; Middle: ISI: 483 msec, CV: 1.1, Hz: 2.4; Bottom: ISI: 814 msec, CV: 1.1, Hz: 1.25.

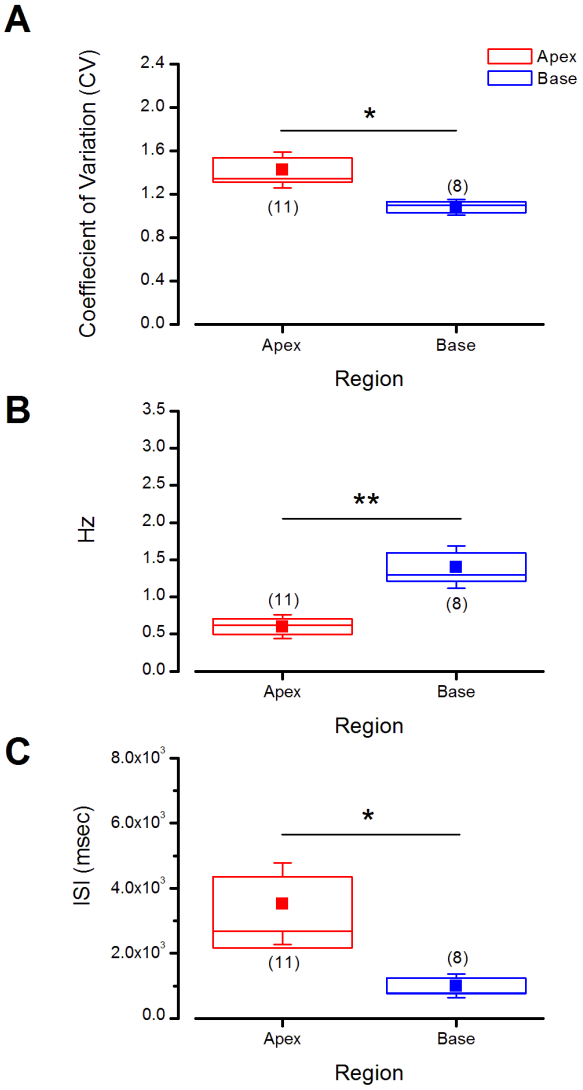

Figure 4-3. **Position-dependent action potential spiking activity in early postnatal SGNs.** ***A,*** Coefficient of variation (CV) was used as a measure for irregular spiking where CV >1 is considered irregular and CV< 1 is considered as regular spiking. Both apical and basal SGNs showed irregular spiking activity, in which apical cells (n =11) showed significantly larger degree of irregularity (1.4 ± 0.1, n =11) compared to basal cells (1.1 ± 0.1 n = 8). ***B,*** Firing rate (Hz) as a function of location. Basal SGNs (1.4 ± 0.2 Hz. n = 8) had significantly higher firing rate than apical cells (0.6 ± 0.1 Hz, n =11). ***C,*** Inter-spike interval (ISI) as a function of location. ISI was significantly shorter in basal SGNs (mean: 999.6 ± 285 msec, median: 785.8 msec, n = 8) compared to apical cells (mean: 3519.8 ± 836.7 msec, median: 2165 msec, n= 11). * $p < 0.05$, ** $p < 0.01$.

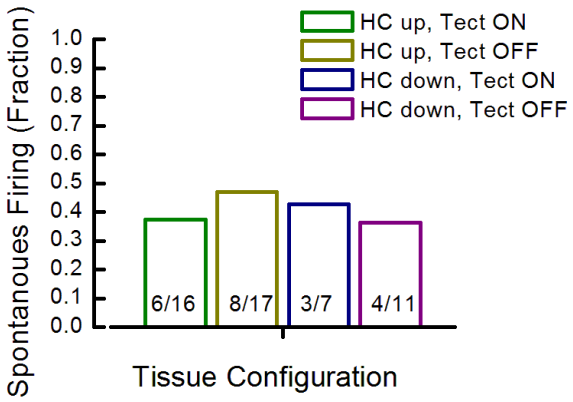

Figure 4-4. **Spontaneous firing in postnatal SGNs is not confounded by SGN cell type or IHC orientation or hair bundle configuration.** No significant difference was found in fraction spontaneous activity in all configurations tested. Spontaneous firing was measured from SGNs age ranging P1-3, in current clamp mode (I=0) for 280 sec. Age and cochlear location was evenly distributed within each configuration. Percentage (fraction) of spontaneous cells with spike rate higher than 0.1 spike/sec. HC up/Tect ON: 0.38, HC up/Tect Off: 0.47, HC down, Tect ON: 0.43, HC down, Tect OFF: 0.36.

DISCUSSION

Here, we provide evidence that early postnatal SGNs fire spontaneous action potentials in a position-dependent manner along the cochlear tonotopic axis. The spontaneous spikes in postnatal SGNs resembled prototypic firing pattern found in other auditory neurons during the development, prior to the onset of hearing (Chapter II). We show that the apical SGNs fire more burst-like, irregular spikes compared to basal SGNs which showed more robust, sustained firing pattern. Apical SGNs had lower firing rate and longer inter -spike intervals, which contributed to the burst-like pattern.

Position-dependent spontaneous firing in postnatal SGNs

These recordings are the first demonstrations in SGNs, showing position-dependent spontaneous firing during the first postnatal week. Previous studies have reported spontaneous firing along the auditory pathway; however, the focus was more on the characterization and developmental acquisition between pre- and post-hearing animals, except one study (Lippe, 1995) which investigated the relationship between spontaneous firing rate and tonotopic position in prehearing avian nucleus magnocellularis (NM) and nucleus laminaris (NL), mammalian equivalent of second and third order auditory neurons. Using *in-vivo* multiunit extracellular recording techniques in embryonic chick NM and NL, Lippe (1995) showed that rate of rhythmic burst activity (mean burst rate: 0.21- 0.71 Hz) increased systematically as a function of tonotopic position, in which higher burst rate was detected in high frequency region of the nuclei. Despite the species and cell type difference, our findings also show position dependent spontaneous firing, in which cells from the base had higher firing rate and shorter inter-

spike interval, and *vice versa* in the apex. This finding also corroborates with findings by Johnson et al. (2011) which showed position-dependent spontaneous activity in postnatal IHCs from mice, rat, and gerbil.

It is important to note that the changes in the spontaneous firing pattern in SGNs were gradual rather than having a clear dichotomy, with some degree of variability seen within the same region. The fact that some of the cells in the apex showed spontaneous firing pattern that were markedly different from the rest of the apical bursting cells, in which the firing consisted of intermittent high burst followed by a very long period of inactivity (**Fig. 4-1**, top and bottom traces) indicates that some degree of heterogeneity in spiking exists within the same cochlear region. It is possible that these low spike,-high bursting cells are reflecting a developmental lag in the apical region of the cochlea, considering the previous finding that showed position dependent spiking activity in IHCs during development (Johnson et al., 2011).

Previously, it was shown in hearing mammals, depending on the presynaptic innervation location within single IHC, SGNs exhibit difference in spontaneous firing rate, irrelative to cochlear tonotopic location (Libermam, 1978; Liberman, 1982). For example, in cats, SGNs innervating the modiolar side of the IHCs have low spontaneous spike rates (< 0.05 spikes/sec, Liberman, 1978), and those innervating the pillar side have high spontaneous spike rates (>18spikes/sec, Liberman, 1978), with low spontaneous cells accounting for 10-15 % of the radial SGN populations. The differences in spike rates within the same IHCs are thought to contribute to the dynamic range of the auditory periphery especially in the apex, thereby enhancing the detection of sounds with varying

levels of sensitivity within the same frequency spectrum (Liberman, 1982; Taberner and Liberman, 2005). Considering that these very low spike, high-bursting spontaneous spiking patterns accounted for ~ 21% of total spiking cells, while some species difference may exist, it is possible that these cells are early prototypes for those low spontaneous firing cells in the mature system. Until today, however, it is unknown whether the differences in spontaneous spike rate in mature SGNs innervating the same IHCs are causal effect reflecting difference in pre- and post -synaptic machinery composition, or due to differences in intrinsic mechanisms such as spontaneous activity during development. If SGN spontaneous activity is strictly IHCs driven, how can one explain the heterogeneity in spontaneous firing in the same cochlear location? These questions await further investigation.

The origin of Spontaneous Activity in SGNs

The findings that postnatal SGNs fire spontaneous activity in a position-dependent manner suggest that these activities are IHC driven. To further validate the mechanism of IHC-dependent spontaneous activity, a straight forward approach would be to use pharmacology to render the IHC activity, such as dihydrostreptomycin (DHS), which are mechanotransduction channel blocker (Marcotti et al., 2005). We have used DHS in order to modulate spontaneous activity in SGNs as previous study indicated the involvement of resting transducer current in spontaneous activity in IHCs (Johnson et al., 2012), however the result was hard to discern in SGNs (data not shown). One possible explanation for this inconclusive data might be due to complexity in spontaneous activity, which is governed by many different sources. This may also explain why teasing out the

origin of spontaneous activity in the developing cochlea has been an enigma to the field. Spontaneous activity in developing cochlea is a neural output manifested by concerted activity that is tightly controlled in time and space. It seems that there is no one single player that is responsible for this neural activity; rather it is a combination of many different mechanisms playing their roles. That is, resting transducer current, efferent modification, non-neural modulation by ATP, and other unknown factors may contribute to spontaneous spiking activity.

While the presence of endogenous spontaneous activity in postnatal SGNs is largely inconclusive (Chen and Lee, 2000), recent finding showed that SGNs fire spontaneous action potentials as early as E14 before they make synaptic contact with the IHCs, indicating early acquisition of action potentials are not IHCs driven (Mars and Spirou, 2012). This striking piece of evidence raises the possibility that spontaneous activity in the developing cochlea is not strictly IHC driven. There may be bi-directional activity, in which SGNendogenous spiking activity governs IHC differentiation and initial development during the early embryonic stages, and that IHC originated Ca^{2+} spikes promote refinement and maturation of sensory maps in the following two postnatal weeks, during which its activity is also modulated by the efferent system and ATP release by the Kölliker organ. Similar to the visual system, where spontaneous activity consists of several waves, it is possible analogous mechanisms apply to cochlear development. Therefore, identifying the transition point between SGN and IHC spontaneous activity may be critical for a better understanding cochlear development.

What we laid out here is a very general survey of the language that the SGNs speak during development, but the field is far behind in deciphering the code. As the word "spontaneous" suggest, this mysterious brain code may carry critical information that can be used for clinical interventions such as stem cell therapy or cochlear implant design. Understanding the neural code for spontaneous activity may increase the chance for SGNs survival for those with deafness, where the survival of SGNs determines the success of cochlear implant intervention. With the recent development of new molecular tools and advances in transgenic animals, in which *in-vivo* cell-specific and time-specific modulation of activity is possible, we may be able to crack the code in near future.

Chapter V. Development of New IHC-SGN Intact Preparation

Chapter V

The findings from Chapter III demonstrated that SGN $I_{h,}$ whose large fraction is carried by HCN1 subunits, contributes to temporal aspects of signal processing by depolarizing SGN resting membrane potentials, accelerating spike latency while minimizing jitter, and synchronizing 8^{th} nerve firing. Additionally, findings in Chapter IV showed evidence that early postnatal SGNs fire spontaneous activity in position-dependent manner, while the source of this acitivty still remains to be investigated. These results prompted the next questions: How is auditory signal transmission achieved in SGNs, especially during early development? How does I_h affect temporal signal processing?

The aim of the present chapter was to develop a new IHC-SGN intact preparation, which allows for mechanical stimulation of IHCs by fluid jet and recording of SGN response properties in simultaneous fashion. Here, a detailed methodology regarding the new preparation development will be explored.

INTRODUCTION

Precise encoding of sound signals into neural code, or spike trains, is a major challenge, yet fundamental to normal auditory processing. One of the most important tasks that the auditory end organ has to face is the rapid and accurate decomposition of sound signals into trains of action potential that the brain can understand. Because sound is not a static property, encoding auditory information is not merely a "sampling" procedure. In order for the brain to perform tasks such as sound discrimination and localization, the auditory system must dynamically extract signal properties, such as frequency and timing, from complex sound waves without compromising the spatio-temporal power of the auditory spectra.

As the primary afferent neurons in the auditory system, SGNs have unique "coding" properties that enable them to faithfully encode incoming signals from their receptor IHCs. The most prominent feature is frequency tuning by spike rate, in which sounds of different frequencies produce maximal firing rate in SGNs at unique cochlear locations, reflecting the tonotopic arrangement of IHCs (Geisler, 1998; Taberner and Lieberman, 2005). Another feature is temporal coding by spike timing. For example, rapid changes in sound signals are encoded by temporal structures of the spike trains (i.e., first spike at onset of sound), as demonstrated by phase locking to sounds below 2 kHz (Geisler, 1998; Lieberman, 1982; Taberner and Lieberman, 2005).

These coding properties evidenced in SGNs by *in-vivo* single unit measurements are combinatory effect of SGNs morphological and intrinsic electrical properties. In the mature system, SGNs innervate IHCs in a one to one ratio, while each individual IHC is

innervated by groups of 20 to 40 SGNs (Liberman, 1980; Spoendlin, 1969). This IHC-SGN innervation pattern ensures that SGNs can encode multiple aspects of the sound stimulus, allowing for precise signal transmission between the IHC and the CNS (Liberman, 1982). In addition, SGN cell bodies express various voltage gated channels along the cochlear axis in a graded manner, aiding the cells to encode signals from the IHCs in a tonotopic fashion (Adamson et al., 2002; Chen et al., 2011; Davis, 2003; Lv et al., 2012).

Why is spike acuity in SGNs important for normal auditory processing? As the first relay station in the auditory system, rapid and faithful transmission of action potentials (APs) in SGNs is critical. Slight temporal "offset" in the AP firing in the afferent neuron can cause detrimental "domino" effects as signals converge in ascending higher order auditory neurons, including those in auditory brainstem and cortex, which rely heavily on temporal information from the auditory nerve to perform tasks, such as sound localization and speech perception (Wightman and Kistler, 1992). For instance, disrupted temporal acuity in SGNs can be particularly challenging for sound discrimination, when there is a competition between incoming auditory signal and background noise, as this will decrease the signal to noise ratio, thus affecting accurate auditory processing.

The previous chapter (Chapter III) demonstrated that I_h in SGN cell bodies, a large fraction carried by HCN1 subunits, depolarizes resting membrane and sag potentials, accelerates rebound spike latency following hyperpolarizaiton, minimizes spike jitter, and enhances synchronized firing at the 8^{th} nerve (Kim and Holt, 2013). These findings

establish the functional significance of I_h in SGN cell bodies. Given that SGNs are critical interface for high fidelity signal processing between IHCs and higher order neurons along the auditory pathway, and that spike acuity in SGNs are critical for normal auditory processing, what is the function of HCN channels in SGN cell body in terms of temporal signal processing?

Recently, Yi and colleagues (2010) have shown the presence of I_h in SGN afferent dendrite and its role in shortening EPSP waveforms, which is thought to enhance reliable signal transmission by preventing EPSP summation at IHC-SGN junctions. From a sensory neurophysiologcial standpoint, this makes sense because action potentials are initiated at or near the afferent nerve terminal where sensory transduction occurs (Carr et al., 1996; Lowenstein and Ishiko, 1960). In most sensory neurons, the nerve terminals are usually packed with several molecular entities, such as sodium channels and myelin, to facilitate salutatory AP conduction down the axonal fiber in an all or none fashion, thus enabling rapid and reliable signal propagation without losing the gain. Thus, the extent to which neuronal cell body contributes to signal coding is unclear.

While SGN afferent synaptic machinery (Sobcowicz, 1982) is critical for ensuring accurate encoding of hair cell activity (Buran et al., 2010; Khimich et al., 2005), it does not necessarily guarantee whether signals at the terminal will propagate centrally without failure. Unlike other sensory neurons, SGNs have unique cyto-architecture. They are bipolar neurons with large cell bodies positioned in the middle, whose configuration can pose additional challenge to the auditory system for normal functioning. That is, the large cell body can act as an electrical sink, which in turn can interfere with the rapid and

precise signal propagation from the afferent dendrite to the SGN soma (Hossain et al., 2005).

One mechanism for overcoming this electrical challenge in SGNs is by the systematic expression of sodium channels (Na_v 1.6) at the peripheral and central initial segments flanking the somata of both type I and type II SGNs and at the receptor-neural junction near the IHC-SGN synapse (Hossain et al., 2005). Based on a computer simulation model, Hossain et al. (2005) showed that deletion of Nav1.6 channels at the peripheral and central initial segments in type II SGNs resulted in complete AP failure, indicating that the clustering of sodium channels near the soma ensures successful signal transmission across the cell body. However, since type I SGNs have larger somata size than type II cells, it is unclear whether flanking of sodium channels near the somata would be sufficient to circumvent the impedance imbalance in primary auditory afferent neurons. While the loose myelination around the soma may reduce the current density loss at the soma, a more direct electrical mechanism may be needed as sustained depolarizing current will be needed to maintain the membrane potential near threshold for efficient AP propagation. Based on the previous findings (Kim and Holt, 2013), it is plausible that the tonic activation of I_h at rest may provide an extra "boost" by depolarizing the resting membrane potential, thereby enhancing temporal acuity for auditory signal transmission between the IHCs and the cochlear nucleus.

In order to understand how I_h affects temporal signal transmission at SGN somata, the goal of the present study was to develop a new intact preparation in which both the organ of Corti and SGNs are intact. For the past few decades, the focus in the field has been on understanding how sound signals are encoded at the IHC-SGN afferent synapse.

Numerous morphological and electrophysiological studies (Goutman and Glowatzki, 2007; Grant et al., 2010; Sobcowicz, 1986) demonstrated that IHC-SGN posses unique morphological (i.e., ribbon synapse) and biophysical mechanism (i.e., multi vesicular release, Ca^{2+} channel clusters around active zone) that leads to tonotopic frequency specificity and dynamic amplitude coding at the afferent fibers. However, less is known about how temporal signal transmission is achieved in SGN somata.

The development of this novel preparation will be a significant contribution to the field at large. Previous studies have investigated auditory nerve response to sound stimuli (Kiang et al., 1965; Liberman, 1978; 1982b), using *in-vivo* single unit recording in hearing mammals. While extracellular recording techniques provide more naturalistic sampling of SGN nerve responses as it preserves the native intracellular milieu of a cell without rupturing the cell membrane; however, it has reduced resolution compared to that of whole-cell, tight-seal technique, in which manipulation of voltage and current is possible at a single cell level. By stimulating the IHCs and recording from the SGN soma simultaneously using the whole-cell, tight-seal technique, this paradigm will better approximate the *in-vivo* situation of signal transmission and provide better understanding on how signal processing is achieved in SGN soma, especially during development.

MATERIALS AND METHODS

Animals All animal experiments and procedures in this study were performed in strict accordance to the protocol approved by the Animal Research Children's Hospital (ARCH) of Boston Children's Hospital (Protocol # 11-04-1959).

IHC-SGN intact preparation Swiss Webster mice (Taconic Farms, Germantown, NY), age ranging between postnatal day (P) 1-4, were used as wild-type. Following rapid decapitation, temporal bones were removed from both sides of the skull and bathed in ice-cold Minimum Essential Medium (MEM) with glutamax (Gibco # 41090, Grand Island, NY), supplemented with 10 mM hydroxy-ethyl piperazineethanesulfonic acid (HEPES; Sigma, St. Louis, MO) and 0.05 mg/mL ampicillin (Sigma) at pH 7.4. The bony labrynth encapsulating the cochlea was chipped away and the whole cochlear turn was isolated from the core, by severing the SGN central fiber tract at the level of modiolus. Stria vascularis and tectorial membrane were gently peeled off, while leaving the rest of the organ of Corti and SGNs intact. Special care was given to minimize damage to the hair bundle and to preserve afferent fiber connection between the organ of Corti and SGN cell bodies. Freshly dissected cochlear tissue were divided into base and apex and mounted flat on glass coverslips such that IHC sterocillia bundles were facing in an upright position to maximize stimulation by fluid jet. The tissues were secured in place beneath a pair of thin glass fibers glued to the cover slips with Sylgard ®184 (Dow Corning, Midland, MI). Cochlear organotypic explants were maintained overnight *in vitro* at 37°C in a humidified incubator (5% CO_2) to allow for recovery from dissection.

To ensure tissue quality, all electrophysiological recording was performed within less than 24 hours of dissection.

Electrophysiology All electrophysiological recordings were made at room temperature (22-24 °C; 73-76 °F). Cochlear organotypic explants were placed into a custom-made recording chamber and viewed under Zeiss Axio Examiner A.1. fixed-stage upright microscope (Oberkochen, Germany) equipped with 63× water-immersion lens, differential interface contrast (DIC), and epifluorescence optics. Explants were bathed in a standard external solution that contained (in mM): 137 NaCl, 0.7 NaH_2PO_4, 5.8 KCl, 1.3 $CaCl_2$, 0.9 $MgCl_2$, 5.6 D-glucose, 10 HEPES, amino acids (1:50, Gibco # 11130), vitamins (1:100, Gibco #11120). The pH was adjusted to 7.4 with NaOH and the measured osmolarity was 308 mOsmol/kg. Recording pipettes (3.5-5.0 MΩ) were pulled from R-6 soda lime capillaries (King Precision Glass, Claremont, CA), using a two-stage vertical pipette puller (PC-10; Narishige, Tokyo, Japan). To minimize pipette capacitance, tips were coated with Ski wax, and filled with standard internal solution that contained (in mM): 135 KCl, 2.5 $MgCl_2$, 2.5 K_2-ATP, 5.0 HEPES, 5.0 EGTA, 0.1 $CaCl_2$; pH 7.4 (KOH), 288 mOsmol/kg. 1. 5 mM (< 2%) Lucifer Yellow CH dipotassium salt (Sigma # L0114) was added to the internal solution for retrograde labeling of SGN afferent fibers to their innervating IHCs via diffusion. All electrophysiological reagents were purchased from Sigma, unless otherwise noted.

SGN response to IHC fluid jet stimulation was recorded in whole-cell, tight-seal technique in both voltage-, and current-clamp configurations, using Axopatch200B (Molecular Devices, Palo Alto, CA) amplifier. SGN somas were held at a holing

potential of -84 mV. Currents were recorded immediately after the cell membrane was broken through at giga-ohm (GΩ) seal. Series resistance (R_s) and membrane capacitance (C_m) were corrected. Both parameters were continuously monitored, in order to ensure stable recording. Compensated residual R_s was below 7 MΩ on average. Signals were filtered at 5 kHz with a low pass Bessel filter and digitized at ≥ 20 kHz using 12-bit low-noise acquisition system, Digidata 1440A (Axon Instruments, Union City, CA), and recorded using pClamp 10 (Molecular Devices, Sunnyvale, CA). Calculated liquid junction potential of -4mV was corrected for voltage. Acquisition data were stored on a PC for offline analyses.

IHC fluid jet stimulation Stimulus pipettes were fabricated from borosilicate glass (internal diameter: 0.86mm; Sutter Instruments, Novato, CA) to a tip diameter of ~ 10-15 μm, using a two-stage vertical pipette puller (PC-10; Narishige, Tokyo, Japan). Stimulus tip was fire polished using MF 200 MicroForge (World Precision Instruments, Sarasota, FL). Pipette was designed to effectively deliver fluid jet stimulation to targeted individual IHC hair bundles (mouse IHC width: 5-7 μm, Russel & Richardson, 1987).

Stimulus pipette was filled with standard external solution as described above and mounted on an electrode holder that connected to a high-speed pressure clamp system, HSPC-1 (ALA Scientific Instruments Inc, Westbury, NY) via a silicon tubing (≤10 cm). The pressure clamp used in this study is an evolved version of previously used pressure clamps (McBride and Hamil 1992; 1995), with following improvements: The newly designed piezoelectric bimorph in current HCPC-1 allowed for stable and efficient pressure and vacuum control without ringing of the valve, and placement of optical

pressure sensor near the piezo element minimized delay (closed loop valve actuation latency: 120 μs) in pressure actuation to a command voltage (Besch et al., 2002).

Fluid jet was driven by application of variable pressure to the rear end of the stimulus pipette, which was tightly controlled by piezoelectric bimorph in the HSPC-1. Fluid jet stimulus was in the form of series of sinusoids waves (10-100Hz, 200 msec) with varying driving voltage (10-50V) in 10 V increments. The input signal to HSPC-1 was driven by pClamp10 (Molecular Devices) and was converted to analog via Digidata 1440A (Axon Instruments). The output of the fluid jet pressure was monitored via internal feedback sensor located inside of the HSPC-1 head stage and the signals were collected in a separate channel to ensure consistency in stimulation quality.

IHC fluid jet stimulation was made from the pillar side (facing OHCs), therefore positive phase of sinusoids indicated deflection of hair bundles away from the tallest stereocillium (i.e., mechanotransudction channel closing). IHC bundle deflection was continuously monitored during the experiment using a vidoe camera with enhanced contrast controller (C2741-62; Hamamatsu, Hamamatsu city, Japan) and intermittent visual inspection through the eyepiece.

IHC-SGN intact preparation fluid-jet recording scheme SGN soma was patched in whole-cell, tight-seal, voltage-clamp configuration, using the same internal solution and recording pipette (3.5-5.2 Ω) as described above. The criteria of stable SGN neuron recording constitutes as follows: Giga Ohm (Ω) seal, low compensated series resistance (R_s) of < 10 MΩ , and a stable resting membrane potential with minimum leak current

(< 50 pA), and no indication of spontaneous activity. Only when the above criteria were all met, the paradigm proceeded with the next step. Once stable recording from SGN was established, fluid jet stimulus pipette was brought close to the apical pole of the IHC hair bundle from the pillar side to identify the IHC innervated by the SGN. The motorized lower body of the microscope allowed for low noise, vibration-free horizontal repositioning of focus from SGNs to IHCs (distance: ~300-500 μm) under 63x objective, while ensuring stability for electrophysiological recordings at both ends. The delivery of fluid jet stimulus (10Hz, 10DV) was confirmed by the deflection of stereocillia bundle by a CCD camera. The stimulus pipette was moved vertically along the row of IHCs by sequential repositioning of the pipette to adjacent individual IHCs via micro manipulator (Narishige), until a response was detected in the already patched SGN. Upon identification of the presynaptic IHC, the position of the stimulus pipette was slightly adjusted to elicit maximal response. A series of sinusoid wave forms (10-100 Hz, 200 msec) with increasing driving voltage (10-50 DV), in 10DV interval, were delivered to IHC hair bundles via fluid jet, and the response was recorded from SGN in current-clamp mode. At the end of the recording, IHC-SGN cellular innervations was visually confirmed by Lucifer yellow retrograde tracing from the patch pipette, illuminated (Xcite ®120Q, Lumen Dynamics, Ontario, Canada) under a GFP filter.

Immunohistochemistry *S*GNs fibers and IHCs connections were verified *post-hoc* by immunohistochemcial labeling. Following electrophysiological recording, cochlear explants were immediately fixed in 4% paraformaldehyde (Electron Microscopy Sciences, Hatfield, PA) in 0.1M PBS (pH 7.4; Gibco) for 20 min at room temperature

(RT). Tissues were then washed with 1X PBS (3 × 5 min) and incubated in 0.1% Triton™ X-100 (Sigma) for 15 min, and blocked in 3% bovine serum albumin and normal goat serum (Jackson Immuno Research Laboratories, Inc., West Grove, PA) in 0.1M PBS for 1 hr at RT. Primary antibody labeling was done using Myo VIIa rabbit polycolonal antibody (1:1000, Proteus Biosciences Inc., Ramona, CA) in block solution overnight at – 4°C. Subsequently, tissues were washed in 0.05% Tween 20 (Invitrogen, Grand Island, NY) in 0.1 M PBS (4 ×10 min), and counter stained with Alexa Fluor® conjugated 633 secondary antibody (goat-anti rabbit, 1:200) and 546 phalloidin (1:200; Invitrogen) for 1 hr at RT. Tissues were washed with 0.05% Tween 20 (4 ×10 min) before mounted using SlowFade® Gold antifade reagent (Invitrogen, Eugene, Oregon). Samples were imaged using Zeiss LSM 700 laser scanning confocal microscope, using either 25× or 63× objectives. Projection images and three-dimensional renderings were created following Z-series acquisition, using Image J.

Data analysis Offline data analyses were performed using Clampfit 10.2 (Molecular Devices) and OriginPro 7.5 (Origin Lab, Northampton, MA). Figures were prepared with OriginPro 7.5 and Adobe Illustrator. Each cell served as its own control. In appropriate conditions, *Student t-test* was performed using statistical features in OriginPro7.5. Difference in means were considered significant if $p < 0.05$. All data were presented as mean ± 1 SEM, unless otherwise specified.

RESULTS

Development of the new IHC-SGN intact preparation

The goal of the present study was to develop a new IHC-SGN intact preparation, in which simultaneous mechanical stimulation of IHCs and recording SGN response properties are possible. With the development of this preparation, we seek to answer questions of how auditory signal processing is achieved in SGNs in relation to IHC activity. Due to the technical difficulty; data from semi-intact IHC-SGN preparations have not been reported. The closest intact preparations that were used in recent studies have utilized puff pipette to deliver high potassium or ATP close to apical pole of hair cells to depolarize their membrane potential while recording the response from the synaptically connected SGNs (Tritsch et al., 2010b; Weisz et al., 2012). However, these preparations were limited and did not explore the relationship between IHC mechanic stimulation and SGN response properties in a physiologically-relevant paradigm.

In order to record SGN firing properties in response to IHCs mechanic stimulation, we designed a paradigm that will maximize the probability of quality recording, while minimizing tissue damage (**Fig. 5-1*A***). The difficulty with this type of preparation is that the physical distance between the IHCs and SGNs is large, making the coupling between the mechanic stimulation and whole-cell, tight-seal recording challenging. With a conventional upright microscope this can be especially difficult, as the whole mount cochlear tissue cannot be visualized within a single visual field at high magnification. To overcome this physical barrier we used an upright microscope mounted on a motorized platform and fixed stage, which allows visualization of the tissue with high magnification

and maneuvering of the mechanic stimulator and patch clamp recording pipette possible. To identify IHCs that connected to SGNs, we favored fluid-jet over piezo-electric driven stiff probes to mechanically stimulate IHCs. Fluid jet is advantageous in that it not only approximates *in-vivo* like situation, but also allows for hair bundle stimulation without having to physically contact the hair bundle with the stimulus probe. We took advantage of this aspect of the fluid jet, which allowed for rapid screening for synaptically connected IHCs, by sweeping the stimulator close to IHCs apical pole in a sequential manner until an SGN response was detected (**Fig. 5-1*B, D, E***). After the IHC was identified, the stimulus pipette was readjusted to maximize hair bundle stimulation in the target IHCs. At the end of the recording session, the synaptic connection between IHCs and SGNs was confirmed by Lucifer yellow retrograde labeling *post hoc* (**Fig. 5-1*C***).

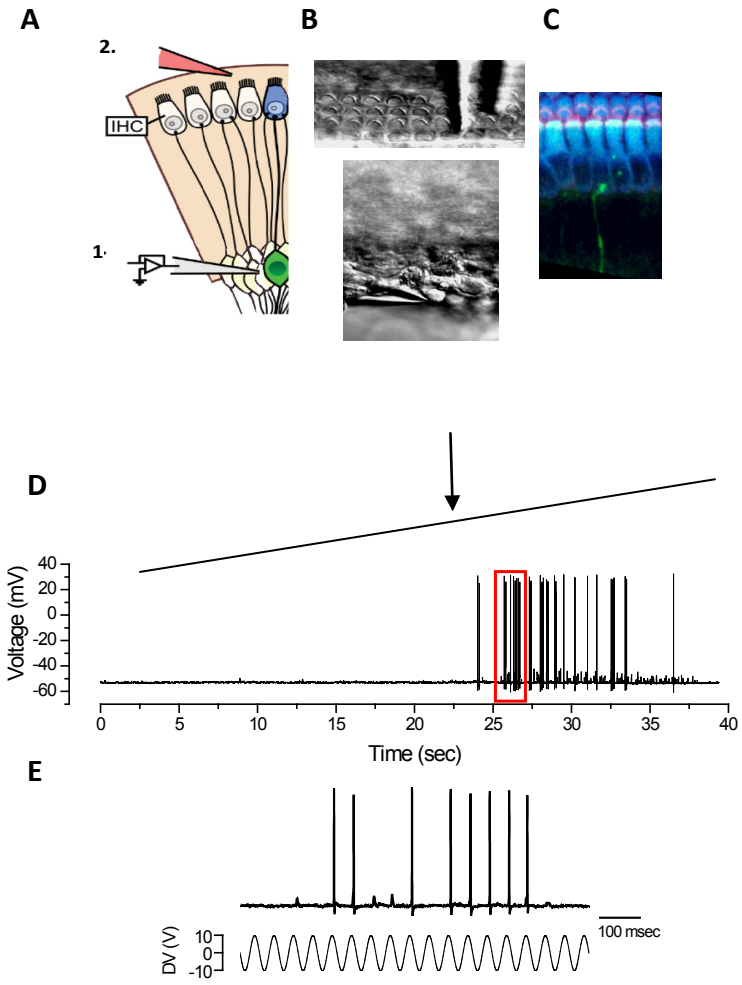

Figure 5-1. **Recording scheme for intact IHC-SGN preparation.** ***A***, Illustration of IHC-SGN intact preparation ***1,*** After stable recording is established in SGNs ***2,*** fluid jet stimulus pipette moves along the IHC row until a response is detected in the patched SGNs (***D***). ***B,*** DIC images of fluid jet stimulating IHCs (top) and SGN patch pipette (bottom). ***C,*** Confocal image of SGN afferent making contact with IHC. Lucifer yellow dye fill was acquired during recording. green: Lucifer yellow, blue: phalloidin, red: myosin7a. ***D,*** Robust SGN (P4, mid-base) response to fluid jet stimulation (10Hz, 10 DV, 40 sec). Ramp indicates sweeping position of the fluid jet stimulus pipette as it was swept across the IHCs row, and black arrow indicates the location where the stimulus probe hit the target IHC. ***E,*** Expanded view of red rectangle in ***D***. The response consisted of mix of APs and EPSPs. APs phase locked to 10Hz sinusoid stimulus with 7.9 msec phase delay. Illustration in ***A*** was modified from Tritsch et al., (2010b), with permission from Nature.

Response properties of SGNs to IHC stimulation by fluid jet

We report here, for the first time, preliminary evidence that early postnatal SGNs are capable of transmitting signals from the IHCs in response to hair bundle stimulation (**Fig. 5-1*D***). Among 48 stable IHC-SGN recordings, a total of 32 cells (65 %) showed evoked responses. Of those, 17 cells (55%) showed modulation of firing rate in response to changes in stimulus frequency (Hz) and driving voltage (DV), indicating the SGN responses were not random, but generated by IHC stimulation.

Evoked response to IHC fluid jet stimulation was achieved in SGNs at all ages tested, between postnatal day (P) 1 to 4 (**Fig. 5-2**). The percentage of evoked reponse, on average, was 84 % across all age group tested. P1 (n = 5) SGNs were able to respond to IHC stimulation, however, the location was limited towards the base of the cochlea. 80 % of responses (4/5 cells) from P1 cells were from basal cells. From P2 and then on, evoked responses were seen in both apical and basal SGNs with almost equal probability (P2 apex: 45%, base 55%; P3 apex; 58%, base: 42%; P4 apex: 55 %, base: 45 %).

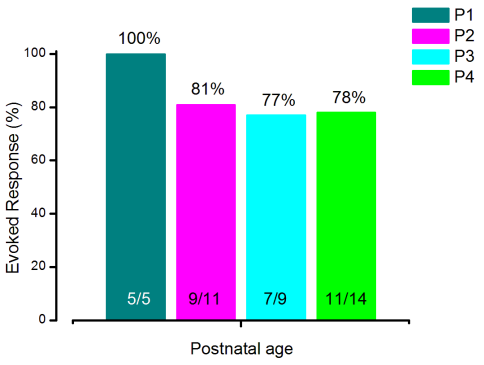

Figure 5-2. **Evoked response in SGNs to IHC mechanical stimulation as a function of postnatal age.** The bar graph shows the percentage of SGNs that showed robust evoked response in response to IHC fluid jet stimulation as a function of postnatal age. No statistical difference was found between all age group tested (P1-4). Fraction at the bottom of the bar graph indicates number of cells showing evoked response/total number of cells recorded per age group.

The general evoked response in SGNs was a mix of action potentials (APs) and subthreshold potentials (EPSPs), all of which showed some degree of entrainment to the stimulation frequency, for low frequency stimulation. **Figure 5-1*D*** illustrates SGN (P4, mid-apex) response to IHC fluid jet stimulation at 10Hz, 10V DV, in current clamp mode. Once the fluid jet hit the synaptically connected IHC, a robust response was detected, which consisted of APs and EPSP like spikes. The response was stable and persisted for the entire duration (~ 14 sec) the fluid jet was stimulating the target IHCs hair bundle, whose synaptic connectivity to SGN was confirmed by Lucifer yellow fill.

In this particular cell (**Fig. 5-3*A, B***), there were 15 APs and 234 EPSPs. The EPSP amplitude distribution for this cell was highly skewed, with mean amplitude of 4.3 ± 0.2 mV and median of 3.2 mV. The inter-spike events for EPSPs were also skewed with mean inter-spike interval of 58.8 ± 7.4 msec and a median of 4.5 msec, at a sinusoidal stimulation of IHC at every 100 msec (10Hz).

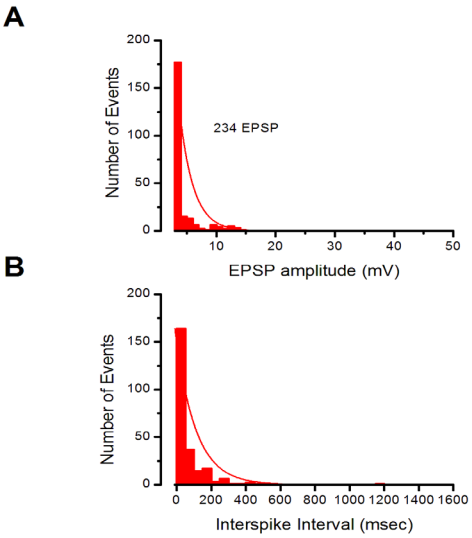

Figure 5-3. **EPSP amplitude and inter-spike interval (ISI) distribution from a SGN in response to IHCs bundle stimulation.** ***A,*** In response to 10Hz IHC fluid jet stimulation, robust EPSPs (234 units) were evoked in the particular SGN (P4, mid-apex). The distribution ESPS amplitude was highly skewed (mean 4.3 ± 0.2 mV; median: 3.2 mV). ***B,*** Inter-spike interval distribution was also skewed, indicating possible coordinated release. (mean ISI: 58.8 ±7.4 msec; median: 4.5 msec)

In order to examine SGN response properties to varying frequency and driving voltage, a series of sinusoids (1000 msec), ranging from 5-100 Hz with varying DV (10-50V) were delivered to IHCs and the response was recorded (**Fig. 5-4**). In a given cell (P4 SGN, apex), the number of EPSP and spikes increased gradually with increasing frequency from 5 to 30 Hz (**Fig. 5-4*B***). However, at frequency higher than 50 Hz, the cells did not show any response. This absence of response at stimulus frequency ≥ 50 Hz may be attributed to the mechanical limitation of fluid jet stimulation to drive fast hair bundle deflections. At frequencies 30 Hz or below, the number of spikes increased with increasing driving voltage and frequencies indicating the EPSP to spike transition (**Fig. 5-4*A***) became more robust as the hair bundle was stimulated with higher intensity and frequency. Interestingly, at DV of 30 or larger the number of spikes did not increase in all frequency level (**Fig. 5-4*C***), suggesting a possible IHC saturation (early postnatal IHC transduction currents saturate with 30Hz fluid jet stimulation; unpublished data, Holt Lab, Dr. BiFeng Pan), synaptic adaptation (Eatock et al., 1991), fatigue or refractoriness in SGNs (Li & Young, 1993). These effects may occur alone or in combination, and are predicted to affect synaptic transmission markedly in the developing cochlea. At the moment, we cannot directly pinpoint the mechanism; however, this preliminary synaptic-transfer pattern raises the possibility that the new IHC-SGN preparation can be used to address those types of questions, with technical fine tuning.

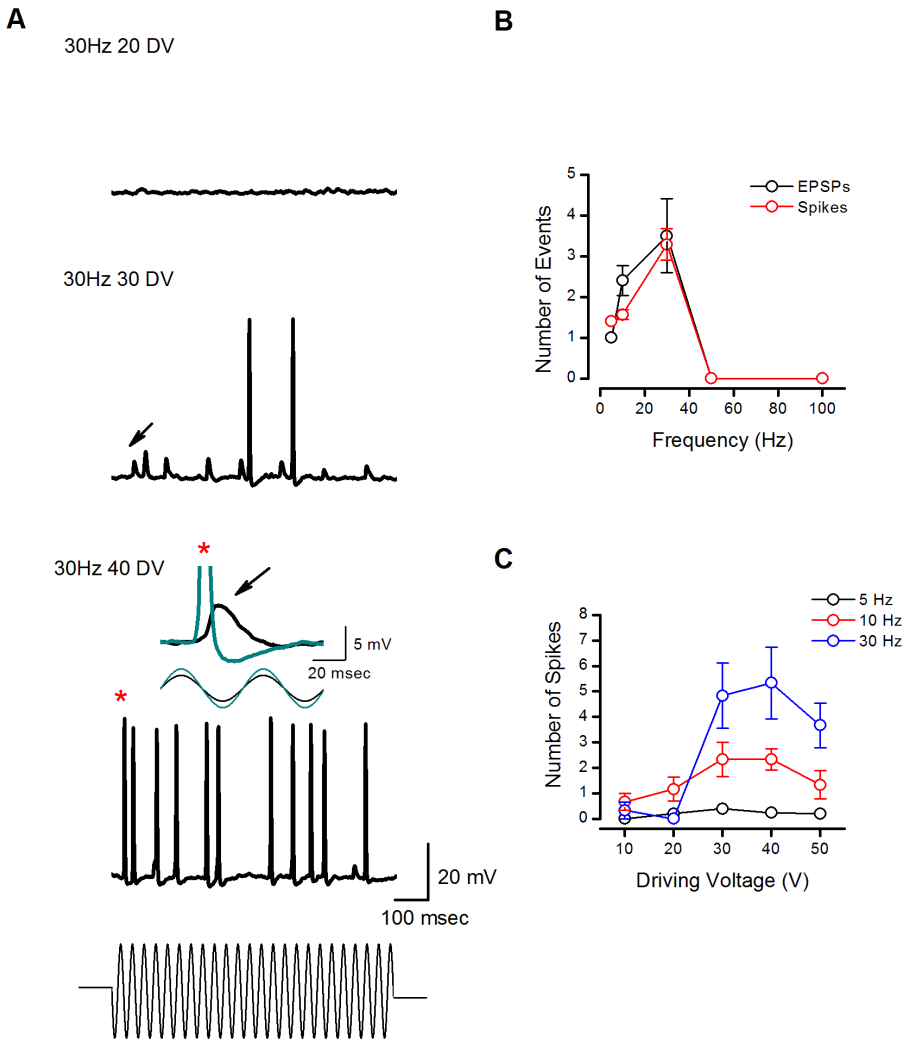

Figure 5-4. **EPSP to spike transition pattern and basic transfer function in SGN in response to IHC fluid jet stimulation.** ***A,*** Example traces of EPSP to Spike transition in the same SGN (P4, mid-base) in response to IHC sinusoid fluid jet stimulation at 30 Hz with increasing intensity. No response was evoked at 20 DV. As the DV increased from 30 to 40 DV, EPSP to spike transition became more robust. The inset in the bottom panel shows high resolution view of subsequent traces superimposed to the same time domain, showing EPSP to spike transition (Black: SGN response to 30 DV, Cyan: SGN response to 40 DV). ***B,*** Number of EPSPs and Spikes as a function of frequency. No response was evoked in frequencies higher than 50Hz. ***C,*** Basic transfer function of SGN in response to IHC fluid jet stimulation. With increasing DV, the number of spikes per cycle increased. The peak was reached at 30DV, 30Hz stimulation.

DISCUSSION

Using the new IHC-SGN intact preparation, the preliminary results presented in this study provide evidence that early postnatal mouse SGNs are capable of transmitting signals from IHCs, as early as P1 at the base in response to mechanical stimulation of IHC by fluid jet. Optimization of the preparation is needed to validate whether the low response rates in SGNs are due to technical limitations of fluid jet or attributable to the system's innate developmental phenomenon. Nonetheless, the findings are the first to show that SGNs are functional and respond to and transmit mechanically driven IHC signals at early developmental stages, before onset of hearing (mice, P10-12; Romand, 1983),

Development of new IHC-SGN preparation and the challenge

During the past decade, great technical advances have been made that broadened our current understanding on signal processing at the IHC-SGN afferent synapse using IHC capacitance recording and afferent bouton recording techniques (Beutner and Moser, 2001; Glowatzki and Fuchs 2002). However, less is known about how signal transmission is achieved in SGN somata in relation to IHC activity. Much of the current literature in SGN physiology are based on *in-vivo* single unit recordings in response to tonal presentation (Kiang et al., 1965; Liberman, 1978; 1982b; Taberner and Liberman 2005), or whole-cell, patch clamp recordings from either semi-intact or dissociated culture system (Adamson et al., 2002; Liu and Davis, 2007; Mo and Davis, 1997). Both approaches have made considerable progress in aiding our knowledge on SGN physiology at both systems and cellular level, however; each presents its own limitations.

The *in-vivo* single unit recording is excellent for assaying normal auditory afferent response across populations of SGN neurons; however, it does not provide high resolution to study the direct link between IHCs and SGNs. On the other hand, both intact and dissociated culture systems have sufficient resolution to study membrane properties of SGNs, but not suitable for addressing systems questions.

The scarcity of the intact preparation to study IHC-SGN signal processing in the field has to do with its technically difficult nature of this preparation. The intact preparation requires a micro dissection technique that will preserve the connection between hair cells and the ganglion without affecting their structural integrity and innervations pattern. In addition, the recording paradigm requires coupling of two separate techniques (SGN whole-cell tight seal technique and IHC mechanic stimulation) in simultaneous fashion, without introducing hindrance to the system itself.

Another challenge with the preparation is the fact that it is a blind study, in which the SGN and IHC synaptic connectivity cannot be visualized unless fluorescence retrograde labeling or other visualization methods are used. In this study, we used Lucifer yellow in the patch pipette to visualize the SGNs afferent dendrite and IHC contact. However, due to phototoxiciy of Lucifer yellow dye (Gaewaller, 1981; Hanani, 2012), the visual confirmation could be only done at the end of the recording session to prevent photodynamic damage to the cell. Thus, for future experiments, use of alternative fluorescence retrograde dye with low photo toxicity or microscope with a sensitive charge coupled device (CCD) camera that allows for real-time visualization of SGN afferent dendrite fill should be considered.

Early postnatal SGNs are capable of transmitting mechanically driven signals from IHCs

Despite all the difficulties presented above, the result in this study shows that postnatal SGNs are capable of transmitting mechanically driven stimulus from the IHCs. The fact that evoked response is seen in SGNs at P1 mostly at the base, with increased response over the next postnatal days in both base and apex is noteworthy as it reflects the spatio-temporal, developmental acquisition of hair cell transduction current. Previously, Lelli et al (2009) have shown that the mechanotransduction apparatus in mouse hair cells become functional at P0 starting at the base followed in the apex at P2, and acquire gradual maturation over the first postnatal week, indicating that the postnatal IHCs are capable of generating transduction current when mechanically stimulated. In addition, gross mature IHC-SGN innervation patterns are present at birth (Echteler, 1992; Sobcowicz, 1986) and the ribbon synapses between IHC and SGNs become functionally mature during the first postnatal week (Khimich, 2005; Huang et al. 2007; Pujol et al. 1998). Recently it was also shown that cochlear nucleus is able to transmit signals by afferent electrode stimulation at P4 in mice (Mars and Spirou, 2012), suggesting not only the peripheral synapse but also the central synapse are fully functional at early developmental stages to relay signals. In line with the previous morphological and functional studies, our finding extends the evidence that the cochlear sensory epithelium, especially SGNs, are capable of transmitting mechanically evoked signals at much earlier stages than what is believed to be at the onset of hearing.

In response to IHCs fluid jet stimulation, SGNs showed responses that included EPSPs and APs. Neither EPSPs nor APs showed complete entrainment to the stimulus,

however, the number of EPSPs increased as the frequency (Hz) and the intensity (as measured as a function of DV) of sinusoid stimulations increased. The occurrence of EPSP to spike transition became more robust and frequent as the stimulus intensity and frequency increased, showing synaptic transfer function. Interestingly, the SGNs stopped responding to IHC mechanic stimulation at frequency higher than 50 Hz at all intensity level. This phenomenon was not limited to cells with certain age or location, but was seen in all SGNs tested, raising the possibility that this was due to technical limitation of fluid jet. Compared to piezo-electric driven stiff probe stimulation, fluid jet driven by pressure clamp system has much narrow dynamic range in delivering high-frequency stimulations. One cannot also rule out the very short stereocilliary length of IHCs (Russell and Richardson, 1987), which makes the efficient delivery of high frequency stimulation to targeted hair bundle much difficult.

Optimization of fluid jet technique

Fluid jet has been widely used in hair cell mechanotransduction studies (Denk and Webb, 1992; Géléoc et al., 1997; Holt et al., 1997; Kros et al., 1992). The advantage of using fluid jet over stiff probe stimulation is that it closely approximates the *in-vivo* IHC stimulation, where IHC stereocillia displacement is a result of fluid mechanics coupled to basilar membrane motion and tectorial membrane sheer in response to traveling sound wave in the fluid filled cochlea (Guinan, 2012; Nowontny and Gummer, 2006).

While fluid jet is limited in the range of high frequency stimulus delivery confounded by the physical limit of pressure clamp system, previous study by Kros et al. (1992) have shown robust and faithful phase locking response in trasducer current in P1-

2 days old mouse IHCs at frequency as high as 119 Hz. The fact that we did not see SGNs responses in stimulus frequency over 50 Hz thus, prompts the need for technical optimization of fluid jet in order to obtain reliable recording condition. A couple of initial measures can be taken to improve the current fluid jet technique. The silicon tube that connects the stimulus holder to the fluid jet head stage, which contains the piezo-bimorph, can be made short to reduce the dead volume and increase the actuation speed of stimulus, thereby increasing the efficiency for high frequency stimulation. Another consideration is to bring the fire polished stimulus pipette very close to the IHC bundle without damaging the cell (Denk and Webb, 1992; Kros et al., 1992). By shortening the distance between the target and the fluid jet stimulator, one can eliminate potential physical errors.

Among other things, the key for efficient stimulus delivery in fluid jet lies on the calibration of the fluid jet stimulus. The disadvantage with fluid jet is that the force applied on hair bundle is unknown. In the literature, researchers have used photodiodes to indirectly measure the force by measuring the deflection of a photodiode with known mass at the tip of the stimulus pipette by gravity (Géléoc et al., 1997; Kros et al., 1992). However, as other factors, such as the distance of the fluid jet to the hair bundle, viscous drag caused by the fluid environment near the tissue, and difference in stimulus tip diameter and its angle of approach, can introduce differences in actual force estimation (Kros et al., 1992), thus, in our experiment we did not estimate the force. Instead, we assumed the driver voltage was proportional to the pressure applied to the bimorph, and

the tip diameter of 10-15 μm was adequate for delivering the DV to the target IHC without creating vibration to the cells nearby.

While still preliminary, our findings indicated a basic transfer function in SGNs in response to IHC mechanic stimulation. This result is promising as it opens up the possibility that this preparation can be used as a platform to ask synaptic transfer function type of questions in SGNs. At current stage, we cannot pinpoint the mechanisms contributing to the transfer function; with fine tuning of the paradigm we foresee the immediate application of this preparation. The current fluid jet system cannot measure the hair bundle displacement directly, but with additional introduction of the stiff-probe mechanotransducer into the paradigm, it is possible to investigate synaptic delay, adaption, and electrical tuning (Crawford and Fettiplace, 1981) properties in SGNs in relation to IHC activity. Further, these technical improvements will help answer the original question as to how HCN channel contributes to temporal aspects of signal transmission between the IHC and SGNs.

Signal processing in developing SGNs

In many mammals, during the two postnatal weeks, many structural and functional changes occur in the cochlea and any hindering of this process can introduce a destructive consequence for the cochlear to mature properly and function to its full spectrum. One of the most mysterious aspects of cochlear development is the presence of spontaneous activity that is thought to govern many of these important developmental processes (Chapter II). During this period, the cochlea does not respond to airborne sound-driven signals but only transmit the spontaneous generated signals, which have a

prototypic pattern that consists of rhythmic burst firing (< 10 Hz) followed by a period of quiescence or reduced discharge activity.

Currently, it is not known whether the auditory system is tuned to only transmit low frequency spontaneous spikes across the system during the first two postnatal weeks. Our data indicate that early postnatal SGNs are capable of transmitting mechanically driven, low-frequency IHC signals. Given that mature SGNs can phase lock to sound stimulus up to 2 kHz *in-vivo* (Geisler, 2008; Taberner and Liberman, 2005) it has yet to be discerned whether these early postnatal SGNs are also capable of transmitting high frequency singles like their mature counterparts or whether they are limited to transmitting low frequency signals as transient developmental phenomena. A definitive answer to this question will further allow us to better understand spontaneous activity in cochlea and how its signal transmission is achieved between the IHCs and SGNs.

Based on current findings, that early postnatal SGNs are responsive to mechanically driven, low frequency stimulation, one interesting question that is impending to be asked is whether spontaneous activity in SGNs can be masked by IHCs stimulation, and whether it will have any developmental consequences. From a clinical therapeutic point of view, this will be a valuable piece of information, as exogenous electrical stimulation have been shown to be critical factor in maintaining the survival of SGNs after IHCs loss (Ryugo et al., 2005). With the boom of viral mediated gene therapy and cochlear implant technology in recent years (Akil et al., 2012; Bedrosian et al., 2006; Moore and Shanon, 2009; Simonelli et al., 2010), deciphering the code, the spoken language between the IHCs and SGNs will have an immense impact on clinical

intervention. For example, delivering spontaneous activity- like stimulation to grafted SGN stem cells may increase their chance to integrating into the system and acquiring functional properties and connections.

In conclusion, here we report a current advancement in developing new IHC-SGN intact preparation and present results that early postnatal SGNs are capable of transmitting signals from IHCs in response to mechanical stimulation. The information we gathered here currently is at a very infant stage, however; it already has shown possibilities of how this new platform can be used to shed light onto some of the very important questions that have yet to be answered in the field of auditory physiology, especially during development.

Chapter VI: Conclusions and Future Directions

Spiral ganglion neurons (SGNs) are the primary afferent neurons in the mammalian cochlea that convey signals from the receptor hair cells to higher order auditory neurons, in trains of action potentials that the brain can understand. Our ability to detect, localize, and perceive sound is a result of the dynamic signal processing that occurs in the auditory system, and SGNs are the first order auditory neurons in that very process. As their bipolar morphology manifests, in which their peripheral fibers extend to hair cells and their central fibers project to central nucleus, SGNs are the sole bridge point between the cochlear hair cells and the brain. Without proper functioning SGNs, the brain will no longer be able to accurately register the analog elements of sounds into digital representation for *real-time* processing, thus, there will be an instant disconnect between the physical world of sound and its perception. Given this, the significance of SGNs in auditory signal processing is absolutely clear and their importance in the auditory system should not be overlooked.

For the past few decades the focus of the field has gravitated towards elucidating the detailed biophysical mechanism of hair cell mechanotransduction and physiology at the cellular level. SGNs, situated deep in the bonny Rosenthal's canal in the cochlear modiolus, on the other hand, have long resisted the attempts to study their electrophysiological properties. The bone encapsulation and the cell body myelination provide extra protection for these neurons, at the same time, however; they limit the physical access, making the physiological study of SGNs challenging. Despite the difficulty, a few pioneering *in-vivo* single unit studies have showed that SGNs exhibit frequency tuning and phase locking properties to sounds, and adapt when presented with

prolonged sound stimuli, much like that of their counterpart hair cells (Kiang et al., 1965; Liberman 1982b; Johnson 1980; Smith, 1977; Taberner and Liberman, 2005). Due to limited resolution and access, it has been hard to discern to what extent these properties are shaped by the intrinsic properties of SGNs. Therefore, the prevailing view has been that SGNs are passive entities that simply relay auditory signals from their receptor hair cells to the brain.

During the past two decades, a considerable advancement has been made in electrophysiological techniques to study SGNs at the cellular level. With the development of SGN *in-vitro* whole-cell, tight-seal, voltage-clamp technique (Santos-Sachi, 1993), the functional role of SGNs could be tested more directly, and ever since, the long held assumptions have been slowly unraveling. That is, it is no longer true that SGNs are "*conveyer belts*" that simply relay signals from one end to the next.

Recent findings indicate that the signal processing in SGNs involves a much more complex and tailored processes that require more than just simple propagation of signals. From a sensory neurobiological stand point this makes sense, where nonlinearity is essential for sensory signal processing. Peripheral sensory neurons are tuned to create neural representations by capturing the salient feature of the sensory input without losing its gain. Therefore, it is not particularly surprising that SGNs are endowed with mechanisms that enhance auditory signal processing.

SGNs incorporate distinct morphological and signature electrophysiological coding strategies to resolve precision and temporal acuity of incoming signals from their receptor hair cells. One way to achieve efficient signal transfer between IHC and SGNs

is frequency-specific-coding by expression of various voltage-gated ion channels. The systematic expression of voltage-gated ion channels enhances cells' dynamic range, enabling SGNs to faithfully encode graded membrane potentials of hair cells into trains of action potentials.

Given that SGNs harbor diverse voltage-gated ion channels to shape their firing properties, which ultimately contribute to high-fidelity signal transfer between IHCs and SGNs, examining the ionic conductance and the function of voltage-gated channels expressed in SGNs are critical for better understanding the complexities of auditory processing in SGNs.

The first part of the work in this thesis examines the functional significance of hyperpolarization-activated, cyclic nucleotide-gated (HCN) channels in SGNs (Chapter III). By utilizing molecular and electrophysiological recording techniques *in-vitro* and *in-vivo* in SGNs from WT and *Hcn*-deficient mice, I demonstrated that 1) SGNs express *Hcn1, 2*, and *4* mRNA, with *Hcn1* being the most highly expressed at both neonatal and adult stages. 2) HCN1 is the most prominent subunit contributing to biophysical characteristics of SGN I_h. 3) I_h contributes to depolarized resting potentials, sag and rebound potentials, accelerates rebound spikes following hyperpolarization, and minimizes jitter in spike latency for small depolarizing stimuli. 4) Auditory brainstem responses (ABR) of *Hcn1*-deficient mice, which showed longer latency in the 8^{th} nerve firing, suggest that I_h contributes to synchronized spike timing in SGNs. In summary, these findings indicate that I_h contributes to SGN membrane properties and plays a role in

temporal aspects of signal transmission between the cochlea and the brain, critical for normal auditory function.

The findings from this study contribute to the current understanding of SGN auditory signal processing in several important ways: Taking advantage of molecular (q-RT PCR) and whole-cell, tight-seal electrophysiology techniques in both WT and *Hcn*-deficient mice, this study was the first that corroborated the molecular composition of HCN channels to SGN I_h biophysical characteristics *in-vitro*. In addition, this work have shown that the biophysical characteristic of I_h in the neonatal stage extend to adult stages, showing that I_h is developmentally regulated. The detailed functional analysis of I_h using *in-vitro* current-clamp recording further revealed, for the first time, that I_h in SGN cell body contributes to membrane properties, rebound spike precision, and synchronized action potential firing, which was also validated at systems level *in-vivo* by recording compound action potential firing at the 8th nerve using ABR. The finding that *Hcn1*-deficient mice show delayed 8th nerve firing, in conjunction with *in-vitro* findings, provides robust and powerful evidence that HCN channels in SGNs, HCN1 in particular, contributes to temporal acuity in auditory signal processing.

Human patients with auditory neuropathy have normal hearing and cognitive abilities; however, they show difficulty in understanding speech, perceiving sounds in noisy environments, discriminating soft sound, and localizing sound source using intensity differences and spectral cues. These patients show aberrant ABR in the 8th nerve region, while their cochlear microphonics are intact (Starr et al., 1991; Zeng et al., 1999; 2005). The aberrant or almost non-existent ABR signal in the 8th nerve indicates

abnormal unsynchronized firing, which is attributed to disrupted timing in neural coding at the primary afferent (Starr et al., 1991; Zeng et al., 2005). Although HCN1 related auditory pathophysiology has not been identified or reported previously in the literature, this begs the attention for investigating *Hcn1* as potential auditory neuropathy candidate. As such, the current finding from Chapter III reinforces the importance of studying SGN firing properties and how the basic knowledge acquired can be applied for better understanding auditory neuropathy and devising diagnostic and treatment strategies for related disorders.

In order to fully appreciate signal processing in SGNs as a whole, Chapter IV focuses on spontaneous activity in postnatal SGNs. While much attention has been given to the sensory driven signal processing in SGNs, the activity-independent neural activity that persists during the first two postnatal weeks before the onset of hearing is now only becoming to unveil. Before the cochlea is able to speak the language of sound, the system is tuned to speak this unknown language that seems to carry critical information for normal development of the cochlea. This mysterious neural code has been thought to be involved with IHC maturation, IHC-SGN synapse pruning, and SGN survival and maintenance (Chapter II). Today, the general understanding in the field is that spontaneous activity has a cochlear origin; however, how this activity is generated and sustained during the development is not well understood.

In chapter IV, I show evidence that postnatal SGNs fire spontaneous action potentials whose pattern differ along the cochlear tonotopic axis, reflecting the position-

dependent spontaneous Ca^{2+} spike patterns in immature IHCs. This finding raises the possibility that spontaneous activity in postnatal SGNs is IHCs driven. Future experiments are needed to delineate whether IHC transducer current has any effect in SGN spontaneous activity, however; this is the first report to show cochlear location-dependent spontaneous activity in murine SGNs before the onset of hearing.

While further systematic approach to dissect the mechanism and origin of this spontaneous activity in SGNs are in high demand, any information acquired here will be of particular interest, as it will provide a better understanding of functional development of the auditory system and related auditory dysfunctions. The knowledge acquired by decoding spontaneous activity can be used for better devising cochlear implants and clinical interventions such as SGN stem cell therapy or future adeno-associated virus (AAV) mediated gene therapy, where successful integration and survival of newly grafted cells into the host system is high importance for promising clinical outcome for those with hearing impairments.

To investigate temporal signal processing in SGNs with much higher resolution that approximates the *in-vivo* situation, Chapter V explores in great detail about the methodology and strategy for developing a new preparation, in which both IHC and SGNs are intact, and simultaneous mechanical stimulation of IHCs and path-clamp recording from synaptically connected SGN are possible. Prior to this advancement, the physiological approach in the field was rather compartmentalized, focusing on one cell type at a time. By combining the two most essential players in cochlear signal processing, this new preparation is expanding the methodological boundary in auditory physiology.

The new IHC-SGN intact preparation has a great potential to be used as a new *ex-vivo* model system to understand auditory signal processing in SGNs in relation to IHC activity. While still preliminary, using the new IHC-SGN intact preparation, I demonstrated that SGNs are capable of transmitting signals from IHCs in response to mechanical stimulation of hair bundles as early as P1 at the base. A basic transfer function was also evidenced in SGNs in response to IHC mechanic stimulation, indicating that the new preparation can be applicable for asking signal processing related questions, with improved technical fine tuning.

Much of current knowledge on auditory signal processing at the IHC-SGN synapse comes from studies utilizing IHC capacitance measurements or EPSC recordings from afferent boutons. While these measures have enhanced our understanding on cochlear synaptic physiology immensely; however, it is crucial to take into account that these findings are based on IHC depolarization, and not to graded receptor potentials changes elicited by hair bundle stimulation. With the new preparation, while technical improvement is still needed, it will be possible to explore the relationship between mechanotransduction and synaptic transfer function, and further assay SGN response properties along the tonotopic axis using physiological stimulations. The preliminary evidence I present herein, proved the use of this preparation for asking those types of questions are feasible in the near future.

Considering the technical difficulty and the cost associated with the development of the new IHC-SGN preparation, it is tempting to suggest computer simulation as an alternative. Albeit the fact that the auditory system uses complex computational

algorithms for signal reprocessing, the difficulty lies in that the cochlea uses both electrical and mechanoelectrical (analog) processes to set the first stage of signal transduction. This would require implementation of a computation system that will integrate biological analog circuitry into digital system, which has its own limitation, and the explanation is beyond the scope of this thesis. While there are several analog-integrated, *in-silico*, afferent model systems available (Lazarro, 1991), there are limits to the extent to which computational models can predict or even approximate *biology*. One must also take into account that even those computer model systems that have clear performances, have their algorithm parameters set based on data from physiological experiments. This is not to say, however; that the new preparation will have no limitation in approximating the *in-vivo* system. The most powerful outcome is when the two methods, experimental and computational, can be combined in parallel. Until then, experimental paradigms, such as the new IHC-SGN preparation, are necessary for understanding auditory signal processing at the basic level. The fundamental knowledge acquired here, in conjunction with *in-silico* models, can later applied for development of new generation speech recognition devices or hearing aids with minimized technical and computational glitches. And the development of the new IHC-SGN preparation is now only in the very infant stage of this whole process.

FUTURE DIRECTIONS

Here I provided foundation for the new IHC-SGN intact preparation and showed evidence of signal transmission between IHC and SGNs during early postnatal stages.

With technical fine tuning of the new preparation, it will be interesting to see whether signal transfer function is affected in SGNs of *Hcn1*- deficient mice compared to their WT littermate cohorts.

During development, SGNs make transient synaptic contacts with multiple IHCs before making a mature synaptic contact with one IHC following pruning. However, it is unknown whether those transient synapses are functional or have any physiological significance. Using the new IHC-SGN preparation it will be interesting to test whether the transient synapses are indeed functional by stimulating IHCs and recording the response from the SGN cell body that make transient synaptic contact.

In this thesis, I have provided evidence for spontaneous activity in postnatal SGNs that mirrors the spontaneous activity pattern in the immature IHCs. Given that spontaneous activity in postnatal SGNs is governed by IHC activity, it will be interesting to assay the developmental consequences in SGN when spontaneous activity is absent.

One of the limitations in addressing the specific role of spontaneous activity in SGNs for auditory neural circuit development is the experimental approach that has been used in the field. In many cases, the functional role of spontaneous activity has been indirectly derived from unilateral cochlear ablation studies. However, in this case, it is difficult to attribute the experimental result to the sole absence of spontaneous activity because cochlear ablation can induce other developmental abnormalities. To circumvent this problem, many researchers have started to use congenital deafness animal models, in which spontaneous activity is completely absent due to non-functional IHCs (Leao et al., 2006). The congenital deafness animal mice provide better experimental control compared to the ablation studies, however it is hard to attribute whether the effects seen

are due to absence of spontaneous activity *per se* or due to absence of sound-evoked activity.

Given these experimental limitations, it is critical to develop an *in-vivo* animal model in which the IHC activity can be manipulated in a time-specific, cell-specific manner. Utilizing this animal model, in combination with the new IHC-SGN intact preparation, one will be able to investigate the developmental consequences of spontaneous activity modculation, more specifically its effect on IHC-SGN synapse maturation, by testing the functionality and fidelity of signal transmission in SGNs by modulating IHC activity.

Recent advancement in development of high throughput molecular tools and optical imaging systems, innovative mouse genetic tools, such as *cre-lox* system and optogenetics, have led to remarkable increase in knowledge for cochlear development and auditory signal processing. By combining these available techniques with the new IHC-SGN intact preparation, we will be a step closer in answering many outstanding and long held questions in auditory physiology.

Looking beyond: Neuroscience at large

The cochlea is an excellent model system to study neuronal circuit development. During the first two postnatal weeks, the auditory system undergoes extensive developmental changes to acquire a mature system with exquisitely ordered neural structure that is capable of processing complex sound signals with sub microsecond accuracy. Compared to CNS, cochlea has a less complex, yet highly ordered system as

evidenced by tonotopic specialization, with a well defined input and output structure. Additionally, the neural refinement occurs in a given time window, making it a great system to study neural development and refinement. Therefore, the establishment of the new preparation will not only contribute to understanding IHC-SGN signal processing, but also can be used as a model system to investigate important questions in neurobiology, such as activity dependent pruning.

References

Adamson CL, Reid MA, Mo Z-L, Bowne-English J, Davis RL (2002) Firing features and potassium content of murine spiral ganglion neurons vary with cochlear location. *J Comp Neurol* 447:331-350.

Aizenman CD, Linden DJ (1999) Regulation of the rebound depolarization and spontaneous firing patterns of deep nuclear neurons in slices of rat cerebellum. *J Neurophysiol* 82:1697-1709.

Akil O, Seal RP, Burke K, Wang C, Alemi A, During M, Edwards RH, Lustig LR (2012) Restoration of hearing in the VGLUT3 knockout mouse using virally mediated gene therapy. *Neuron* 75:283-293.

Altomare C, B. Terragni B, Brioschi C, Milanesi R, Pagliuca C, Viscomi C, Moroni A, Baruscotti M, DiFranceso D (2003) Heteromeric HCN1-HCN4 channels: a comparison with native pacemaker channels from the rabbit sinoatrial node. *J Physiol* 549:347-359.

Araki S, Atsushi K, Seldon HL, Shepherd RK, Funasaka S, Clark GM (1998) Effects of chronic electrical stimulation on spiral ganglion neuron survival and size in deafened kittens. *Laryngoscope* 109:687-695.

Bakondi G, Pór A, Kovács I, Szucs G, and Rusznák Z (2009) Hyperpolarization-activated, cyclic nucleotide-gated, cation non-selective channel subunit expression pattern of guinea-pig spiral ganglion cells. *Neuroscience* 158:1469-1477.

Bal R, Oertel D (2000) Hyperpolarization-activated, mixed-cation current (I_h) in octopus cells of the mammalian cochlear nucleus. *J Neurophysiol* 84:806-81.

Banks MI, Pearce RA, Smith PH (1993) Hyperpoarziation-activated cation current (I_h) in neurons of the medial nucleus of the trapezoid body: voltage-clamp analysis and enhancement by norepinephrine and cAMP suggest a modulatory mechanism in the auditory brainstem. *J Neurophysiol* 70:1420-1432.

Bedrosian JC, Gratton MA, Brigande JV, Tang W, Landau J, Bennett J (2006) In vivo delivery of recombinant viruses to the fetal murine cochlea: transduction characteristics and long term effect on auditory function. *Mol Ther* 14:328-335.

Besch SR, Suchyna T, Sachs F (2002) High-seeped pressure clamp. *Pflugers Arch* 445:161-166.

Berglund AM, Ryugo DK (1987) Hair cell innervation by spiral ganglion neurons in the mouse. *J Comp Neurol* 255:560-570.

Beurg M, Fettiplace R, Nam JH, Ricci AJ (2009) Localization of inner hair cell mechanotransducer channels using high-speed calcium imaging. *Nat Neurosci* 12:553-558.

Beutner D, Moser T (2001) The presynaptic function of mouse cochlear inner hair cells during development of hearing. *J Neuorsci* 21:4593-4599.

Biel M, Wahl-Schott C, Michalakis S, Zong X (2009) Hyperpolarization-activated cation channels: From gens to function. *Physiol Rev* 89:847-885.

Blankenship AG, Feller MB (2010) Mechanisms underlying spontaneous patterned activity in developing neural circuits. *Nat Rev Neurosci* 11:18-29.

Blankenship AG, Ford KJ, Johson J, Seal RP, Edwards RH, Copenhagen DR, Feller MB (2009) Synaptic and extrasynaptic factors governing glutamatergic retinal waves. *Neuron* 62:230-241.

Bok J, Zha X-M, Cho Y-S, Green SH (2003) An extracellular locus of cAMP-dependent protein kinase action is necessary and sufficient for promotion of spiral ganglion neuronal survival by cAMP. *J Neuorsci* 23:777-787.

BoSmith RE, Briggs I, Sturgess NC (1983) Inhibitory actions of ZENECA ZD7288 on whole-cell hyperpolarization activated inward current (I_f) in guinea-pig dissociated sinoatrial node cells. *Br J Pharmacol* 10:343-349.

Brandt A, Striessing J, Moser T (2003) $Ca_v1.3$ channels are essential for development and presynaptic activity of cochlear inner hair cells. *J Neurosci* 23:10832-10840.

Bregman A (1990) *Auditory Scene Analysis: The Perceptual Organization of Sound.* The MIT Press, Cambridge, MA. pp. 792.

Brenowitz S, Trussel LO (2001) Maturation of synaptic transmission at End-bulb synapses of the cochlear nucleus. *J Neurosci* 21:9487-9498.

Brown MC (1987) Morphology of labeled afferent fibers in the guinea pig cochlea. *J Comp Neurol* 260:591-604.

Brownell WE, Bader CR, Bertrand D, de Ribaupierre Y (1985) Evoked mechanical responses of isolated cochlear outer hair cells. *Science* 227:194-196.

Buran BN, Strenzke N, Neef A, Gundelfinger ED, Moser T, Liberman MC (2010) Onset coding is degraded in auditory nerve fibers from mutant mice lacking synaptic ribbons. *J Neurosci* 30:7587-7597.

Cant NB (1998) Structural Development of the Mammalian Auditory Pathways. In: *Development of the Auditory System.* Rubel EW, Popper AN, Fay RR (Eds.), Springer, New York, NY. pp. 15-413.

Carr RW, Pianova S, McKemy DD, Brock JA (2009) Action potential in the peripheral terminals of cold-sensitive neurons innervating the guinea-pig cornea. *J Physiol* 587:1249-1464.

Chen C (1997) Hyperpolarization-activated current (I_h) in primary auditory neurons. *Hear Res* 110:179-190.

Chen WC, Davis RL (2006) Voltage-gated and two-pore domain potassium channels in murine spiral ganglion neurons. *Hear Res* 222:89-99.

Chen WC, Xue HZ, Hsu YL, Liu Q, Patel S, Davis RL (2011) Complex distribution patterns of voltage-gated calcium channel α-subunits in the spiral ganglion. *Hear Res* 278:52-68.

Chen Z, Kujawa SG, Sewell W (2007) Auditory sensitivity via rapid changes in expression of surface AMPA receptors. *Nat Neurosci* 10:1238-1240.

Crawford AC, Fettiplace R (1981) An electrical tuning mechanism in turtle cochlear hair cells. *J Physiol* 312:377-412.

Davis RL (2003) Gradients of neurotrophins, ion channels, and tuning in the cochlea. *The Neuroscientist* 9:311-316.

Denk W, Holt JR, Shepherd GM, Corey DP (1995) Calcium imaging of single stereocilia in hair cells: localization of transduction channels at both ends of tip links. *Neuron* 15:1311-1321.

Denk W, Webb WW (1992) Forward and reverse transduction at the limit of sensitivity studied by correlating electrical and mechanical fluctuations in frog saccular hair cells. *Hear Res* 60:89-102.

DiFrancesco D (1986) Characterization of single pacemaker channels in cardiac sino-atrial node cells. *Nature* 324:470-473.

DiFrancesco D, Tortora P (1991) Direct activation of cardiac pacemaker channels by intracellular cyclic AMP. *Nature* 351:145-147.

Dulon D, Jagger DJ, Lin X, Davis RL (2006) Neuromodulation in the spiral ganglion: shaping signals from the organ of corti to the CNS. *J Membr Biol* 209:167-175.

Eatock RA, Weiss TF, Otto KL (1991) Dependence of discharge rate on sound pressure level in cochlear nerve fibers of the alligator lizard: implication for cochlear mechanisms. *J Neurophysiol* 65:1580-1597.

Echteler SM (1992) Developmental segregation in the afferent projections to mammalian auditory hair cells. *Proc Natl Acad Sci USA* 89:6324-6327.

Echteler SM, Nofsinger YC (2000) Development of ganglion cell topography in the postnatal cochlea. *J Comp Neurol* 425:436-446.

Elgoyhen AB, Vetter DE, Katz E, Rothlin CV, Heinemann SF, Boulter J (2001) α10: A determinant of nicotinic cholinergic receptor function in mammalian vestibular and cochlear mechanosensory hair cells. *Proc Natl Acad Sci USA* 98:3501-3506.

Farris HE, Wells GB, Ricci AJ (2006) Steady-state adaptation of mechanotransduction modulates the resting potential of auditory hair cells, providing an assay for endolymph [Ca^{2+}]. *J Neurosci* 26:12526-12536.

Fay RR, Popper AN (2000) Evolution of hearing in vertebrates: the inner ears and processing. *Hear Res* 149:1-10.

Fekete DM, Rouiller EM, Liberman MC, Ryugo DK (1984) The central projections of intracellularly labeleld auditory nerve fibers in cats. *J Comp Neurol* 229:432-450.

Felix II RA, Fridberger A, Leijon S, Berrebi AS, Magnusson AK(2011) Sound rhythms are encoded by postinhibitory rebound spiking in the superior paraolivary nucleus. *J Neurosci* 31:12566-12578.

Feller MB (1999) Spontaneous correlated activity in developing neural circuits. *Neuron* 22:653-656.

Forge A, Becker D, Casalotti S, Edwards J, Marziano N, Nevill G (2003) Gap junctions in the inner ear: comparison of distribution patterns in different vertebrates and assessment of connexin composition in mammals. *J Comp Neurol* 467:207-231.

Forsythe ID (2007) A fantasia on Kölliker's organ. *Nature* 450:43-44.

Friauf E, Lohmann C (1999) Development of auditory brainstem circuitry. *Cell Tissue Res* 297:187-195.

Fuchs PA, Sokolowski BHA (1990) The acquisition during development of Ca^{2+}-activated potassium current by cochlear hair cells of the chick. *Proc R Soc Lond B* 241:122-126.

Galli L, Maffei L (1988) Spontaneous impulse activity of rat retinal ganglion cells in prenatal life. *Science* 242:90-91.

Gans C (1992) An overview of the evolutionary biology of hearing. In: *The Evolutionary Biology of Hearing*, Webster DB, Fay RR, Popper AN (Eds.), Springer Verlag, New York, NY. pp. 3-13.

Gähwiler BH (1981) Labeling of neurons within CNS explants by intracellular injection of Lucifer yellow. *J Neurobiol* 12:187-191.

Geisler CD (1998) *From Sound to Synapse. Physiology of the Mammalian Ear*. New York: Oxford University Press, New York, NY. pp, 396.

Géléoc GS, Lennan GW, Richardson GP, Kros CJ (1997) A quantitative comparison of mechanoelectrical transduction in vestibular and auditory hair cells of neonatal mice. *Proc Biol Sci* 264:611-621.

Ginzberg RD, Morest DK (1984) Fine structure of cochlear innervation in the cat. *Hear Res* 2:109-127.

Glowatzki E, Fuchs PA (2000) Cholinergic synaptic inhibition of inner hair cells in the neonatal mammalian cochlea. *Science* 288:2366-2368.

Glowatzki E, Fuchs PA (2002) Transmitter release at the hair cell ribbon synapse. *Nat Neurosci* 5:147-154.

Goldberg GS, Moreno AP, Lampe PD (2002) Gap junctions between cells expressing connexin 43 or 32 show inverse permselectivity to adenosine and ATP. *J Biol Chem* 277:36725-36730.

Goodyear RJ, Kros CJ, Richardson GP (2006) The Development of Hair Cells in the Inner Ear. In: *Vertebrate hair cells.* Eatock RA, Fay RR, Popper AN (Eds.), Springer, New York, NY. pp. 20-94.

Goutman JD, Fuchs PA, Glowatzki E (2005) Facilitating efferent inhibition of inner hair cells in the cochlea of the neonatal rat. *J Physiol* 556:49-59.

Goutman JD, Glowatzki E (2007) Time course and dependence of transmitter release at single ribbon synapse. *Proc Natl Acad Sci USA* 104:16341-16346.

Grant L, Yi E, Glowatzki E (2010) Two modes of release shape the postsynaptic response at the inner hair cell ribbon synapse. *J Neurosci* 30:4210-4220.

Guinan JJ Jr (2012) How are inner hair cells stimulated? Evidence for multiple mechanical drives. *Hear Res* 292:35-50.

Gummer AW, Mark RF (1994) Patterned neural activity in brain stem auditory area of a prehearing mammal, the tammar wallaby (*Macropus eugenii*). *Neuro Report* 5:685-688.

Hanani M (2012) Lucifer yellow-an angel rather that the devil. *J Cell Mol Med* 16:22-31.

Hanse E, Durand GM, Garaschuk O, Konnerth A (1997) Activity dependent wiring of the developing hippocampal neuronal circuit. *Semin Cell Dev Biol* 8:35-42.

Hansen MR, Bok J, Devaiah AK, Zha X-M, Green SH (2003) Ca^{2+}/Calmodulin-dependent protein kinase II and IV both promote survival but differ in their effects on axon growth in spiral ganglion neurons. *J Neurosci Res* 72:169-184.

Hanson MG, Landmesser LT (2004) Normal patterns of spontaneous activity are required for correct motor axon guidance and the expression of specific guidance molecules. *Neuron* 43:687-701.

Harris NC, Constant A (1995) Mechanism of block by ZD 7288 of the hyperpolarzation-activated inward rectifying current in guinea pig substantia nigra neurons in vitro. *J Neurophysiol* 74:2366-2378.

Hashisaki GT, Rubel EW (1989) Effect of unilateral cochlea removal on anteroventral cochlear nucleus neurons in developing gerbils. *J Comp Neurol* 283:5-73.

Hauser M (1997) *Evolution of Communication*. The MIT Press, Cambridge, MA. pp.760.

Hegarty JL, Kay AR, Green SH (1997) Trophic support of cultured spiral ganglion neurons by depolarization exceeds and is additive with that by neurotrophin or cAMP and requires elevation of $[Ca^{2+}]_i$ within a set range. *J Neurosci* 17:1959-1970.

Herrmann SJ, Stieber J, Ludwig A (2007) Pathophysiology of HCN channels. *Eur J Physiol* 454:517-522.

Hinosoja R (1977) A note on development of Corti's organ. *Acta Otalaryngol* 84:238-251.

Holt JR, Corey DP, Eatock RA (1997) Mechanoelectrical transduction and adaptation in hair cells of the mouse utricle, a low-frequency vestibular organ. *J Neurosci* 17:8739-8748.

Horwitz GC, Lelli A, Gélécoc GS, Holt JR (2010) HCN channels are not required for mechanotransduction in sensory hair cells of the mouse inner ear. *PLoS One* 5: e 8627.

Horwitz, GC, Risner-Janiczek J, Jones SM, Holt JR (2011) HCN channels expressed in the inner ear are necessary for normal balance function. *J Neurosci* 31:16814-16825.

Hossain WA, Antic SD Yang Y, Rasband MN Morest DK (2005) Where is the spike generator of the cochlear nerve? Voltage-gated sodium channel sin the mouse cochlea. *J. Neurosci.* 25:6857-6868.

Housley GD (2000) Physiological effects of extracellular nucleotides in the inner ear. *Clin Exp Pharm Physiol* 27:575-580.

Huang LC, Thorne PR, Housely GD, Montgomery JM (2007) Spatiotemporal definition of neurite outgrowth, refinement and retraction in the developing mouse cochlea. *Development* 134:2925-2933.

Hudspeth AJ (1985) The cellular basis of hearing: the biophysics of hair cells. *Science* 230:745-752.

Ishii TM, Takano M, Ohmori H (2001) Determinants of activation kinetics in mammalian hyperpolarization-activated cation channels. *J Physiol* 537:93-100.

Ishii TM, Takano M, Xie LH, Oma A, Ohmori H (1999) Molecular characterization of the hyperpolarization-activated cation channel in rabbit sinoatrial node. *J Biol Chem* 274: 12835-12839.

Ito K, Dulon D (2002) Nonselective cation conductance activated by muscarinic and purinergic receptors in rat spiral ganglion neurons. *Am J Physiol Cell Physiol* 282:1121-1135.

Johnson DH (1980) The relationship between spike rate and synchrony in responses of auditory-nerve fibers to single tones. *J Acoust Soc Am* 68:1115-1122.

Johnson SL, Eckrich T, Kuhn S, Zampini V, Franz C, Ranatunga KM, Roberts TP, Masetto S, Knipper M, Kros CJ, Marcotti W (2011) Position-dependent patterning of spontaneous action potentials in immature cochlear inner hair cells. *Nat Neurosci* 14:711-718.

Johnson SL, Kennedy HJ, Holley MC, Fettiplace R, Marcotti W (2012) The resting transducer current drives spontaneous activity in prehearing mammalian cochlear inner hair cells. *J Neurosci* 32:10479-10483.

Johnson SL, Marcotti W, Kros CJ (2005) Increase in efficiency and reduction in Ca^{2+} dependence of exocytosis during development of mouse inner hair cells. *J Physiol* 563:177-191.

Jones TA, Jones SM (2000) Spontaneous activity in the statoacoustic ganglion of the chicken embryo. *J Neurophysiol* 83:1452-1468.

Jones TA, Jones SM, Paggett KC (2001) Primordial rhythmic bursting in embryonic cochlear ganglion cells. *J Neurosci* 21:8129-8135.

Jones TA, Jones SM, Paggett KC (2006) Emergence of hearing in the chicken embryo. *J Neurophysiol* 96:128-141.

Jones TA, Leake PA, Snyder RL, Stakhovskaya O, Bonham B (2007) Spontaneous discharge patterns in cochlear spiral ganglion cells before the onset of hearing in cats. *J Neuropshysiol* 98:1898-1908.

Kamiya K, Takahashi K, Kitamura K, Momoi T, Yoshikawa Y (2001) Mitosis and apoptosis in postnatal auditory system of the C3H strain. *Brain Res* 901:296-302.

Kandler K, Clause A, Noh J (2009) Tonotopic reorganization of developing auditory brainstem circuits. *Nat Neurosci* 12:711-717

Kane KL, Long-Guess CM, Gagnon LH, Ding D, Salvi RJ, Johnson KR (2012) Genetic background effects on age-related hearing loss associated with *Cdh23* variants in mice. *Hear Res* 283:80-88.

Katz E, Elgoyhen AB, Gomez-Casati ME, Knipper M, Vetter DB, Fuchs PA, Glowatzki E (2004) Developmental regulation of nicotinic synapses on cochlear inner hair cells. *J Neurosci* 24:7814-7820.

Kawashima Y, Géléoc GS, Kurima K, Labay V, Lelli A, Asai Y, Makishima T, Wu DK, Della Santina CC, Holt JR, Griffith AJ (2011) Mechanotransduction in mouse inner ear hair cells requires transmembrane channel-like genes. *J Clin Invest* 121:4796-4809.

Kelly M (2007) Cellular commitment and differentiation in the organ of Corti. *Int J Dev Biol* 51:571-583.

Khimich D, Nouvian R, Pujol R, Tom Dieck S, Egner A, Gundelfinger ED, Moser T (2005) Hair cell synaptic ribbons are essential for synchronous auditory signaling. *Nature* 434: 889-894.

Kiang NY, Liberman MC, Gage JS, Northrup CC, Dodds LW, Oliver ME (1984) Afferent innervation of the mammalian cochlea. In: *Comparative Physiology of Sensory Systems*. Bolis, L., Keynes, R.D., Maddrell, H.P. (Eds.), Cambridge University Press, Cambridge, UK. pp. 143-161.

Kiang NY, Rho JM, Northrop CC, Liberman MC, Ryugo DK (1982) Hair-cell innervation by spiral ganglion cells in adult cats. *Science* 217:175-177.

Kiang NY, Watanabe T, Thomas EC, Clark LF (1965) *Discharge Patterns of Single Fibers in the Cat's Auditory Nerve,* Vol. 35. The M.I.T. Press, Cambridge, MA.

Koch U, Grothe B (2003) Hyperpolarization-activated current (I_h) in the inferior colliculus: distribution and contribution to temporal processing. *J Neurophysiol* 90:3679-3687.

Kodak VC, Sanes DH (1995) Synaptically evoked prolonged depolarizations in the developing auditory system. *J Neurophysiol* 74:1611-1620.

Kopp-Scheinpflug C, Tozer AJB, Robison SW, Tempel BL, Hennig MH, Forsythe ID (2011) The sound of silence: Ionic mechanisms encoding sound termination. *Neuron* 71:911-925.

Kros CJ (2007) How to build an inner hair cell: Challenges for regeneration. *Hear Res* 227:3-10.

Kros CJ, Crawford AC (1990) Potassium currents in inner hair cells isolated from the guinea-pig cochlea. *J Physiol* 421:263-291.

Kros CJ, Ruppersberg JP, Rüsch A (1998) Expression of a potassium current in inner hairs cells during development of hearing in mice. *Science* 394:281-284.

Kros CJ, Rüsch A, Richardson GP (1992) Mechano-electrical transducer currents in hair cells of the cultured neonatal mouse cochlea. *Proc Biol Sci* 249:185-193.

Langer P, Grudner S, Rusch A (2003) Expression of Ca^{2+} activated BK Channel mRNA and its splice variant in the rat cochlea. *J Comp Neurol* 455:281-284.

Lazzaro JP (1991) Biologically-based auditory signal processing in analog VLSI. *IEEE Asilomar Conference on Signal, Systems, and Computers*. pp. 790-794.

Leake PA, Hradek GT, Chair L, Snyder RL (2006) Neonatal deafness results in degraded topographic specificity of auditory nerve projections to the cochlear nucleus in cats. *J Comp Neurol* 497:13-31.

Leake PA, Hradek GT, Rebscher SJ, Snyder RL (1991) Chronic intracochelar electrical stimulation induces selective survival of spiral ganglion neurons in neonatally deafened cats. *Hear Res* 54:251-271.

Leake PA, Hradek GT, Vollmer M, Rebscher SJ (2007) Neurotrophic effects of GM1 ganglioside and electrical stimulation of cochlear spiral ganglion neurons in cats deafened as neonates. *J Comp Neurol* 501:837-853.

Leake PA, Stakhovskaya O, Hradek GT, Hetherington AM (2008) Factors influencing neurotrophic effects of electrical stimulation in the deafened developing auditory system. *Hear Res* 242:86-99.

Leao RN, Sun H, Svahn K, Bertson A, Youssoufian M, Paolini AG, Fyffe REF, Walmsley B (2006) Topographic organization in the auditory brainstem of juvenile mice is disrupted in congenital deafness. *J Physiol* 571:563-578.

Lelli A, Asai Y, Forge A, Holt JR, Géléoc GS (2009) Tonotopic gradient in the developmental acquisition of sensory transduction in outer hair cells of the mouse cochlea. *J Neurophysiol* 101:2961-2973.

Li L, Parkins CW, Webster DB (1999) Does electrical stimulation of deaf cochleae prevent spiral ganglion degeneration? *Hear Res* 133:27-39.

Li J, Young ED (1993) Discharge-rate dependence of refractory behavior of cat auditory –nerve fibers. *Hear Res* 69:151-162.

Liberman MC (1978) Auditory-nerve response from cats raised in a lownoise chamber. *J Acoust Soc Am* 63:442-455.

Liberman MC (1980) Morphological differences among radial afferent fibers in the cat cochlea: an electron-microscopic study of serial section. *Hear Res* 1:45-63.

Liberman MC (1982a) Single-neuron labeling in the cat auditory nerve. *Science* 216:1239-1241.

Liberman MC (1982b) The cochlear frequency map for the cat: labeling auditory nerve fibers of known characteristic frequency. *J Acoust Soc Am* 72:1441-1449.

Liberman MC, Brown MC (1986) Physiology and anatomy of single olivocochlear neurons in the cat. *Hear Res* 24:17-36.

Lieberman MC, Gao J, He DZ, Wu X, Jia S, Zuo J (2002) Prestin is required for electromotility of the outer hair cells and for the cochlear amplifier. *Nature* 419:300-304.

Liberman MC, Oliver ME (1984) Morphometry of intracellularly labeled neurons of the auditory nerve: correlation with functional properties. *J Comp Neurol* 223:163-176.

Liberman MC, Simmons DD (1985) Application of neuronal labeling techniques to the study of the peripheral auditory system. *J Acoust Soc Am* 78:312-319.

Lin X, Chen S (2000) Endogenously generated spontaneous spiking activities recorded from postnatal spiral ganglion neuron in vitro. *Dev Brain Res* 119:297-305.

Lippe WR (1994) Rhythmic spontaneous activity in the developing avian auditory system. *J Neurosci* 14:1486-1495.

Lippe WR (1995) Relationship between frequency of spontaneous bursting and tonotopic position in the developing avian auditory system. *Brain Res* 703:205-213.

Liu Q, Davis RL (2007) Regional specification of threshold sensitivity and response time in CBA/CaJ mouse spiral ganglion neurons. *J Neurophysiol* 98:2215-2222.

Lousteau RJ (1987) Increased spiral ganglion cell survival in electrically stimulated deafened guinea pig cochleae. *Laryngoscope* 97:836-842.

Lowenstein WR, Ishiko N (1960) Effects of polarization of the receptor membrane and of the first Ranvier node in a sense organ. *J Gen Physiol* 43:981-998.

Lu CC, Appler JM, Houseman EA, Goodrich LV (2011) Developmental profiling of spiral ganglion neurons reveals insights into auditory circuit assembly. *J Neurosci* 31:10903-10918.

Ludwig A , Budde T, Stieber J, Moosmang S, Wahl C, Holthoff K, Langebartels A, Wotjak C, Munsch T, Zong X, Feil S, Feil R, Lancel M, Chien KR, Konnerth A, Pape HC, Biel M, Hofmann F (2003) Absence epilepsy and sinus dysrhythmia in mice lacking the pacemaker channel HCN2. *EMBO J* 22:216-224.

Ludwig A, Zong X, Jeglitsch M, Hofmann F, Biel M (1998) A family of hyperpolarization-activated mammalian cation channels. *Nature* 393:587-591.

Ludwig A, Zong X, Stieber J, Hullin R, Hofmann F Biel M (1999) Two pacemaker channels from human heart with profoundly different activation kinetics. *EMBO J* 12:2323-2329.

Luo L, Brumm D, Ryan AF (1995) Distribution of non-NMDA glutamate receptor mRNAs in the developing rat cochlea. *J Comp Neurol* 36:372-382.

Lustig LR, Leake PA, Snyder RL, Rebscher SJ (1994) Changes in the cat cochlear nucleus following neonatal deafening and chronic intracochlear electrical stimulation. *Hear Res* 74:29-37.

Lüthi A, McCormick DA (1998) Periodicity of thalamic synchronized oscillations: the role of Ca^{2+} mediated upregulation of I_h. *Neuron* 20:553-563.

Lv P, Sihn C-R, Wang W, Shen H, Kim HJ, Rocha-Sanchez SM, Yamoah EN (2012) Posthearing Ca^{2+} currents and their roles in shaping the different modes of firing of spiral ganglion neurons. *J Neurosci* 32:6314-6330.

Lv P, Wei D, Yamoah EN (2010) K_v7-type channel currents in spiral ganglion neurons: involvement sensory neural hearing loss. *J Biol Chem* 45:34699-34707.

Marcotti W, Johson SL, Holley MC, Kros CJ (2003a) Developmental changes in the expression of potassium currents of embryonic, neonatal and mature mouse inner hair cells. *J Physiol* 548: 383-400.

Marcotti W, Johson SL, Kros CJ (2004) A transiently expressed SK current sustains and modulates action potential activity immature mouse inner hair cells. *J Physiol* 560:691-708.

Marcotti W, Johnson SL, Rüsch A, Kros CJ (2003b) Sodium and calcium current shape action potentials in immature mouse inner hair cells. *J Physiol* 552:743-761.

Marcotti W, Kros CJ (1999) Developmental expression of the potassium current $I_{k,n}$ contributes to maturation of mouse outer hair cells. *J Physiol* 520:653-660.

Marcotti W, van Netten SM, Kros CJ (2005) The aminoglycoside antibiotic dihydrostreptomycin rapidly enters mouse outer hair cells through the mechano-electrical transducer channels. *J Physiol* 567:505-521.

Mars GS, Spirou GA (2012) Embryonic assembly of auditory circuits: spiral ganglion and brainstem. *J Physiol* 590:2391-2408.

McBride DW Jr, Hamill OP (1992) Pressure-clamp: a method for rapid step perturbation of mechanosensitive channels. *Pflugers Arch* 421:606-612.

McBride DW Jr, Hamill OP (1995) A fast pressure-clamp technique for studying mechanogated channels. In: *Single-channel recording*. Sakmann B. Neher E (Eds.), Plenum, New York, NY. pp. 329-340.

Meister M, Wong ROL, Baylor, DA, Shatz CJ (1991) Synchronous bursts of action potentials in ganglion cells of the developing mammalian retina. *Science* 252:939-943.

Meyer AC, Moser T (2010) Structure and function of cochlear afferent innervation. *Curr Opin Otolaryngol Head Neck Surg* 18:441-446.

McKay SM, Oleskevich S (2007) The role of spontaneous activity in development of the endbulb of Held synapse. *Hear Res* 230:53-63.

Mo ZL, Adamson CL, Davis RL (2002) Dendrotoxin-sensitive K^+ currents contribute to accommodation in murine spiral ganglion neurons. *J Physiol* 542:763-778.

Mo Z-L, Davis RL (1997) Heterogenous voltage dependence of inward rectifier currents in spiral ganglion neurons. *J Neurophysiol* 78:3019-3027.

Moody WJ (1998) Control of spontaneous activity during development. *J Neurobiol* 37:97-109.

Moody WJ, Bosma MM (2005) Ion channel development, spontaneous activity, and activity-dependent development tin nerve and muscle cells. *Physiol Rev* 85:883-941.

Moore DR (1982) Late onset of hearing in the ferret. *Brain Res* 253:309-11.

Moore DR, Shannon RV (2009) Beyond cochlear implants: awakening the deafened brain. *Nat Neurosci* 12:686-691.

Moosmang S, Biel M, Hofmann F, Ludwig A (1999) Differential distribution of four hyperpolarization-activated cation channels in mouse brain. *J Biol Chem* 380:975-980.

Mostafapour SP, Cochran SL, Del Puero NM, Rubel EW (2000) Patterns of cell death in mouse anteroventral cochlear nucleus neurons after unilateral cochlea removal. *J Comp Neurol* 426:561-571.

Müller M (1996) The cochlear place-frequency map of the adult and developing Mongolian gerbil. *Hear Res* 94:148-156.

Nagtegaal AP, Borst JG (2010) In vivo dynamic clamp study of I_h in the mouse inferior colliculus. *J Neurophsyiol* 104:940-948.

Niedzielski AS, Wenthold RJ (1995) Expression of AMPA, kainite, and NMDA receptor subunits in cochlear and vestibular ganglia. *J Neurosci* 13:3496-3509.

Nolan MF, Malleret G, Dudman JT, Buhl DL, Santoro B,Gibbs E, Vronskaya S, Buzsáki G, Siegelbaum SA, Kandel ER, Morozov A (2004) A behavioral role for dendritic integration: HCN1 channels constrain spatial memory and plasticity at inputs to distal dendrites of CA1 pyramidal neurons. *Cell* 119:719-732.

Nolan MF, Malleret G, Lee KH, Gibbs E, Dudman JT, Santoro B, Yin D, Thompson RF, Siegelbaum SA, Kandel ER, Morozov A (2003) The hyperpolarization-activated HCN1channel is important for motor learning and neuronal integration by cerebellar Purkinje cells. *Cell* 115:551-564.

Nowotny M, Gummer AW (2006) Nanomechanics of the subtectorial space caused by electromechanics of cochlear outer hair cells. *Proc Natl Acad Sci U S A* 103:2120-2125.

Pan B, Géléoc GS, Asai Y, Horwitz GC, Kurima K, Ishikawa K, Kawashima Y, Griffith AJ, Holt JR (2013) TMC1 and TMC2 are components of the mechanotransduction channel in hair cells of the mammalian inner ear. *Neuron* 79:504-515.

Parks TN (1979) Afferent influences on the development of the brain stem auditory nuclei of the chicken: otocyst ablation. *J Comp Neurol* 183:665-677.

Parks TN (1997) Effects of early deafness on development of brain stem auditory neurons. *Ann Otol Rhinol Laryngol Suppl* 168:37-43.

Perkins KL (2006) Cell-attached voltage-clamp and current-clamp recording and stimulation techniques in brain slices. *J Neurosci Methods* 154:1-18.

Perkins RE, Morest DK (1975) A study of cochlear innervation patterns in cats and rats with the Golgi method and Nomarski optics. *J Comp Neurol* 163:129-158.

Platzer J, Engel J, Schrott-Fischer A, Stephan K, Bova S, Chen H, Zheng H, Striessnig J. (2000) Congenital deafness and sinoatrial node dysfunction in mice lacking class D L type Ca^{2+} channels. *Cell* 102:89-97.

Pujol R, Lavigne-Rebillard M, Lenoir M (1998) Development of sensory and neural structures in the mammalian cochlea. In: *Development of the auditory system*, Rubel EW, Fay RR (Eds.), Springer-Verlag, New York, NY. pp. 146-192.

Reid MA, Flores-Otero J, Davis RL (2004) Firing patterns of type II spiral ganglion neurons in vitro. *J Neurosci* 24:733-742.

Robertson D (1976) Possible relation between structure and spike shapes of neurons in guinea pig cochlear ganglion. *Brain Res* 109:487-496.

Robertson D (1984) Horseradish peroxidase injection of physiologically characterized afferent and efferent neurons in the guinea pig spiral ganglion. *Hear Res* 15:113-121.

Robertson D, Sellick PM, Patuzzi R (1999) The continuing search for outer hair cell afferents in the guinea pig spiral ganglion. *Hear Res* 136:151-158.

Robinson RB, Siegelbaum SA (2003) Hyperpolarization-activated cation currents: From molecules to physiological function. *Annu Rev Physiol* 65:453-480.

Roehm PC, Hansen MR (2005) Strategies to preserve or regenerate spiral ganglion neurons. *Curr Opin Otolaryngol Head Neck Surg* 13:294-300.

Romand MR, Romand R (1987) The ultrastructure of spiral ganglion cells in the mouse. *Acta Otolaryngol* 104:29-39.

Romand R (1983) Development of the cochlea. In: *Development of Auditory and Vestibular Systems.* Romnd R (Ed), Academic Press, New York, NY. pp. 47-88.

Romand R (1984) Functional properties of auditory nerve fibers during postnatal development in kitten. *Exp Brain Res* 56:395-402.

Royeck M, Horstmann MT, Remy S, Reitze M, Yaari Y, Beck H (2008) Role of axonal Na_v 1.6 sodium channels in action potential initiation of CA1 pyramidal neurons. *J Neuryphysiol* 100:2380-2008.

Rubel EW, Fritzsch B (2002) Auditory system development: Primary auditory neurons and their targets. *Annu Rev Neurosci* 25:51-101

Ruel J, Chen C, Pujol R, Bobbin RP, Puel JL (1999) AMPA-preferring glutamate receptors in cochlear physiology of adult guinea-pig. *J Physiol* 518:667-680.

Russel FA, Moore DR (1999) Afferent reorganization within the superior olivary complex of the gerbil: development and induction by neonatal, unilateral cochlear removal. *J Comp Neurol* 352:607-625.

Russel IJ, Richardson GP (1987) The morphology and physiology of hair cells in organotypic cultures of the mouse cochlea. *Hear Res* 31:9-24.

Rusznák Z, Szűcs G (2009) Spiral ganglion neurons: an overview of morphology, firing behavior, ionic channels and function. *Eur J Phsyiol* 457:1303-1325.

Rübsamen R, Lippe WR (1998) Cochlear Function. In: *Development of the auditory system.* Rubel EW, Popper AN, Fay, RR. (Eds.), Springer, New York, NY, pp.193-270.

Ryugo DK, Kretzmer EA, Niparko JK (2005) Restoration of auditory nerve synapses in cats by cochlear implants. *Science* 310:1490-1492.

Salih, SG, Housley GD, Raybould NP, Thorne PR (1999) ATP-gated ion channel expression in primary auditory neurons. *Neuroreport* 10:2579-2586.

Sanes DH, Walsh EJ (1998) The development of central auditory processing. In: *Development of the Auditory System* Rubel EW, Popper AN, Fay RR (Eds.), Springer-Verglag, New York, NY. pp. 271-314.

Santoro B, Chen S, Lüthi A, Pavlidis P, Shumyatskky GP, Tibb GR, Siegelbaum SA (2000) Molecular and functional heterogeneity of hyperpolarization-activated pacemaker channels in the mouse CNS. *J Neurosci* 20:5264-5275.

Santos-Sacchi J (1993) Voltage-dependent ionic conductances of Type I spiral ganglion cells from the guinea pig inner ear. *J Neurosci* 13:3599-3611.

Saunders JC, Coles RB, Gates BR (1973) The development of evoked responses in the cochlea and cochlear nuclei of the chick. *Brain Res* 63:59-74.

Sher EA (1971) The embryonic and postnatal development of the inner ear of the mouse. *Acta Otolaryngol Suppl* 285:1-77.

Simmons DD, Mason-Gieseke LM, Hendrix TW, Morris K, Williams SJ (1991) Postnatal maturation of spiral ganglion neurons: A horseradish peroxidase study. *Hear Res* 55:81-91.

Simonelli F, Maguire AM, Auricchio A et al. (2010) Gene therapy for Leber's congenital amarosis is safe and effective through 1.5 years after vector administration. *Mol Ther* 18:643-650.

Smith RL (1977) Short-term adaptation in single auditory nerve fibers: some post-stimulatory effects. *J Neurophysiol* 40:1098-1111.

Sobkowicz HM, Rose JE, Scott GE, Levenick CV (1986) Distribution of synaptic ribbons in the developing organ of Corti. *J Neurocytol* 15:693-714.

Sobkowicz HM, Rose JE, Scott GE, Slapnick SM (1982) Ribbon synapses in the developing intact and cultured organ of Corti in the mouse. *J Neurosci* 2:942-957.

Sonntag M, Englitz B, Koopp-Scheinpflug C, Rübsamen R (2009) Early postnatal development of spontaneous and acoustically evoked discharge activity of principal cells of the medical nucleus of the trapezoid body: an in vivo study in mice. *J Neurosci* 29:9510-9520.

Spoendlin II (1969) Innervation pattern of the organ of Corti of the cat. *Acta Oto-Iaryngol* 67:239-254.

Spoendlin H (1973) The innervation of the cochlea receptor. In: *Mechanisms in Hearing*. Moller AR (Ed.), Academic Press, New York, NY. pp.185-229.

Stacy RC, Demas J, Burgress RW, Sanes JR, Wong RO (2005) Disruption and recovery of patterned retinal activity in the absence of acetylcholine. *J Neurosci* 25:9347-9357.

Stakhovskaya O, Hradek GT, Snyder RL, Leake PA (2008) Effects of age at onset of deafness and electrical stimulation on the developing cochlear nucleus in cats. *Hear Res* 243:69-77.

Starr A, McPherson D, Patterson J, Don M, Luxford W, Shannon R, Sininger Y, Tonakawa L, Waring M (1991) Absence of both auditory evoked potentials and auditory percepts dependent on timing cues. *Brain* 114:1157-1180.

Stieber J, Herrmann S, Feil S, Löster J, Feil R, Biel M, Hofmann F, Ludwig A (2003) The hyperpolarization-activated channel HCN4 is required for the generation of pacemaker action potentials in the embryonic heart. *Proc Natl Acad Sci USA* 100:15235-15240.

Strata F, Atzori M, Molnar M, Ugolini G, Tempia F, Cherubini E (1997) A pacemaker current in dye-couple hilar interneurons to the generation of giant GABAergic potentials in developing hippocampus. *J Neurosci* 17:1435-1446.

Stuart G, Häusser M (1994) Initiation and spread of sodium action potentials in cerebellar purkinje cells. *Neuron* 13:703-712.

Szabó ZS, Harasztosi CS, Sziklai I, Szûcs G, Rusznák Z (2002) Ionic currents determining the membrane characteristics of type I spiral ganglion neurons of the guinea pig. *Eur J Neurosci* 16:1887-1895.

Taberner AM, Liberman MC (2005) Response properties of single auditory nerve fibers in the mouse. *J Neurosphysiol* 93:557-569.

Tao HW, Zhang LI, Engert F, Poo M (2001) Emergence of input specific LTP during development of retinoectal connections in vivo. *Neuron* 31:569-580.

Tierney TS, Russell A, Moore DR (1997) Susceptibility of developing cochlear nucleus neurons to deafferentation-induced death abruptly ends just before the onset of hearing. *J Comp Neurol* 378:295-306.

Tritsch NX, Bergles DE (2010a) Developmental regulation of spontaneous activity in the mammalian cochlea. *J Neurosci* 30:1539-1550.

Tritsch NX, Rodríguez-Contreras A, Crins TT, Wang HC, Borst JG, Bergles DE (2010b) Calcium action potentials in hair cells pattern auditory neuron activity before hearing onset. *Nat Neurosci* 13:1050-1052.

Tritsch NX, Yi E, Gale JE, Glowatzki E, Berlges DE (2007) The origin of spontaneous activity in the developing auditory system. *Nature* 450:50-55.

von Békésy G (1970) Travelling waves as frequency analysers in the cochlea. *Nature* 225:1207-1209.

Walsh EJ, McGee J (1987) Postnatal development of auditory nerve and cochlear nucleus neuronal responses in kittens. *Hear Res* 28:97-116.

Wang W, Kim HJ, Lv P, Tempel B, Yamoah EN (2013) Association of the K_v1 family of K^+ channels and their functional blueprint in the properties of auditory neurons as revealed by genetic and functional analyses. *J Neurophysiol* 110:1751-1764.

Weisz CJ, Glowatzki E, Fuchs PA (2009) The postsynaptic function of type II cochlear afferents. *Nature* 461:1126-1129.

Weisz CJ, Glowatzki E, Fuchs PA (2014) Excitability of type II cochlear afferents. *J Neurosci* 34:2365-2373.

Weisz CJ, Lehar M, Hiel H, Glowatzki E, Fuchs PA (2012) Synaptic transfer from outer hair cells to type II afferent fibers in the rat cochlea. *J Neurosci* 32:9528-9536.

Wightman FL, Kistler DJ (1992) The dominant role of low-frequency interaural time differences in sound localization. *J Acoust Soc Am* 91:1648-1661.

Wong ROL, Meister M. Shatz CJ (1993) Transient period of correlated bursting activity during development of the mammalian retina. *Neuron* 11:923-938.

Yamada R, Kuba H, Ishii TM, Ohmori H (2005) Hyperpolarization-activated cyclic nucleotide-gated chation channels regulate auditory coincidence detection in nucleus laminaris of the chick. *J Neurosci* 25:8867-8877.

Yi E, Roux I, Glowatzki E (2010) Dendritic HCN channels shape excitatory postsynaptic potentials at the inner hair cell afferent synapse in the mammalian cochlea. *J Neurophysiol* 103:2532-2543.

Zeng F-G, Kong Y-Y, Michalewski HJ, Starr A (2005) Perceptual consequences of disrupted auditory nerve activity. *J Neurophysiol* 93:3050-3063.

Zeng F-G, Oba S, Garde S, Sininger Y, Starr A (1999) Temporal and speech processing deficits in auditory neuropathy. *Neuroreport* 10:3429-3435.

Zhang LI, Bao S, Merzenich MM (2002) Disruption of primary auditory cortex by synchronous auditory inputs during a critical period. *Proc Natl Acad Sci USA* 99:2309-2314.

Zhang LI, Poo M-M (2001) Electrical activity and development of neural circuits. *Nat Neurosci Suppl* 4:1207-1214.

Zhang LI, Tao HW, Holt CE, Harris WA, Poo M (1998) A critical window for cooperation and competition among developing retinotectal synapses. *Nature* 395:37-44.

Zheng J, Lee S, Zhou ZJ (2004) A developmental switch in the excitability and function of the starburst network in the mammalian retina. *Neuron* 44:851-864.

Zheng J, Lee S, Zhou ZJ (2006) A transient network of intrinsically bursting starburst cells underlies the generation of retinal waves. *Nat Neurosci* 9:363-371.

Zheng QY, Johnson KR, Erway LC (1999) Assessment of hearing in 80 in-bread strains of mice by ABR threshold analyses. *Hear Res* 130:94-10.